1 Title Page

Title: Human-computer interactions predict mental health

Subtitle: MAILA - a **MA**chine learning framework for **I**nferring **L**atent mental states from digital **A**ctivity

Authors:

Veith Weilnhammer[1,2], Jefferson Ortega[3], David Whitney[1,3,4]

Affiliations and Contribution:

[1] Helen Wills Neuroscience Institute, University of California Berkeley, USA
[2] Max Planck UCL Centre for Computational Psychiatry and Ageing Research, London, UK
[3] Department of Psychology, University of California Berkeley, USA
[4] Vision Science Group, University of California Berkeley, USA

Corresponding Author:

Veith Weilnhammer
email: veith.weilnhammer@gmail.com
web: https://veithweilnhammer.github.io/

2 Summary

Feelings, thoughts, and intentions shape the way we move. This paper shows that cursor and touchscreen activity, two universal components of human-computer interactions, reveal the mental state of the person behind the screen, reaching state-of-the-art biomarker precision at zero marginal cost.

3 Abstract

Scalable assessments of mental illness, the leading driver of disability worldwide, remain a critical roadblock toward accessible and equitable care. Here, we show that human-computer interactions encode multiple dimensions of self-reported mental health and their changes over time.

We introduce MAILA, a MAchine-learning framework for Inferring Latent mental states from digital Activity. We trained MAILA to predict 1.3 million mental-health self-reports from 20,000 cursor and touchscreen recordings recorded in 9,000 online participants. The dataset includes 2,000 individuals assessed longitudinally, 1,500 diagnosed with depression, and 500 with obsessive-compulsive disorder. MAILA tracks dynamic mental states along three orthogonal dimensions, generalizes across contexts, and achieves near-ceiling accuracy when predicting group-level mental health. The model translates from general to clinical populations, identifies individuals living with mental illness, and captures signatures of psychological function that are not conveyed by language.

Our results demonstrate how everyday human-computer interactions can power passive, reliable, dynamic, and maximally scalable mental health assessments. The ability to decode mental states at zero marginal cost sets new benchmarks for precision medicine and public health, while raising important questions about privacy, agency, and autonomy online.

4 Introduction

Mental illness is the leading cause of disability worldwide[1,2]. Despite their impact, symptoms often go undetected for years[3,4]. Delayed access to care increases the risk of poor outcomes[5].

Language, the medium through which mental health is commonly expressed and understood, is not sufficient to close the gap between symptom onset and access to care. Mental illness can make it difficult to recognize and articulate the experiences that give rise to distress[6]. Feelings of shame, stigma, and language barriers may prevent people from reaching out[7,8]. In support systems with limited resources, shared moments of communication are often difficult to achieve[9]. While fluent in conversation and, to some extent, reflective of human cognition[10], large language models still lack the contextual understanding required for responsible deployment[11].

Efforts to develop more accessible and efficient mental health care are therefore expanding from language-based assessments, such as interviews and questionnaires, to non-verbal markers, including polygenic risk scores[12–14], neuroimaging[15,16], wearable technology[17,18], cognitive tasks[19,20] and digital behaviors[21,22]. Human-computer interactions like cursor and touchscreen activity are of particular interest, because they are generated by virtually every consumer grade device, recorded continuously at zero cost, and independent of language, introspection, and social expectations[23]. Finding a mind-body connection in these digital behaviors would mean that mental states, and their changes, can be decoded every time a person uses a computer, tablet, or smartphone[21–31].

The idea that mental states are expressed in movement is supported by centuries of research on facial expression, posture, gait, and gestures[32,33]. According to motor-control theory, actions rely on internal models that are continuously shaped by ongoing affective and cognitive processes[34,35]. It therefore stands to reason that human-computer interactions, like other forms of motor behavior[32–35], encode signatures of mental states, including those central to mental health.

So far, however, the extent to which human-computer interactions reflect mental states remains an open question. Previous attempts have been limited by small, homogeneous samples that restrict statistical power and external validity[36]. Many have focused on narrowly defined features that may overlook the high-dimensional nature of human-computer interactions[37,38]. In addition, prior work has mostly targeted binary diagnostic traits rather than the dynamic and continuous fluctuations in mental health that matter most in psychology, medicine, and neuroscience[39,40].

Here, we introduce MAILA, a machine learning framework for inferring latent mental states from digital activity, and the MAILA dataset, a large-scale collection of human-computer interactions annotated with self-reports about mental health. Our results confirm that cursor movements and touchscreen activity, two universal components of human-computer interactions, reflect the mental state of the person behind the screen. MAILA extracts signatures of psychological function that have so far remained untapped, setting a new benchmark in the accuracy, cost-efficiency, scalability, and ecological validity of mental-health biomarkers.

5 Results

To test whether mental states can be decoded from human-computer interactions, we recorded cursor and touchscreen activity during a variety of digital activities and at multiple times in 9000 unique participants who answered 67 questions about their current psychological distress and well-being. We evaluated MAILA on structured and open-ended digital behaviors, repeated assessments, and participants with and without a diagnosed mental illness.

We tracked cursor movements in 4,000 participants from the general population who completed a structured questionnaire interface designed to mimic everyday computer use (Supplemental Figure S1). 2,000 of the 4,000 baseline participants repeated the assessment at a later time. Among the follow-up participants, 600 completed a non-mental health survey, and another 600 played an interactive decision-making game. Separately, we also recorded touchscreen activity in 5,000 participants who completed a creative drawing task and a mobile version of the questionnaire interface. Among these, 3500 came from the general population, 1,000 self-identified as diagnosed with depression, and 500 reported living with obsessive-compulsive disorder (OCD).

We projected each participant into two spaces, one defined by patterns of human-computer interaction, and one defined by self-reported mental health, and trained MAILA to map from one to the other (Figure 1).
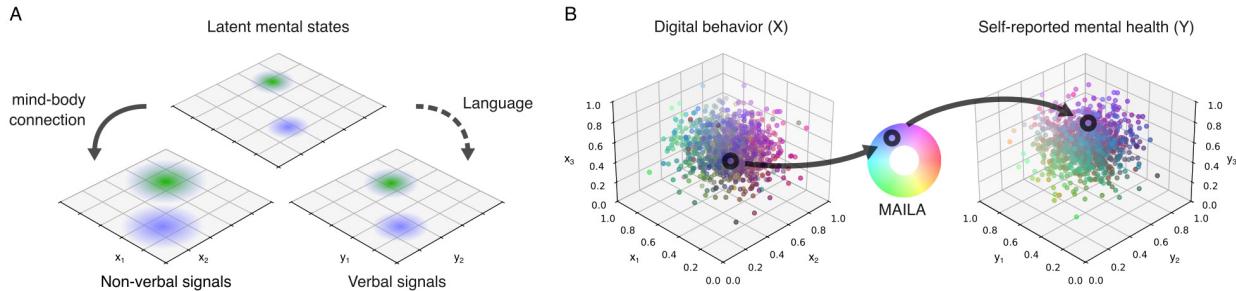

Figure 1. Decoding mental states from digital behavior. MAILA predicts mental states from cursor and touchscreen activity, two integral components of everyday interactions with computers and handheld devices. **A.** Verbal and non-verbal signals encode latent mental states, illustrated for two distinct experiences (blue and green) that differ along two dimensions (e.g., sadness and anxiety). Verbal signals are precise but sparse; non-verbal signals are noisy but ubiqituous and observed at much lower cost. **B.** We obtained 20,000 cursor and touchscreen recordings and labelled them with 1.3 million self-reports provided by 9,000 unique participants. Each participant is represented as a point in the space of digital behavior $X^{N \times C}$, where C denotes features of human-computer interaction (x_1-x_3), and as a point in the space of mental health $Y^{N \times Q}$, where Q represents dimensions that describe mental states (illustrated here by the dimensions y_1-y_3 for N individuals). MAILA decodes self-reported mental health from data-driven features of human-computer interactions.

5.1 The space of human-computer interaction

MAILA uses unsupervised representation learning to encode each participant's cursor or touch-screen activity as a distribution over stereotyped movement patterns. We segmented each recording, containing on average $2.46 \times 10^4 \pm 462.35$ screen-normalized coordinates, into partially overlapping windows of 100 consecutive samples. A long short-term memory autoencoder, pretrained on naturalistic human-computer interactions[41], transformed each segment into a 50-dimensional movement embedding. We pooled the embeddings across all participants N and grouped them into C = 500 K-means clusters, each representing a distinct, recurring pattern of human-computer interaction. MAILA then computes, for individual participants, the proportion of segments assigned to each cluster (Supplemental Figure S2-4).

This process transforms the recorded cursor or touchscreen activity into a $X^{N \times C}$ feature matrix. Each row in X defines a participant's location in the space of digital behavior, i.e., a C-dimensional distribution over recurring patterns of human-computer interaction.

5.2 The space of mental health

The MAILA dataset annotates all recorded human-computer interactions with continuous mental health self-reports. We measured psychological distress and wellbeing as two distinct but related domains of mental health[42]. We assessed distress using 53 items across 10 subscales, including depression, anxiety, phobic anxiety, somatization, interpersonal sensitivity, psychoticism, paranoia, hostility, and clinically relevant features. We quantified wellbeing using 14 items across 3 subscales, covering emotional, social, and psychological experiences (Supplemental Table S1, Supplemental Figure S5-6).

To obtain ground-truth measures of mental health while preventing trivial decoding, we built a custom web interface that induced naturalistic human-computer interactions while decoupling cursor and touchscreen activity from the content of self-reports. Cursor and touch movements in everyday digital environments typically follow horizontal, vertical, and diagonal paths that reflect how users navigate between central content and peripheral controls[41]. Our response interface mirrored this pattern by placing self-report elements at random central locations and navigation elements for advancing the survey at fixed corner positions (Supplemental Figures S7-8).

Participants answered items such as "How much are you distressed by feeling fearful?" or "To what extent do you feel happy?" on a continuous scale from "Not at all" to "Very much". Questions appeared in random order, and responses were given by moving a cursor or dragging a dot onto a response line whose start and endpoint were independently randomized on every trial. MAILA's inputs were derived from the entire cursor or touchscreen recording, without labeling the final response position or indicating when a specific question was answered. This design ensured that

the model's input contained no direct information about the chosen rating, even when MAILA was trained on data collected during questionnaire completion (Supplemental Figure S9). To further demonstrate non-trivial decoding, we tested whether models calibrated in this way generalized to digital behavior recorded outside the mental-health self-report context, whether models trained directly on free-form behavior could still predict mental health, and whether MAILA generalized to open-ended human-computer interactions in a public dataset[41].

The interface measured distress and wellbeing with internal consistency of 0.91 Cronbach's α. Test-retest correlations reached 0.86 for follow-up intervals shorter than one week, and declined to 0.69 after eight weeks, indicating that the interface was highly reliable over short intervals, while sensitive to meaningful changes in mental health that accumulate over time. Individual items were related but not redundant, and grouped into subscales that captured coherent variance in mental health (see Methods for psychometric details).

We organized the continuous self-reports in a $Y^{N \times Q}$ mental health matrix, where Q represents individual items, dimension-specific scores, and global questionnaire scores, scaled from 0 to 1. Each row in this matrix defines a location in the space of psychological distress and wellbeing, i.e., a Q-dimensional description of the experiences that define mental health. We observed a wide range of mental health profiles that spanned the full continuum from distress to wellbeing at an average inter-quartile range of 0.49 ± 0.01, indicating substantial variability across participants (Supplemental Figure S5).

5.3 Linking human-computer interaction to mental health

Together, $X^{N \times C}$ and $Y^{N \times Q}$ form a paired representation of digital behavior and mental health. We trained support vector regression machines to predict self-reported mental states from patterns of human-computer interaction, and evaluated model performance on held-out participants using 5-fold cross-validation and generalization to independent datasets (Figure 1). We quantified predictive power using rank-based correlation with the ground truth (R), the root mean squared error relative to the range of the target variable (e), and the area under the received operating characteristic curve (AUC) as a threshold-free measure of discriminative performance across arbitrary percentiles. All results were compared against randomly permuted baselines (p, 10^6 permutations).

5.4 Cursor movements predict mental health

We recorded cursor movements in 4,000 participants who completed the interface on their desktop or laptop computer. Based on the cursor data alone, MAILA predicted overall levels of distress (R = 0.26, p < 10^{-6}) and wellbeing (R = 0.18, p < 10^{-6}), as well as inter-individual differences in depression, anxiety, phobic anxiety, somatization, interpersonal sensitivity, psychoticism, paranoia,

hostility, clinically-relevant features, and emotional, social, and psychological wellbeing in held-out participants ($R = 0.2 \pm 0.02$, $p = 4.8 \times 10^{-11}$, across dimensions). The model's continuous predictions discriminated between higher versus lower symptom burden at arbitrary percentile cutoffs with an average AUC of 0.6 ± 0.01. While each dimension was predicted by an independent regression model, MAILA recovered the dimensional structure of mental health: the predicted inter-dimension correlations differed from the true correlations by only 5.32% of the possible range ($p < 10^{-6}$; Figure 2, Supplemental Figure S10).
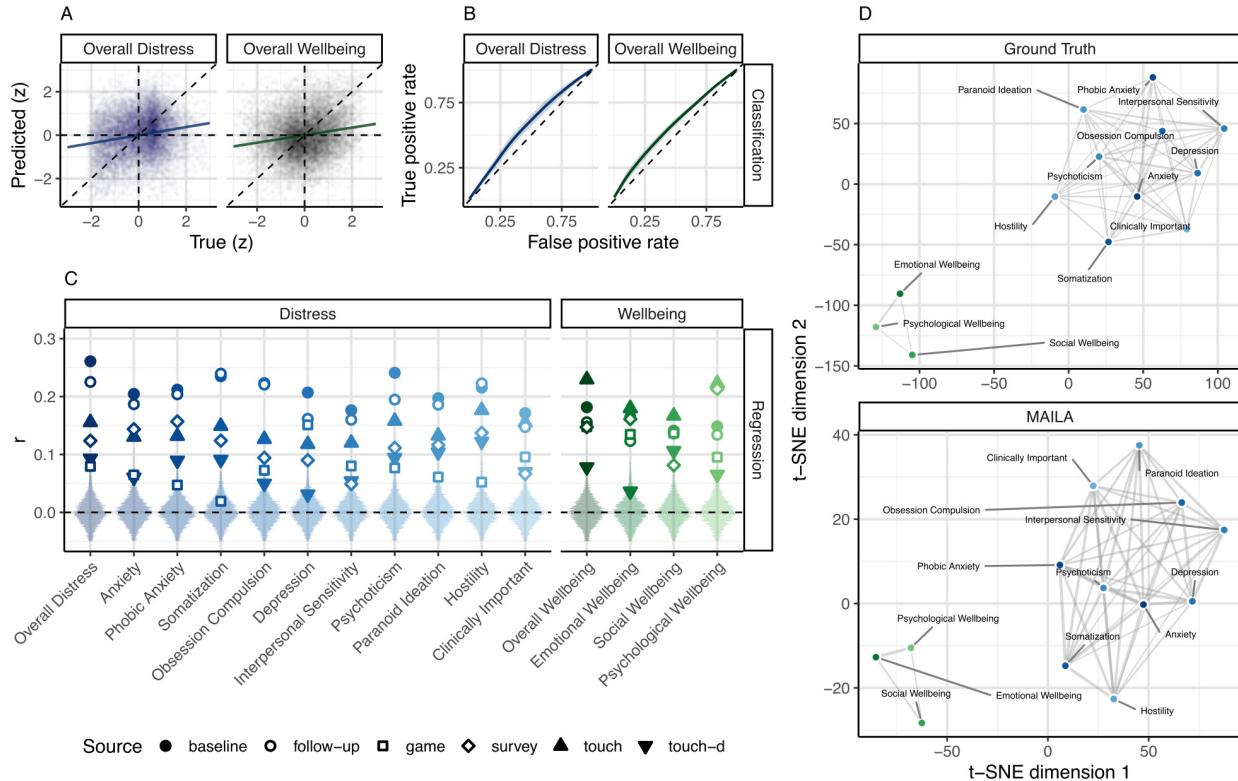

Figure 2. Human-computer interactions predict mental health. MAILA predicts multiple dimensions of mental health from brief cursor and touchscreen recordings. The model generalizes across contexts and time while preserving the correlation structure of mental health. **A.** Predicted versus true distress and wellbeing scores (z-score), alongside ordinary-least-squares regression. **B.** ROC curves for classifying higher versus lower distress and wellbeing across datasets and percentile cutoffs between 10% and 90%, based on MAILA's continuous predictions. Solid lines indicate averages; shaded ribbon spans the 95% confidence interval. **C.** Correlations of MAILA's predictions with the self-reported ground truth across dimensions. Violin plots show null distributions; points mark observed correlation from baseline, follow-up, survey, game, and touch datasets (filled: 5-fold cross-validation; unfilled: frozen models applied to another dataset). **D.** Two-dimensional embeddings of correlations among mental health dimensions in the ground truth and in MAILA. Line thickness corresponds to the strength of positive correlations.

With MAILA, less than 12 minutes of cursor tracking approximated self-reported mental health with the precision of state-of-the-art biomarkers, including polygenic risk scores[12–14], neuroimaging[15,16],

wearable technology[17,18], cognitive tasks[19,20], and digital behaviors[21,22]. While accuracy varies across studies, modalities, and sample size, established predictors typically yield correlations below 0.2 with inter-individual differences in cognition or psychopathology[16,19], and reach AUCs between 0.55 and 0.7 for binary psychiatric outcomes such as depression, anxiety, or schizophrenia[12,13,43].

MAILA matched this performance with fully passive data that can be extracted at zero marginal cost from any consumer grade device. Predictions derived from random splits of each participant's cursor movements correlated at $R = 0.81 \pm 4.93 \times 10^{-3}$, demonstrating a level of reliability that exceeds many experimental markers of mental health[44] (Supplemental Figure S11). In the following, we show how this cost-precision trade-off enables MAILA to decode dynamic and specific mental states across populations, contexts and time, and to approach near-ceiling accuracy when multiple observations are combined.

5.5 MAILA tracks changes in mental health

Static predictors such as polygenic risk scores, structural imaging, or demographic traits cannot detect changes in mental health, which are central to early intervention and personalized care. To understand whether human-computer interactions encode temporally specific patterns that reflect dynamic mental states, we calibrated MAILA on cursor movements from 4,000 participants at baseline and applied it, without retraining, to a subgroup of 2000 participants who repeated the same task 5 to 76 days later. In contrast to the analyses above, which assessed MAILA's ability to predict mental health in held-out participants at a single time point, we asked whether MAILA could decode within-person changes over time from cursor movements alone.

Between baseline and follow-up, participants reported median mental-health changes of 19.49% (inter-quartile range: 10.33%) relative to the maximum response range. These self-reported changes were closely mirrored by the difference in MAILA's predictions between baseline and follow-up ($R = 0.48 \pm 0.01$), which discriminated between improved or worsened mental health at an average AUC of $0.73 \pm 6.06 \times 10^{-3}$ and closely followed the correlation structure of self-reported changes in mental health ($e = 5.04\%$, $p < 10^{-6}$; Figure 3, Supplemental Figure S10). Models trained at baseline remained robust in predicting distress ($R = 0.16$, $p < 10^{-6}$), wellbeing ($R = 0.16$, $p < 10^{-6}$), and their subdimensions at follow-up ($R = 0.18 \pm 0.02$, $p = 8.59 \times 10^{-10}$, Figure 2). Errors did not increase with the interval between recordings ($p = 1$).

Predicting within-participant change yielded stronger correlations than predicting between-person differences within a dataset. This increase in precision suggests that mental health predictions become more accurate when participants contribute training data at an earlier time point. MAILA's ability to track change remained robust when predicting change without any access to ground truth labels, using only model predictions for participants held out during cross-validation at baseline ($R = 0.15 \pm 0.01$, $p = 4.69 \times 10^{-24}$, Supplemental Figure S12). This confirms that models can

8

track changes in an individual's mental health from digital behavior alone, but that tracking is substantially improved in the clinically realistic setting where baseline information is available.

Together, our results indicate that cursor movements encode state markers of mental health. Human-computer interactions thus encode signals that could support early detection, treatment evaluation, and risk monitoring between clinical visits.
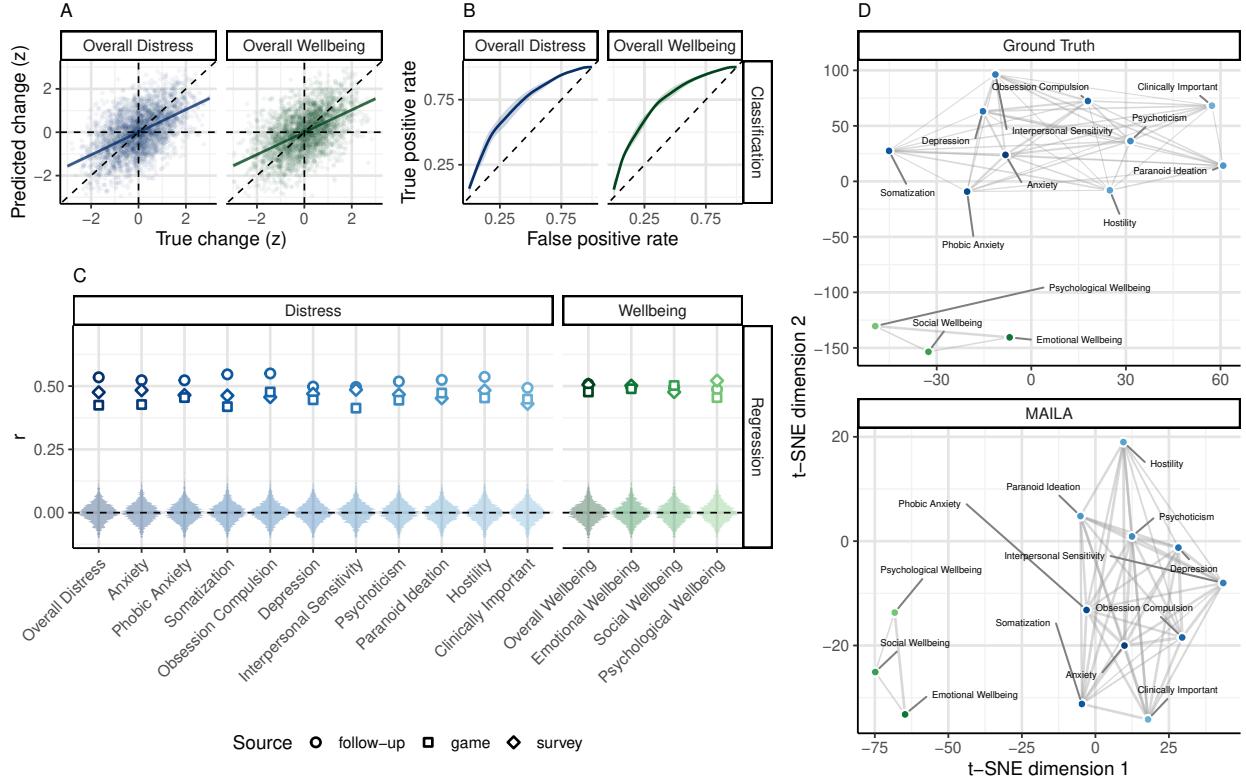

Figure 3. Human-computer interactions predict changes in mental health. MAILA is sensitive to dynamic mental states, enabling real-time monitoring of psychological distress and wellbeing. **A.** Predicted versus true changes in overall distress and wellbeing between baseline and follow-up (z-score), alongside ordinary-least-squares regression. **B.** ROC curves for classifying higher versus lower distress and wellbeing scores at follow-up relative to baseline, based on MAILA's continuous predictions. Solid lines indicate averages across the three datasets; shaded ribbons span the 95% confidence interval. **C.** Correlation between predicted and true change across dimensions. Violin plots show null correlations; points mark observed correlation from follow-up, survey, and game data. **D.** Two-dimensional t-SNE embeddings of correlations among true and predicted changes in mental health. Line thickness corresponds to the strength of positive correlations.

5.6 MAILA generalizes across contexts

Mental health assessments require measures that remain valid across contexts[45]. Questionnaires and structured clinical interviews achieve this robustness through standardization, where the format, sequence, timing, and instructions ensure that each participant is assessed under comparable

9

conditions. Models that work with passive real-time signals such as human-computer interactions, by contrast, sacrifice standardization for scalability and ecological validity, which causes them to suffer from lower accuracy and increased bias when applied outside their training distribution[45].

To test MAILA's ability to generalize across contexts, we trained models on cursor movements recorded at baseline and applied them, without retraining, to two separate subgroups recruited at follow-up. Each subgroup included 600 participants who used the response interface for a task unrelated to mental health: one completed a non-psychological survey (Supplemental Table S2); the other played an interactive decision-making game[46].

As expected, responses in both tasks carried no above-chance information about participants' mental health (Supplemental Figure S13). Human-computer interactions recorded in these contexts were not predictive of survey ($R = 0.01 \pm 0.03$, $p = 0.28$) or gameplay behavior ($R = 0.02 \pm 0.02$, $p = 0.09$; Supplemental Table S2). Any ability to decode psychological distress or wellbeing in these settings must therefore arise from how people move the cursor, rather than from how they responded to specific survey questions or game events.

Models trained at baseline successfully predicted overall distress (survey: $R = 0.12$, $p < 10^{-6}$, game: $R = 0.08$, $p = 0.03$), wellbeing (survey: $R = 0.15$, $p < 10^{-6}$, game: $R = 0.15$, $p < 10^{-6}$), and their subdimensions (survey: $R = 0.08 \pm 0.03$, $p = 5.17 \times 10^{-7}$, game: $R = 0.08 \pm 0.02$, $p = 4.64 \times 10^{-6}$; Figure 2) based only on the human-computer interactions collected during survey completion and gameplay. MAILA distinguished between higher versus lower symptom burden at an average AUC of $0.56 \pm 7.57 \times 10^{-3}$ and $0.55 \pm 7.46 \times 10^{-3}$, respectively, and remained highly sensitive to mental health changes over time with only survey ($R = 0.48 \pm 0.01$, AUC $= 0.73 \pm 7.22 \times 10^{-3}$) or game data as follow-up inputs ($R = 0.45 \pm 0.01$, AUC $= 0.72 \pm 0.01$, Figure 3).

At the time of survey and game experiments, each participant also repeated the mental-health task used for training at baseline. Relative to this context, MAILA produced consistent mental-health estimates for the same held-out individual (survey: $R = 0.22 \pm 0.01$ $p = 1.51 \times 10^{-14}$; game: $R = 0.11 \pm 0.02$, $p = 1.7 \times 10^{-9}$). Errors remained within the baseline distribution (Supplemental Figure S14).

Together, our generalization experiments demonstrate that the mind-body connection leaves a robust and context-invariant signature in the way people move the cursor. Everyday human-computer interactions encode information about the mental state of the person behind the screen of a desktop or laptop computer.

5.7 Mental health is encoded in structured touchscreen activity

Mobile technology has become the primary medium of everyday digital activity[47]. Today, 96% of internet users access the web via smartphones, and 64% of global traffic is generated by hand-

held devices[48]. To confirm that mental states are also encoded in touch-based human-computer interactions, we trained and tested MAILA in an independent group of 3,500 general population participants who completed the questionnaire interface on their smartphone or tablet. From touchscreen activity alone, MAILA predicted overall distress (R = 0.16, p < 10^{-6}), wellbeing (R = 0.23, p < 10^{-6}), and their subdimensions (R = 0.15 ± 0.02, p = 4.18 × 10^{-10}; Figure 2). Based on its continuous predictions, the model discriminated between higher versus lower symptom burden at an average AUC of 0.57 ± 0.02.

5.8 Mental health is encoded in free-form human-computer interaction

Our response interface induced structured patterns of cursor and touchscreen activity that mirrored everyday human-computer interaction, where users move between central contents and peripheral control elements (Supplemental Figures S7-8). To test whether MAILA can generalize beyond rigid user interfaces, we asked all 4,000 touchscreen participants to complete a series of prompted drawings on their phones or tablets before starting the questionnaire. Each prompt, for example, "Draw a spaceship" or "Draw the digits 036", specified only what to draw, but not how (see Supplemental Table S3 for all prompts and Supplemental Figure S15 for example drawings). These drawing tasks elicited free-form, creative digital behavior with no direct link to mental health, providing a stringent test of MAILA's ability to generalize beyond structured human-computer interactions.

Remarkably, with only the free-from touchscreen activity as its input, MAILA predicted overall distress (R = 0.09, p < 10^{-6}), wellbeing (R = 0.08, p < 10^{-6}), and their subdimensions (R = 0.07 ± 0.02, p = 6.26 × 10^{-7}). Across arbitrary percentile cutoffs, participants with higher versus lower symptom burden were distinguished with an average AUC of 0.54 ± 7.57 × 10^{-3} (Figure 2). Despite relying on entirely different interaction modes, independent models trained on the structured touchscreen interface and the drawing behavior converged on correlated predictions for the same held-out participants (R = 0.06 ± 0.02, p = 1.2 × 10^{-6}). Errors decreased by 4.31 ± 0.18% (p < 10^{-6}) when predictions from the two touchscreen recordings were combined, indicating that MAILA's precision can be improved through repeated measurements across contexts[21].

5.9 MAILA predicts mental health across demographics

Bias is a major concern when applying predictive models to people who differ in age, gender, or cultural background, since unequal performance across demographic groups is known to amplify existing disparities in care[45]. The MAILA dataset spans online participants aged from 18 to 85 years, with 48.45% identifying as female and 47.02% as male. We recruited participants with 96 different nationalities from 55 countries of residence, representing varied ethnicities and a wide range of employment and student statuses (Supplemental Figures S16-17). While no dataset can fully

reflect global populations[49], our sample's diversity provides a meaningful foundation for testing whether MAILA's predictions generalize fairly. We observed stable prediction errors across demographic groups (median F = 1.06; Supplemental Figure S16), indicating that demographic factors do not systematically modulate inferences from human-computer interactions in a way suggestive of algorithmic bias.

5.10 Human-computer interactions predict 3 orthogonal dimensions of mental health

Our results demonstrate that brief everyday digital activities, such as completing surveys, playing games or drawing pictures, provide a window onto the mental state of the person behind the screen. A key question that follows is whether patterns of human-computer interaction encode particular thoughts and emotions that shape the content of psychological distress and wellbeing, or whether they reflect only a general tendency toward poor or good mental health.

Clinicians often rely on structured interviews and questionnaires to map an individual's position in multidimensional spaces of mental health. By asking about experiences such as depression, anxiety, or connectedness, they construct a high-dimensional profile that guides decision-making. Yet, unlike Euclidean spaces where axes are orthogonal and independent, many language-based descriptions of mental health are interrelated[50]. Low mood, for example, is frequently accompanied by social withdrawal and persistent worry. These covariations were also present in MAILA dataset: participants who felt more distressed reported lower wellbeing (and vice versa, R = -0.25 ± 0.02). Higher scores on one dimension were accompanied by higher scores on others (distress dimensions: R = 0.66 ± 0.02; wellbeing dimensions: 0.73 ± 0.09; Figure 2-3, Supplemental Figure S6).

Such shared variance is often taken to reflect a global factor capturing an individual's propensity toward distress[50]. A possible implication is therefore that alignment with this global factor alone may be enough for MAILA to predict multiple correlated dimensions of mental health, without any specificity to their content. To evaluate whether human-computer interactions encode differentiated markers beyond a one-dimensional scalar of distress, we transformed the $Y^{N \times Q}$ mental health matrix into a set of orthogonal principal components (PC). Each PC captured an independent source of variation of self-reported mental health in the MAILA dataset (Figure 4).

Based on the recorded human-computer interactions alone, MAILA successfully predicted the location of held-out participants on the first 3 PCs of mental health, which together explained 37.91% of the variance across all calibration and generalization datasets. PC1 reflected a general distress-to-wellbeing axis and was decoded at R = 0.16 ± 0.04 ($p < 10^{-6}$). PC2 separated depression and interpersonal sensitivity from other types of distress (R = 0.22 ± 0.04, $p < 10^{-6}$). PC3 placed somatization and hostility on one end, obsessive-compulsive symptoms and interpersonal sensitivity on the other, and anxiety, depression, psychoticism, and paranoia in between (R = 0.2 ± 0.07, p = 0). MAILA's continuous predictions separated participants with higher versus lower scores with

AUCs of 0.57 ± 0.02 for PC1, 0.62 ± 0.02 for PC2, and 0.6 ± 0.02 for PC3 (arbitrary percentile thresholds). The model remained highly sensitive to within-participant mental-health changes (R $= 0.36 \pm 0.04$, p $= 7.53 \times 10^{-8}$), differentiating their direction with an average AUC of 0.68 ± 0.03 (across PC1-3, Figure 4).
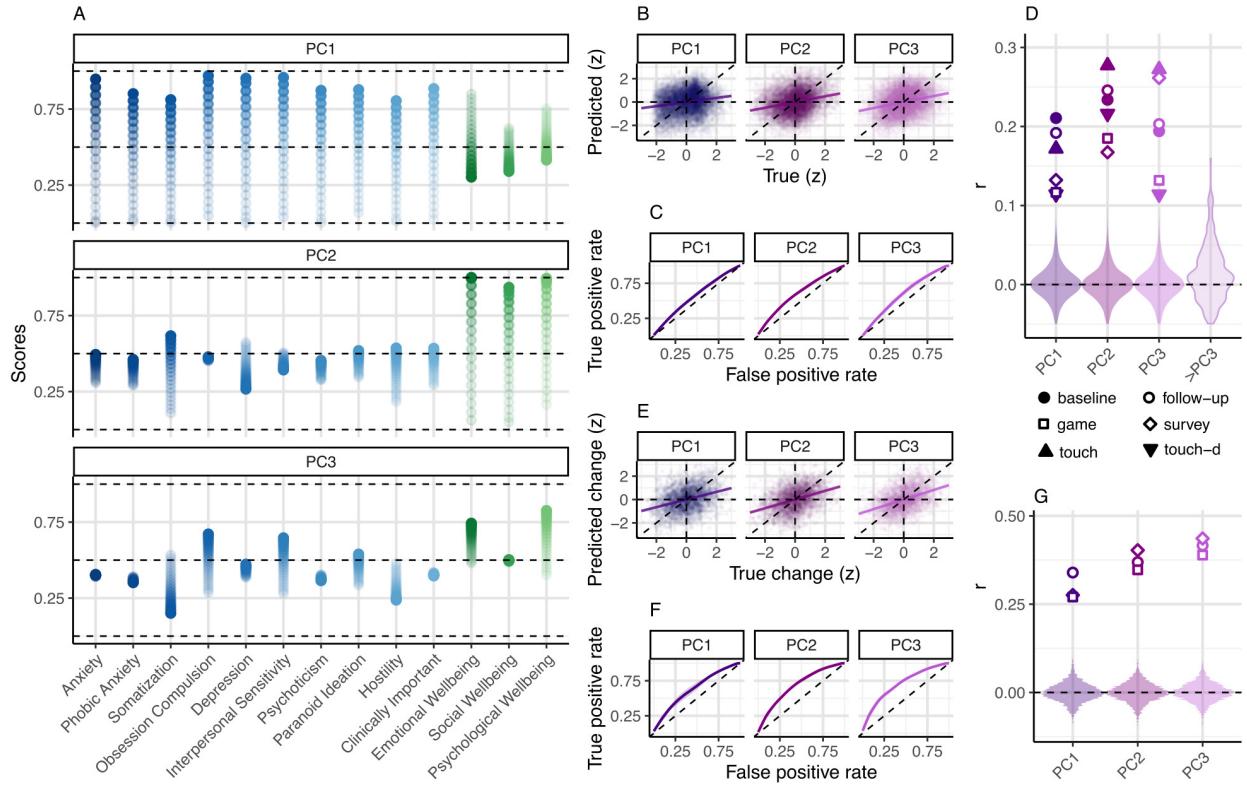

Figure 4. Human-computer interactions predict three orthogonal dimensions of mental health. MAILA predicts dynamic mental states across three principal components (PCs) of mental health, encoding information about the level (PC1) and the origins (PC2-3) of distress. **A.** Loading direction of reported scores (increasing from low to high opacity) on the PCs. **B.** Predicted versus true overall scores for the PC1-3 (z-score), alongside ordinary-least-squares regression. **C.** ROC curves across all sources and percentile cutoffs. Bold lines show average ROC curves per PC; shaded ribbons indicate 95% confidence intervals. **D.** Predictive performance across PCs. Violins show null distributions; points mark observed correlation from baseline, follow-up, survey, game, and touch datasets (filled: five-fold cross-validation; unfilled: frozen models applied to another dataset). **E.** Predicted versus true changes between baseline and follow-up in PC space (z-score). **F.** ROC curves for classifying higher versus lower PC scores at follow-up relative to baseline. **G.** Correlations between predicted and true changes across PCs. Violin plots show null distributions; points mark observed correlations.

MAILA's ability to predict PC1-3 confirms that human-computer interactions contain information not only about the level, but also about the content of challenging mental states. By aligning with multiple orthogonal dimensions of mental health, MAILA distinguished between different ways in which people experience distress, such as whether symptoms are more affective, somatic, or inter-

personal. We found weaker predictions beyond PC3 ($R = 0.01 \pm 3.58 \times 10^{-3}$), suggesting that human-computer interactions capture the most dominant axes of variation of self-reported mental health in the MAILA database.

5.11 MAILA tracks group-level mental heatlh

As a consequence of MAILA's individual-level precision, aggregated predictions are expected to yield highly accurate group-level estimates as residual errors cancel out (Supplemental Figure S18). To explore the models' utility for population-level mental health monitoring, we tested whether MAILA can, from human-computer interactions alone, predict and replicate established demographic and environmental effects on mental health. In line with previous reports, our ground-truth self-reports suggested that mental health was modulated by employment status, with unemployed and part-time employed individuals reporting higher distress and lower wellbeing than retired or full-time employed participants[51]. We also observed an effect of age, with older adults reporting lower distress and higher wellbeing[52]. Participants who identified as female tended to report higher distress than participants who identified as male[53]. Finally, aggregating self-reports by local time revealed a diurnal pattern across participants, who reported higher wellbeing in the early morning and increasing distress as the day progressed, consistent with a morning peak in positive affect and a gradual rise in negative affect toward nightfall[54].

From human-computer interactions alone, and without access to any demographic or temporal information, MAILA recovered the effects of employment[51] ($R = 0.67$, $p = 7.89 \times 10^{-9}$), gender[53] ($R = 0.67$, $p = 6.8 \times 10^{-5}$), age[52] ($R = 0.97$, $p < 10^{-6}$), and time-of-day[54] ($R = 0.47$, $p = 5.91 \times 10^{-11}$; Figure 5). Temporal tuning curves, obtained by shifting predicted and true diurnal signals, peaked at zero lag, indicating that human-computer interactions capture shared circadian fluctuations in mental state (Figure 5E).

To explore MAILA's ability to decode group-level mental health from non-experimental behavior, we applied models trained on the MAILA dataset to open-ended human-computer interactions from 19 users who collectively contributed 2,550 hours of cursor activity across 160,000 sessions[41], including activities such as web browsing, file management, office applications, coding, and entertainment. Using only these naturalistic cursor movements as input, we replicated the circadian fluctuations within individual participants, confirming that the time-of-day effect was not driven by selection bias (Figure 5F). On longer timescales, predictions from one session resembled those from adjacent sessions rather than shifting abruptly, while preserving the correlation between mental health dimensions seen in the MAILA dataset (Supplemental Figure S19).

Together, these results validate MAILA against established demographic and environmental influences. Human-computer interactions provide a scalable signal for real-time, cost-free public mental-health monitoring across contexts.
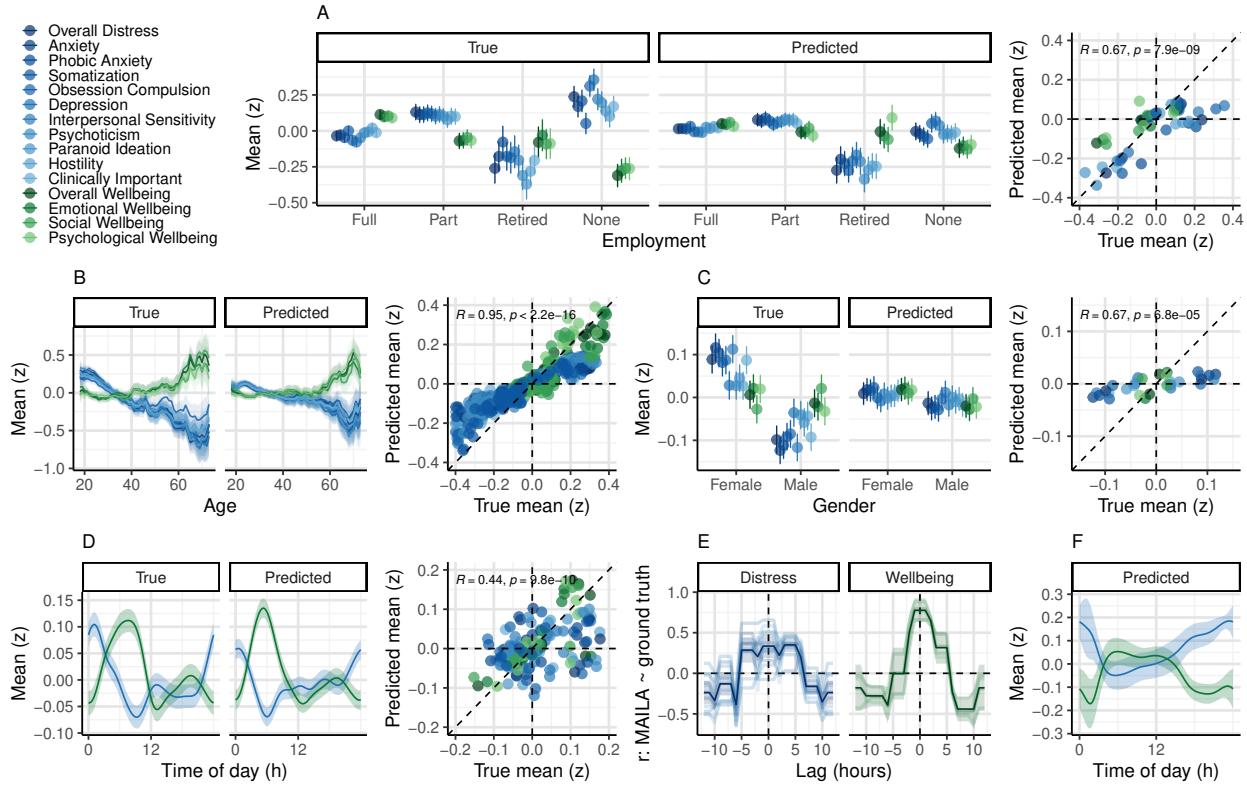
Figure 5. Human-computer interactions track group-level mental heatlh. MAILA recovers established demographic and temporal predictors of psychological function. **A.** Ground truth and predictions for distress and wellbeing by employment status (z-scored). Error bars indicate the 95% confidence interval. The right panel plots predicted versus true group-level means. **B.** Ground truth and predictions for distress and wellbeing by age. Shaded areas indicate the 95% confidence interval. **C.** Ground truth and predictions for distress and wellbeing by gender. **D.** Ground truth and predictions for depression (blue) and emotional wellbeing (green) across hours of the day. Shaded areas indicate the 95% confidence interval (left panel). The right panel shows predicted versus true group-level means for each hour across all dimensions. **E.** Lag-dependent correlations between true and predicted scores across time-of-day bins. Thin lines show individual dimensions; shaded areas show group means ± 95% CI for distress and wellbeing. Correlations peak near zero lag, indicating that MAILA captures slow shared diurnal structures in mental state. **F.** Frozen MAILA models applied to open-ended cursor movements (external dataset) replicate the circadian mental health fluctuations in 19 individuals, each of whom contributed multiple session at varying times in the day.

5.12 MAILA generalizes to clinical populations

An important requirement for digital tools like MAILA is the ability to measure mental health both within and beyond clinical populations[30,31]. We therefore tested MAILA in 1,000 participants who reported a history of depression, and 500 participants who reported a history of OCD. Both groups completed the free-form drawing task as well as the touchscreen version of the questionnaire inter-

face. Within each diagnostic group, participants were stratified into four equally sized subgroups based on functional impairment and medication status.
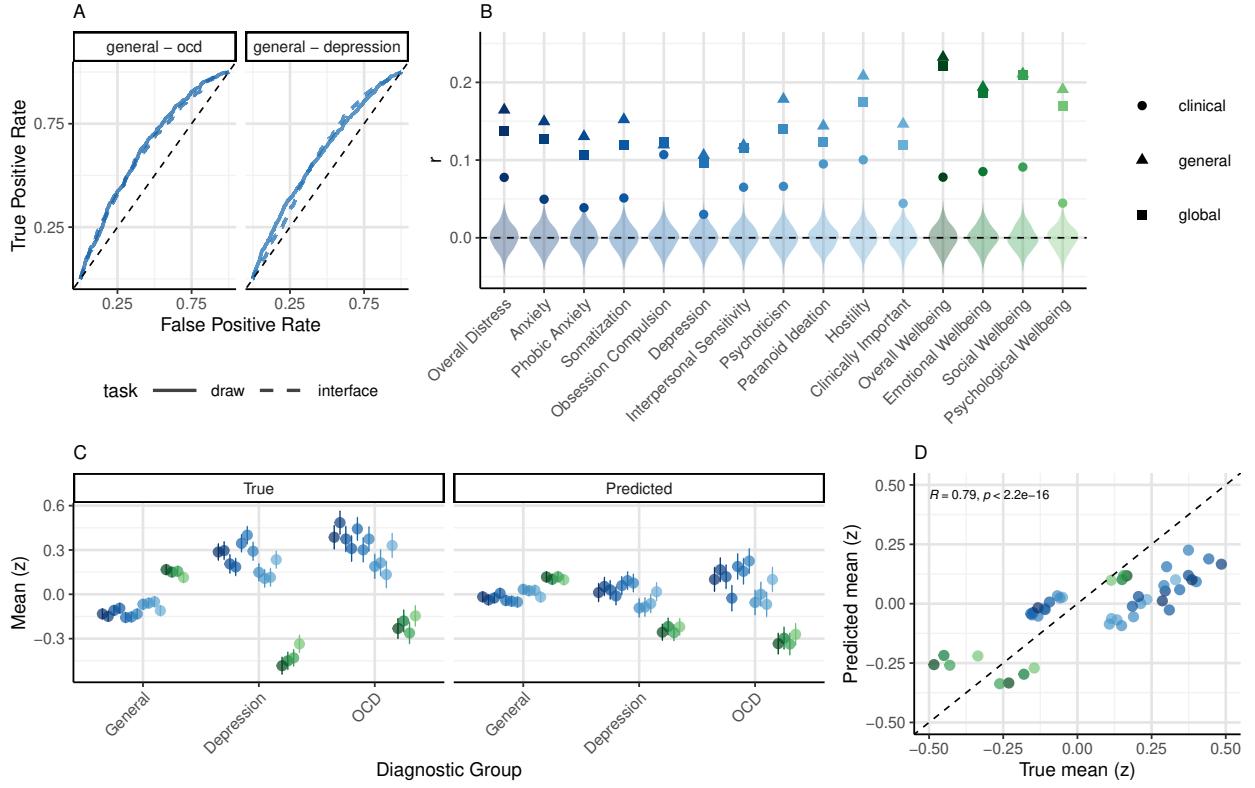

Figure 6. MAILA generalizes to clinical populations. Human-computer interaction differentiate people with depression and OCD from the general population and encode variation in psychological function within clinical groups. **A.** ROC curves for differentiating participants with a self-reported diagnosis of OCD (left) and depression (right) from the general population. Dashed and solid lines denote classification based on touch-based drawing and questionnaire interface, respectively. **B.** Group-level performance across dimensions in models trained on all participants (general and clinical populations). Markers denote correlation within general, clinical, and the joint (global) population. Violin plots show null distributions. **C.** Average ground truth (left) and predictions (right) for dimensions of distress (blue) and wellbeing (green) by population (z-scored). Errorbars mark 95% confidence intervals. **D.** Predicted versus true group-level averages across groups and dimensions.

Prior genome-wide associations studies have shown strong genetic correlations between clinician-assigned and self-reported diagnoses[14]. Evaluating MAILA on these labels therefore not only addresses the question of generalization to people living with mental illness, but also validates the model's predictions against established diagnostic traits. With only MAILA's touchscreen encoding as their input, support vector classifiers distinguished individuals with a self-reported history of mental illness from the general population at an AUC of 0.64 for depression and an AUC of 0.7 for OCD, irrespective of whether predictions were made from structured or free-form touchscreen

activity (Figure 6). Functional impairment (p = 0.86) and psychiatric medication (p = 0.12) did not affect classification performance.

MAILA matched the performance of behavioral markers derived from wearable devices[18] and performed slightly better than polygenic risk scores and imaging biomarkers for depression[12], while relying only on passive digital signals that are generated during everyday human-computer interactions at zero marginal cost. The model performed comparably to classifiers trained on all available self-reports collected at the same time, which achieved AUCs of 0.75 for depression and 0.76 for OCD, highlighting MAILA's potential as a maximally scalable screening tool that may help shorten the duration of undetected mental illness[55].

As expected, MAILA predicted greater distress related to depressive symptoms in participants with a history of depression (b = $7.7 \times 10^{-3} \pm 2.02 \times 10^{-3}$, p = 1.38×10^{-4}), and greater distress related to obsessive and compulsive symptoms in those with a history of OCD (b = $0.01 \pm 2.73 \times 10^{-3}$, p = 2.93×10^{-6}). MAILA's group-level estimates of distress and wellbeing closely mirrored the ground truth across clinical and non-clinical populations (R = 0.79, p < 10^{-6}).

MAILA retained its ability to capture inter-individual differences across all dimensions within the clinical groups (R = 0.07 ± 0.01, Figure 6), even though people with a self-reported diagnosis experienced more extreme mental states than participants from the general population. This suggests that the model captured depression and OCD not as qualitatively distinct categories, but on a continuum along the dimensions that shape mental health in the general population[40,42]. This ability to generalize supports MAILA's utility for measurement-based care in clinical settings, without the need for diagnosis-specific model tuning.

5.13 MAILA validates and extends cognitive phenotypes of mental health

Conventional mental health assessments rely on predefined indicators of mental health, such as responses to structured interviews and questionnaire items[39]. This hypothesis-driven approach is often mirrored in digital phenotyping, where predefined aspects of behavior, such as screen time or typing speed, serve as proxies for constructs such as diagnoses, traits, or their underlying cognitive mechanisms[17,30,38].

MAILA, by contrast, learns an end-to-end mapping from human-computer interactions to mental health without specifying the underlying signals. Its central assumption is that individuals who are close to each other in the space of mental health also cluster together in the space of human-computer interactions. Such a shared geometry between internal states and observable behavior[34,35] makes it possible to interpret unfamiliar signals through their proximity to familiar ones, and offers a data-driven way to validate hypotheses about the mechanisms of mental illness.

We showcase this ability with respect to belief instability, a cognitive marker that describes how readily people revise their internal models in response to new information. While rigid belief updating has been linked to perseverative thinking in depression and OCD, overly flexible belief updating may lead to erratic or impulsive behavior[46].
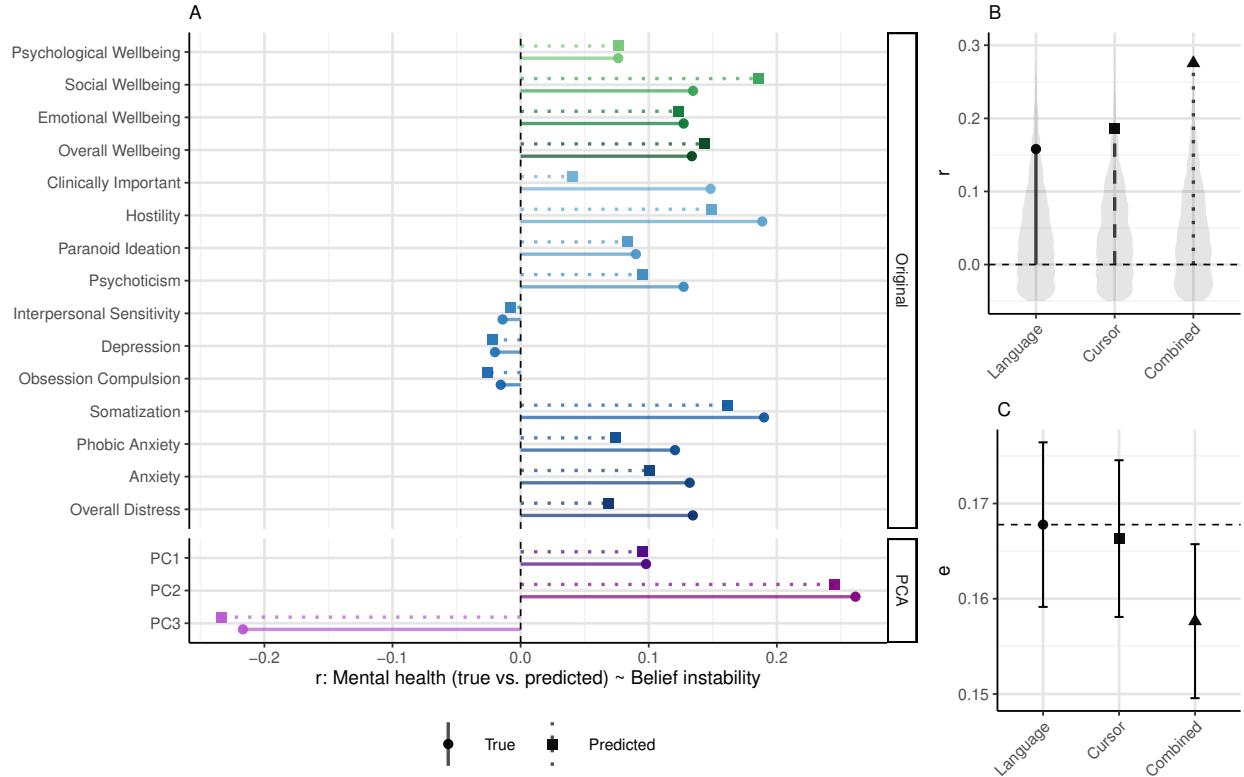

Figure 7. MAILA as a bridge between language and cognitive markers of mental health. Human-computer interactions improve the encoding of belief instability, a transdiagnostic cognitive marker of mental health and illness, relative to self-reports. **A.** Correlations between belief instability and dimensions of mental health, shown for ground truth (round markers) and predicted scores (square markers) along original dimensions (top) and principal components (bottom) of mental health. **B.** Cross-validated prediction of belief instability from cursor embeddings, self-reports (language), and their combination. Violin plots show permuted null distributions; markers indicate observed coefficients **C.** Normalized root mean squared errors (e $\pm$ 95% confidence intervals) for the same models. Dashed line marks the error of predictions from self-reports alone.

In MAILA's gamified generalization experiment, 600 participants completed eight independent rounds of the beads task[46]. In each round, they observed a sequence of colored beads drawn from one of two jars. Each jar contained blue and green beads in different proportions, and all beads within a given round came from the same jar. Participants knew the majority-minority ratio (e.g., 75%:25%) for both jars but were never told which jar was being used. After each draw, they reported a confidence-weighted belief about which jar the beads were coming from. In this task, the entropy of belief updates indexes belief instability: low entropy reflects rigid or stable inferences,

whereas high entropy reflects reactive or erratic updating[56].

Correlations between the dimensions of self-reported mental health and update entropy in the beads task confirmed that belief instability maps mental health along a continuum from reactive to rigid cognition, showing positive associations with hostility and somatization and negative associations with experiences of depression, obsession-compulsion, and interpersonal sensitivity. These relationships persisted when self-reports were replaced by predictions derived solely from cursor movements in held-out participants. From human-computer interactions alone, MAILA recovered the group-level associations between mental states and belief instability at R = 0.7 (p = 4.59×10^{-3}; Figure 7A).

At the individual level, MAILA's movement embeddings predicted unique variance in belief instability over and above all available self-reports (cross-validated partial correlation between cursor movement and update entropy, controlling for self-reports: R = 0.19, p = 3.47×10^{-6}). Self-reports also carried unique, albeit weaker, information about belief instability (R = 0.14, p = 8.55×10^{-4}, controlling for cursor movement). Combining self-reports and cursor-based features achieved the highest performance (R = 0.28, p = 7.64×10^{-12}). Errors in the combined model were significantly lower in comparison to self-reports alone (p = 1.64×10^{-6}; Figure 7B-C).

Together, these results suggest that human-computer interactions encode information about cognition that goes beyond what is conveyed by language. Data-driven markers extracted from everyday digital behavior can therefore validate and extend established phenotypes of mental health.

5.14 Interpreting MAILA

Like many data-driven models, MAILA learns predictive features that do not have immediate verbal interpretations. To explain its performance in terms of intuitive descriptors, we computed 12 established metrics of cursor and touchscreen activity[36] and regressed them onto MAILA's predictions. In participants from the general population, predicted wellbeing was characterized by higher path efficiency, whereas predicted distress was associated with more tortuous trajectories and greater variability in speed (Supplemental Figure S20A).

As an external validation of this feature-mapping approach, we tested whether the behavioral features that MAILA identified as markers of distress and wellbeing differentiated the general population from participants with depression and OCD from the general population. As expected, clinical participants showed elevated distress-related features (p = 1.31×10^{-6}) and reduced wellbeing-related features (p = 4.92×10^{-15}; Supplemental Figure S20B), indicating that MAILA provides a principled way to test whether arbitrary handcrafted features capture meaningful inter-individual differences in mental health.

Between cursor- and touch-based interactions, we observed substantial variability in how hand-crafted metrics related to mental states, including reversals in the direction of association for 37.5% of all features (Supplemental Figure S20A). This instability indicates that intuitive behavioral descriptors struggle to distill consistent or modality-general signatures of mental states. MAILA outperformed models built from handcrafted features across all benchmarks, including lower prediction errors for inter-individual mental health differences in the general population (p $= 1.29 \times 10^{-97}$), higher specificity to the causes of distress and wellbeing (PC1-3, p $= 2.67 \times 10^{-26}$, Supplemental Figure S20C), as well as higher accuracy in classifying depression (AUC $= 0.64$ vs. 0.59) and OCD (AUC $= 0.7$ vs. 0.6).

Handcrafted features require researchers to predefine which aspects of cursor and touchscreen behavior are meaningful, restricting their analysis to a small, theory-driven subset of the signal. By learning directly from the data, MAILA captures a richer and more general representation of mental health. Its predictive accuracy decreased when we reduced the number of group-level clusters, excluded participants from the training set, limited the amount of available test data, or distorted human-computer interactions with increasing levels of random noise (Supplemental Figure S21). These patterns show that behavioral diversity, realistic sample sizes, and longer recordings enhance MAILA's performance, while modest user-side scrambling can substantially reduce unwanted digital profiling.

5.15 Decoding deception and identity from human-computer interaction

Cursor movements and touchscreen gestures underlie nearly all human-computer interactions. Here, we explore two non-mental-health applications of MAILA that have broad implications for trust and accountability in digital environments: lie detection and user identification.

To approximate how well MAILA can detect false self-reports directly from human-computer interaction, we simulated systematically distorted questionnaire profiles by adding Gaussian noise to each participant's true mental-health profile. We then quantified the mismatch between MAILA's predictions and these distorted profiles using the negative Euclidean distance. MAILA's ability to distinguish true from distorted profiles increased monotonically with the magnitude of distortion, rising from an AUC of 0.73 when the added noise had a standard deviation equal to the original item-level variability, to 0.89 when the noise standard deviation was doubled (Supplemental Figure S22). Increasingly inconsistent or fabricated self-reports thus became progressively easier to detect from cursor and touchscreen behavior alone.

To test whether human-computer interactions contain personally identifiable information, we asked whether a support vector classifier could predict participant identity from digital behavior alone. The model was trained on data from 4,000 baseline participants and evaluated on 2,000 follow-up participants. Classification was above chance but weak (accuracy $= 1.75 \pm 0.58\%$, chance level $=$

0.05%, p = 7.51×10^{-4}). With cursor movements as the only available signal, MAILA's ability to identify individuals in large populations was therefore greater than zero, but limited.

In many real-world settings, the user's identity is already known, because they are logged into an account, use a recognized device, or continue a previous session. In these cases, the relevant question is not who is using the device, but whether the same person is still using it. To test whether MAILA can track the continuity of identity over time, we trained a second classifier to determine whether two recordings, one from the baseline dataset, the other from the follow-up dataset, originated from the same or a different participant. The classifier tracked the continuity of identity with an AUC of 0.58 (p < 10^{-6}). Its performance remained unaffected by the delay between recordings (p = 0.85), the degree of change in mental health between sessions (p = 0.62), and MAILA's ability to predict self-reports at follow-up (p = 0.7).

Together, these results suggest that human-computer interactions can be used for lie detection and user identification. The ability to decode information that people may not want to share underscores the urgent need for safeguards against the unintended or unauthorized use of digital biomarkers embedded in cursor and touchscreen activity.

6 Discussion

Overcoming the mental health crisis requires measurements that are scalable, accessible, affordable, and accurate enough to guide decision-making[24,25,28]. Gold-standard tools such as clinical interviews and questionnaires provide high-quality information, but rely on limited availability, shared language, and cultural context. Established biomarkers, including polygenic risk scores[12–14], neuroimaging[15,16], wearable technology[17,18], cognitive tasks[19,20] and digital behaviors[21,22], often encode persistent traits rather than dynamic mental states, depend on active participation, time-consuming protocols, and expensive equipment, generate data that are difficult to store and anonymize, or capture behavior in contexts far removed from everyday life. As a result, current methods occupy a narrow Pareto frontier, where no single tool achieves sufficient accuracy, cost-efficiency, and ecological validity at the same time.

MAILA presents a fundamental advance across multiple roadblocks that have long constrained the assessment of mental health: while decoding psychological distress and wellbeing with state-of-the-art biomarker precision, MAILA scales to billions of devices at zero marginal cost. Its predictions are continuous and dynamic, generalize across populations, contexts, and time, and improve in accuracy when multiple observations are combined. Human-computer interactions may therefore provide a low-burden entry point that identifies and connects individuals at risk with the healthcare system. Once a connection is established, MAILA may enhance the temporal resolution of mental-health monitoring, supporting earlier detection of clinically relevant states[24,25]. When aggregated

at the population level, MAILA provides high-fidelity signals capable of informing early-warning systems, resource allocation, and the design of preventive public-health programs.

Our results indicate that human-computer interactions encode information about mental states that complements and advances verbal descriptions. Most mental health taxonomies have been organized around binary categories, such as depression or anxiety, reflecting a historical link to medical frameworks centered on the presence of pathogenic agents. Tuberculosis, for example, is diagnosed by detecting mycobacterium tuberculosis: either the bacterium is present, confirming the disease, or it is absent, ruling it out. In mental health, no such causal markers exist. Instead, diagnostic categories are shaped by language, history, and culture, grouping together individuals with highly heterogeneous symptoms and treatment responses[14,39,40].

As a data-driven behavioral assessment, MAILA may be sensitive to mental states that traditional language-based assessments obscure[22,57,58]. This may help expand access to care for individuals who struggle to recognize, articulate, or report their experiences, including non-verbal individuals and those facing language barriers[7,8]. Compared with language, human-computer interactions are also less prone to deliberate distortion and may help to reduce biases associated with impression management or social desirability. Discrepancies between MAILA and language-based tools may serve as a consistency check in contexts where self-report reliability is critical. In neuroscience, data-driven predictions from human-computer interactions may provide convergent validity for computational phenotyping[21,22,57]. Because of its scalability, MAILA may help move the biomedical sciences into a data-rich domain, where deep learning is most effective at advancing the study of human cognition, emotion, behavior, and mental health[59].

At the same time, MAILA raises serious ethical considerations around privacy, consent, and autonomy, since it provides sensitive information about an individual's mental state from signals that can be obtained on any digital device. Passive mental health screening, even when well-intentioned, can produce unintended consequences. For example, individuals flagged by automated tools may experience anxiety, stigma, or confusion if results are presented outside of an ecosystem that bridges the last mile toward mental health support[24,25,60].

There is also a danger that predictive mental health technologies will be implemented in contexts that prioritize institutional or economic interests over individual wellbeing. Without strong safeguards, MAILA could be misused in hiring decisions, insurance risk assessments, or unwanted profiling in sectors such as education, immigration, or law enforcement. When used in these contexts, mental health predictions may exacerbate discrimination and reinforce existing inequalities. Preventing such harms requires not only transparent disclosure and opt-in participation but also strong normative and regulatory frameworks that limit use to beneficial contexts.

Predictive models must not be seen as replacements for clinical judgment or personal narratives. Models like MAILA cannot capture the full complexity of lived experience or therapeutic context.

Overreliance on automated indicators risks reducing mental health to a set of quantifiable patterns, potentially marginalizing individuals whose distress does not manifest in ways that are easily measurable. Fairness also demands that these systems be continuously validated across diverse populations and use cases, as behavioral norms, access to technology, and expression of mental states can vary significantly across cultures, languages, age groups, and neurodivergent populations.

To address these challenges, predictive models need to be evaluated against established standards for trustworthy AI. We assessed MAILA in light of the FUTURE-AI framework, a system for assessing the fairness, universality, traceability, usability, robustness, and explainability of AI in healthcare[61]. Supplemental Table S4 summarizes our current alignment with its six guiding principles and identifies priorities for future development. By adopting these recommendations, we aim to advance digital phenotyping in a way that is transparent, inclusive, and ultimately beneficial to those in need of mental health support.

7 Methods

7.1 Resource Availability

7.1.1 Lead Contact

Further information and requests for resources should be directed to and will be fulfilled by the lead contact, Veith Weilnhammer (veith.weilnhammer@gmail.com).

7.1.2 Materials Availability

This study did not generate new unique reagents.

7.1.3 Data and Code Availability

This manuscript was created using the *R Quarto* framework, which integrates all data, code and text within one document. Code and data will become available on https://github.com/veithweilnhammer/maila upon publication.

7.2 The MAILA Dataset

The MAILA dataset is a large-scale dataset that links mental health self-reports with passive digital behavior that can be acquired at zero marginal cost. It comprises ~ 20000 recordings of cursor and touchscreen activity collected between August 2024 and July 2025 (Supplemental Figure S1).

7.2.1 Participants

We recruited 9000 participants through the online research platform Prolific (www.prolific.com). All participants provided informed consent prior to participation. The study was approved by the Institutional Review Board of the University of California, Berkeley, and conducted in accordance with the Declaration of Helsinki. We pre-screened participants for English proficiency and their willingness to answer mental health questions, including sensitive topics such as self-harm or suicidality. We used Prolific's build-in filters to select participants based on hardware (4000 participants on desktop or laptop computers for cursor-based data, 5000 on smartphone or tablets for touch-based data). We applied no additional exclusion criteria and entered all succesfully submitted data to our analysis pipline (Supplemental Figure S1).

The 4000 cursor-based participants came from the general population (no filters applied except the hardware filter). 2000 of them were recruited twice, with a follow-up interval between 5 to 76 days. Participants in the touch-based datasets were recruited once. Of these, 3,500 came from the general population (with no screening beyond the hardware filter), 1,000 self-identified as having a diagnosis of depression, and 500 self-identified as having a diagnosis of OCD. Clinical groups were defined using the "Mental Health Diagnosis Detail" filter and further stratified into four equally sized subgroups based on two dimensions: functional impairment (from the "Mental Illness Daily Impact" filter) and current treatment status ("medication" vs. "none", from the "Mental Health Treatment" filter).

Supplemental Figures S16-17 summarize the demographic composition of our sample. The MAILA dataset includes participants between 18 and 88 years of age, 93 nationalities, ethnicities, 6 types of employment, and a balanced gender distribution (48.45% female, 47.02% male). Demographic distributions were closely aligned between all subsets of the MAILA dataset (see Supplemental Figure S17 for a visualization of age, gender, employment, and ethnicity across subsets).

The recordings had a median duration of of 13.22 minutes. Because the experiment was conducted on the participants' own devices, the interface's sampling rate was determined by the participant's hardware and browser implementation. The median sampling rate was 60Hz for cursor and 60.6Hz for touchscreen activity, with 74.45% of data falling within a ± 5 Hz window around the median. To preserve ecological validity, we did not re-sample or exclude any movement data, requiring all downstream analyses to account for natural variation in hardware at the user end. This design supports the generalizability of the framework to uncontrolled, real-world settings.

7.2.2 Randomized response interface

We developed a custom web-based questionnaire interface in JavaScript that allowed us to collect self-reports while eliciting cursor movements and touchscreen gestures characteristic of everyday

digital activity (Supplemental Figures S7-8). In the interface, a randomized response mapping dissociated the observed human-computer interactions from the semantic content of the responses provided by participants (Supplemental Figures S1 and S9). We used the interface to collect mental health self-reports, survey responses unrelated to mental health, and confidence reports in a gamified decision-making experiment.

At the start of the interface, participants received standardized on-screen instructions and completed a brief training trial. Each trial assessed a single, randomly selected item by guiding participants through a self-paced two-step question-response loop. On the question display, a question appeared in large font at the center of the screen (e.g., "How much are you distressed by feeling blue?"). In the cursor-based interface, participants proceeded by clicking on a circle randomly positioned in one of the screen's four corners. The response display appeared after a short delay (250 ms). The same item was displayed again in smaller font at the top, and a response line appeared at a randomly generated position and orientation. The two endpoints of the line were marked with a green and a blue circle. A reference displayed at the bottom of the screen on every trial explained that the green end corresponded to "Not at all" and the blue end to "Very much".

Response positions were mapped to a continuous scale from 0 to 1, where 0 corresponded to the green end and 1 to the blue end. For instance, if a participant answered "How much are you distressed by feeling blue?" by clicking one-third of the way from green to blue, the recorded response would be 0.33, indicating mild distress. When participants did not click exactly on the response line, the relative distance between the green and blue endpoints was used to compute their response. Clicks were only registered within the diameter spanned by these endpoints. We randomized the position, orientation, and length of the response line on every trial (length range: 15-50% of screen height). As a result, the same response (e.g., "Not at all") could be associated with any absolute screen location. For example, one participant might click in the lower-left quadrant to indicate a distress level of 0.33, while another might click near the center for the exact same distress. Both the question order and the response mappings were independently randomized across participants and items. In the gamified decision-making experiments, the questions were replaced by information about the current outcome of the game (see below for details). Supplemental Figure S9 illustrates how this design ensured that the location of the pointer on the screen was orthogonal to the underlying mental health self-reports.

The touch-based version differed from the cursor-based interface in three ways: first, participants viewed and responded to each item on a single screen; second, participants advanced the questionnaire by pressing a centrally located button at the bottom of the display; third, instead of clicking directly on the response line, participants dragged a response dot, initially placed in one of the four corners, onto the randomly positioned response line. These adjustments accommodated smaller screens and transformed the interaction into a continuous dragging gesture, providing a touchscreen analogue to the continuous cursor movements.

7.2.3 Mental health assessments

We used the interface to assess the participants' mental states using a novel self-report instrument that captured current distress and wellbeing as two complementary domains of mental health[42]. By adapting 67 items (Supplemental Table S1) from established clinical and positive psychology questionnaires[62,63], we mapped mental health across a spectrum of negative and positive states[42]. The distress domain consisted of 53 items grouped into the subdimensions of anxiety, phobic anxiety, somatization, obsession-compulsion, depression, interpersonal sensitivity, psychoticism, paranoid ideation, hostility, and items of clinical relevance. The wellbeing domain comprised 14 items spanning emotional, social, and psychological wellbeing. All items were reworded to fit a digital, continuous-response format (Supplemental Table S1). Rather than using a Likert scale, participants reported their experiences on a continuous scale ranging from 0 ("Not at all") to 1 ("Very much"). Distress and wellbeing items were intermixed and presented in randomized order.

We computed global scores for distress and wellbeing, as well as subdimension scores, by averaging across the respective items. This yielded a mental health matrix $Y^{N \times Q}$, where N is the number of participants and Q the number of mental health features (items, subdimensions, global scores). Each row in this matrix represents an individual's location in a high-dimensional space of mental health, without reference to clinical thresholds or normative cutoffs.

7.2.3.1 Psychometric properties

We evaluated the psychometric properties of the questionnaire interface in terms of internal consistency, item structure, and test-retest reliability. We first assessed the reliability of of our mental health assessments using Cronbach's α, which was high for both distress (0.96) and wellbeing (0.86), indicating strong coherence among items within each scale. The average correlation between each item and the corresponding global score fell within the expected range of well-functioning items (distress: 0.54 ± 0.01; wellbeing: 0.51 ± 0.06). Mean inter-item correlations confirmed that the items within each domain were related but not redundant (distress: $0.31 \pm 3 \times 10^{-3}$; wellbeing: 0.3 ± 0.02). The subdimensions of distress and wellbeing each captured coherent and interpretable variance, as reflected by their correlations with the respective global scores, which ranged from 0.77 to 0.89.

To assess temporal stability, we correlated baseline and follow-up responses for intervals that ranged from 5 to 76 days. For follow-up intervals shorten than a week, test-retest correlations were high for overall distress (0.88) and wellbeing (0.84). Test-retest correlations gradually declined to 0.69 after eight weeks. To evaluate sensitivity to change, we computed the absolute difference between test and retest responses and regressed this value against the time interval between assessments. A linear mixed-effects model with random intercepts for each item revealed that changes in self-reported mental health increased significantly with longer follow-up intervals ($p = 7.7 \times 10^{-3}$).

Together, these validation results indicate that the questionnaire interface provided stable, consistent, and interpretable estimates of mental health, while remaining sensitive to real-world variation in psychological state over time.

7.2.3.2 Principal component analyses

To test whether human-computer interactions encode differentiated information about the content of mental health, rather than only a global distress factor, we decomposed the mental health matrix $Y^{N \times Q}$ into orthogonal principal components (PCs). Each PC defined an independent axis of variation in self-reported mental health across participants. We trained independent models to predict PC scores from cursor and touchscreen data, and evaluated their performance across baseline, follow-up, survey, game, and touch datasets.

7.2.4 Generalization experiments

The response interface dissociated the content of self-reported mental health (i.e., to what degree a participant endorsed a specific item of the assessment) from cursor movements and touchscreen activity recorded during questionnaire completion. This calibration procedure minimized the amount of data required to link motor behavior to mental health. At the same time, it recorded human-computer interactions in the cognitive context of self-reflection about mental health. Whether this context constrains or enhances generalization remains an open question: on the one hand, cursor and touch dynamics elicited during introspection may differ from those in everyday digital activity; on the other hand, activating a mental health context may amplify behavioral signatures that are diagnostic across settings.

To assess the robustness of models calibrated in this way, we evaluated MAILA on independent datasets that varied in content, task structure, and cognitive context. Within the MAILA dataset, the generalization structure was nested: all cursor-based recording originated from a baseline assessment of 4,000 participants from the general population. Of these, 2,000 completed a follow-up session. Within this follow-up group, two additional subsets of 600 participants each completed (i) a non-psychological survey and (ii) a gamified decision-making task. We further tested frozen MAILA models on an external public dataset of open-ended human-computer interactions, including web browsing, file management, office applications, coding, and entertainment, with multiple sessions per participant[41].

7.2.4.1 Non-psychological survey

We recorded cursor movements while participants answered general survey questions unrelated to mental health (Supplemental Table S2). The task interface and randomized response mapping were

identical to the calibration paradigm, isolating the effect of content while keeping the motor context constant.

7.2.4.2 Gamified decision-making task

Participants completed a gamified version of the beads task, a probabilistic reasoning paradigm used as a transdiagnostic marker of altered decision-making in computational psychiatry[46]. At the beginning of each of six rounds, one of two jars was selected at random: a "blue jar" containing mostly blue beads and some green, or a "green jar" containing mostly green beads and some blue. The majority-minority ratio (e.g., 75:25) was displayed, but the identity of the majority color was hidden. Each round consisted of eight sequential bead draws. After each draw, participants viewed the bead and an updated count of blue and green draws in the current round. They then indicated their certainty about which jar the beads were coming from on a continuous scale ranging from "100% certain: green jar" to "100% certain: blue jar." The report interface was identical to the questionnaire interface outlined above. Across the six rounds, participants observed 48 bead draws and provided 48 certainty judgments. Cursor movements were recorded throughout the entire game. With the same interface logic and randomized response mapping as the calibration dataset, this task extended MAILA from survey completion to a novel interactive context involving sequential evidence accumulation, probabilistic reasoning, and gamification.

7.2.4.3 Naturalistic cursor movements

We applied MAILA, without retraining, to naturalistic cursor movements from the Boğaziçi dataset[41], downloaded 07/01/2024. This dataset comprises continuous recordings of cursor activity from 24 individuals, totaling approximately 2,550 hours of active computer use. Cursor movements were logged via a custom Python application that continuously captured mouse actions, timestamps, window titles, and contextual details of user interactions. Following the authors' protocol, we analyzed data from 19 participants who contributed sufficient training and testing data.

7.3 MAILA

To model the relationship between human-computer interaction and mental states, we developed MAILA, a machine learning framework that transforms raw cursor and touchscreen activity into a data-driven movement feature matrix $X^{N \times C}$ (N = number of participants, C = number of movement features) and predicts the associated self-report matrix $Y^{N \times Q}$ (Q = number of mental health features).

7.3.1 Inputs

We segmented screen-normalized cursor and touchscreen positions $(a_t, b_t) \in [0,1]^2$ with a sliding window of fixed length $L = 100$ and stride $\delta = 10$ samples. For each participant n, this yields S_n segments $X_i^{L \times 2}$:

$$X_i = \begin{bmatrix} a_{i,1} & b_{i,1} \\ \vdots & \vdots \\ a_{i,L} & b_{i,L} \end{bmatrix}$$

7.3.2 Autoencoder

Each movement segment $X_i^{L \times 2}$, represented as a sequence of 2D cursor positions $\{x_{i,t}\}_{t=1}^{L}$, is passed through a long short-term memory (LSTM) autoencoder to obtain a compact latent representation of movement dynamics.

Encoder. The encoder LSTM (hidden dimension $H = 64$) processes the input segment X_i as a sequence of 2D cursor positions and outputs a hidden state at each time step. The final hidden state h_L summarizes the full trajectory and is linearly projected into a latent embedding of size $E = 50$:

$$h_t = \text{LSTM}_{\text{enc}}(x_{i,t}, h_{t-1}), \qquad z_i^{1 \times E} = \sigma(W_z h_L + b_z).$$

Here, $x_{i,t} \in [0,1]^2$ is the 2D cursor position for segment i at time step t, h_t is the recurrent hidden state of the encoder at time t, and h_L is the final hidden state summarizing the full trajectory. The latent vector $z_i^{1 \times E}$ is obtained by projecting h_L through a linear layer (W_z, b_z) followed by a sigmoid activation that bounds each latent unit to $(0,1)$ for interpretability.

Decoder. To reconstruct the input sequence, the latent code $z_i^{1 \times E}$ is repeated across all time steps to form the matrix $Z_i^{L \times E}$:

$$Z_i = \begin{bmatrix} z_i \\ \vdots \\ z_i \end{bmatrix}, \qquad Z_i^{L \times E}.$$

This repeated latent sequence is then passed through a second LSTM (hidden dimension $H = 64$), followed by a linear output layer and a sigmoid activation that maps hidden states back to normalized 2D cursor coordinates:

$$\hat{x}_{i,1:L} = \sigma(W_o \, \text{LSTM}_{\text{dec}}(Z_i) + b_o), \qquad \hat{x}_{i,t} \in [0,1]^2.$$

The same architecture allows extraction of latent features through the encoder or reconstruction from any latent vector using the decoder. The sigmoid output ensures that all predicted coordinates remain within the normalized input range.

We trained the autoencoder on an independent public cursor tracking dataset[41] for 100 epochs, using a batch size of 128 and a learning rate of 0.001. Training minimized the mean squared reconstruction error:

$$\mathcal{L}_{\text{recon}} = \frac{1}{L} \sum_{t=1}^{L} \|x_{i,t} - \hat{x}_{i,t}\|^2.$$

The final validation loss after training was 0.000052. Supplemental Figure S3 shows examples of original and reconstructed cursor movements from the MAILA dataset.

7.3.3 Movement feature representation

MAILA pools all segment embeddings $z_i^{1 \times E}$ across participants and clusters them using K-means into $C = 500$ discrete clusters:

$$\mathcal{C} = \{c_1, \ldots, c_C\}, \qquad z_i \mapsto \arg\min_j \|z_i - c_j\|.$$

Each cluster represents a recurring movement motif as captured in the latent space of the autoencoder at the group level. For each participant n, MAILA computes the proportion of their S_n segments assigned to each cluster, resulting in a movement feature vector $m_n^{1 \times C} \in [0,1]^C$ that sums to 1:

$$m_{n,j} = \frac{1}{S_n} \sum_{i=1}^{S_n} \mathbb{I}[\, z_i \in \mathcal{C}_j \,].$$

Stacking these feature vectors yields the movement matrix $X^{N \times C}$, where each row describes a participant's distribution over clusters of human-computer interaction (Figure 2B-C). For model evaluation, clustering was fit on the training data only. The resulting centroids were held fixed when assigning cluster memberships in test data.

7.3.4 Prediction of mental health

MAILA uses the movement feature matrix $\mathrm{X}^{N \times C}$ to predict participants' self-reported mental health features from the matrix $\mathrm{Y}^{N \times Q}$. MAILA approximates the decoding function $f(X; \delta)$: $X \to Y$, which maps cursor or touchscreen activity to latent mental states as indicated by the questionnaire responses in $\mathrm{Y}^{N \times Q}$.

To implement $f(X; \delta)$, we trained one support vector regressor (SVR, radial basis function kernel, $C = 1.0$, $\epsilon = 0.1$, automatic kernel scaling) per mental-health feature:

$$\hat{y}_{n,q} = f_q(x_n; \delta_q) = \mathrm{SVR}_q(x_n), \qquad q = 1, \ldots, Q.$$

Here, δ_q denotes the SVR parameters for feature q, and x_n is the movement feature vector of participant n. We evaluated model performance in two complementary settings. First, we assessed predictive accuracy using 5-fold cross-validation with non-overlapping participant IDs, ensuring that all data from a given participant appeared in a single fold. Second, to assess generalizability across time and context, we trained models on the full calibration dataset and evaluated them on independent follow-up and generalization datasets. Clustering was fit on the calibration data only, and the resulting centroids were held fixed when assigning cluster memberships in test datasets.

After training independent SVR models for each target item, we averaged held-out predictions and targets by participant and dimension (depression, anxiety, phobic anxiety, somatization, interpersonal sensitivity, psychoticism, paranoia, hostility, clinically relevant features, emotional, psychological, and social wellbeing) to obtain per-participant dimensional estimates, including overall distress (mean across all distress dimensions) and overall wellbeing (mean across all wellbeing dimensions).

Model performance was quantified using three complementary metrics. First, Spearman's rank correlation coefficient (R) captured the rank-order correspondence between predicted and observed values. Second, the normalized root mean squared error (e) measured absolute deviations while accounting for the outcome's scale, defined as the square root of the mean squared error normalized by the range of the outcome variable. Third, the area under the receiver operating characteristic curve (AUC) assessed discriminative performance. To compute AUC, continuous SVR outputs were treated as ranking scores and ground-truth responses were binarized at the 10th, 25th, 50th, 75th, and 90th percentiles of the empirical outcome distribution. This procedure enabled evaluation of model sensitivity across multiple cut-offs along the mental-health continuum. Together, these metrics provide complementary assessments of prediction accuracy, error magnitude, and classification performance.

To compare the multivariate structure of mental health across ground-truth scores and MAILA's predictions, we computed dimension-wise correlation matrices, converted them into dissimilarities

(D = 1 - R), and embedded them with t-SNE (perplexity = 6). We display the first two dimensions for visualization. Raw correlation matrices are displayed in Supplemental Figure S10.

7.3.5 Internal reliability

To assess the internal reliability of MAILA, we quantified the consistency of its predictions across two independent subsets of human-computer interaction data from the same individuals. For each participant, we randomly divided the LSTM-derived movement embeddings into two non-overlapping halves (50/50 splits), with split boundaries randomized independently to avoid systematic alignment across participants. The clustering step was performed on one split only, and the resulting cluster centroids were then transferred to the other split to construct its corresponding feature matrix. This yielded two independent feature matrices $X_{1/2}^{N \times C}$, each associated with the same mental health response matrix $Y^{N \times Q}$.

For each mental-health item, we trained independent MAILA models on the self-reports from one split and applied them to the opposite split. The procedure was then repeated in the reverse direction, resulting in two independent prediction vectors per participant. The correlation between these cross-split predictions served as an estimate of model reliability relative to a null distribution generated by random permutation of one prediction vector.

7.3.6 Prediction of changes in mental health

To evaluate whether the human-computer interactions track within-person changes in mental health over time, we trained MAILA on the baseline features $X_{baseline}$ with the corresponding targets $y_{baseline}$, and applied the frozen models to the baseline and follow-up features $X_{followup}$, the features extracted from behavior during the non-mental health survey X_{survey}, or the gamified decision-making experiment X_{game}. Centroids were defined from baseline data alone and applied to the follow-up embeddings. We correlated the difference between the ground-truth reports,

$$y_{followup} - y_{baseline}$$

with the predicted difference,

$$\hat{y}_{followup/survey/game} - \hat{y}_{baseline}$$

Here, $\hat{y}_{baseline}$ was obtained from a model that had access to that participant's baseline data, reflecting the clinical situation in which a ground-truth rating is available at baseline while follow-up data remain unseen. In a control analysis, we computed $\hat{y}_{baseline}$ using 5-fold cross-validation,

ensuring that each participant's baseline data were also held out from model training. We used AUC to assess MAILA's ability to discriminate between increased versus decreased scores at follow-up relative to baseline.

7.3.7 Demographics

To test whether MAILA's predictive performance differed across demographic groups, we grouped participants by age (binned by decade), gender, nationality, ethnicity, employment/student status, and country of residence. For each demographic variable, we fit a linear mixed-effects model with prediction error as the outcome, the demographic category as a fixed effect, and participant ID as a random intercept. We applied Type III ANOVAs to evaluate the main effect of each demographic factor while accounting for unbalanced group sizes.

7.3.8 Group-level mental health

To evaluate whether MAILA can support population-level mental health monitoring, we tested its ability to reproduce established demographic and temporal patterns in mental health from human-computer interactions alone. For each participant and mental-health dimension, ground-truth questionnaire scores and MAILA predictions were z-scored before aggregation. We then computed group-level means by binning participants according to age (years), employment status (full-time, part-time, retired, job seeking), gender, and local time-of-day (hour). For each grouping variable, we quantified alignment between MAILA and ground truth by computing Spearman's rank correlations between true and predicted group-level means across bins.

To assess whether these temporal effects generalized to within-participant patterns in open-ended human-computer interaction, we applied frozen models to an external dataset[41] and aggregated MAILA predictions and ground-truth scores by local hour within individuals.

To estimate how MAILA's prediction errors translate into performance in larger groups, we conducted simulations of population-level monitoring under realistic noise levels (Supplemental Figure S18). We first generated synthetic "true" mental-health scores by sampling from a Gaussian distribution with fixed mean and variance. We then created corresponding "predicted" scores by adding noise such that the normalized root mean squared error between true and predicted values matched the range observed for MAILA in our empirical analyses. For each simulated population and group size, we computed group-level means and variances for both the true and predicted scores, and quantified alignment by correlating the true group-level statistics with their predicted counterparts.

7.3.9 Clinical generalization

To evaluate MAILA in clinical populations, we analyzed touchscreen data from 1,000 participants who self-identified with a diagnosis of depression and 500 with a diagnosis of OCD. The clinical groups provided information on functional impairment and psychiatric medication status for stratification. We trained support vector classifiers (SVC, radial basis function kernel, C = 1.0, ϵ = 0.1, automatic kernel scaling) to discriminate clinical from general-population participants based on their movement features and quantified performance with AUC.

To assess sensitivity to inter-individual differences within clinical groups, we trained models on the full sample (including both general and clinical participants) using 5-fold cross-validation and computed Spearman's rank correlations between ground truth and predicted scores within the depression and OCD groups. We applied linear mixed-effects models to test whether MAILA predicted mental health profiles aligned with expected group characteristics, that is, higher depression scores among participants who self-identified with a history of depression and higher OCD symptoms among those who self-identified with a history of OCD.

7.3.10 Decoding belief instability from human-computer interaction

To derive a behavioral marker of belief instability, we analyzed trial-by-trial confidence updates from the gamified decision-making task. In each round, participants observed eight sequential draws from one of two jars with known bead ratios but unknown majority color. After each draw, they provided a confidence-weighted belief about which jar generated the sequence. We quantified the signed entropy of belief updates as:

$$\Delta b_t = b_t - b_{t-1}, \qquad H_t = -|\Delta b_t| \log |\Delta b_t|$$

where $b_t \in [0,1]$ denotes the belief at trial t. H_t captures both the magnitude and the direction of belief revisions: large, variable updates produce high signed entropy (reflecting reactive or unstable updating), whereas small, consistent updates produce low signed entropy (reflecting rigid or stable updating). For each participant, we averaged H_t across all rounds to obtain a single belief-instability score.

To examine how belief instability relates to mental health, we correlated the signed-entropy scores with self-reported mental-health dimensions, and repeated the same analysis using MAILA's predicted mental-health scores (derived from cursor movements in held-out participants). Alignment between ground-truth and MAILA-derived mental-health correlations was quantified using Spearman's R, computed by correlating the vector of true correlations with the corresponding vector obtained from predictions across mental-health dimensions.

To test whether belief instability could be predicted directly from human-computer interaction, we trained SVR models under 5-fold cross-validation using three feature sets: (i) MAILA's movement feature matrix $X^{N \times C}$, (ii) the self-report matrix $Y^{N \times Q}$, and (iii) the concatenation $[X; Y]$. For each fold, the model predicted the signed-entropy score for unseen participants, and predictive accuracy was quantified using Spearman's R and the normalized root mean squared error (e).

7.3.11 Human-interpretable features

For each participant, we computed a set of human-interpretable movement features F, including average speed, kurtosis, jerk, movement area, relative idle time, path efficiency, turn angle, tortuosity, turn rate relative to distance, horizontal-vertical bias, speed entropy, and speed fluctuation rate. We estimated linear regression coefficients by regressing each z-scored feature independently onto the first three principal components (PC1-PC3) of mental health, using both the true and predicted PC scores derived from MAILA. This provided an interpretable mapping between motor features, MAILA's predictions, and their ground truth.

To directly compare the predictive utility of handcrafted features against MAILA, we replaced the original feature matrix $X^{N \times C}$ with the handcrafted feature matrix $X'^{N \times F}$, where F is the number of human-interpretable features. We then trained SVR to map from X' to the mental health matrix $Y^{N \times Q}$. By applying the cross-validation procedures as outlined above, we assessed how well handcrafted features could approximate the participants' mental health self-reports, and compared their performance against MAILA's $X^{N \times C}$ matrix in terms of e, R, and AUC.

7.3.12 Information loss

We assessed MAILA's robustness to information loss by training and testing support vector regression models to predict scores on each dimensions of distress and wellbeing while implementing four types of data degradation: (1) noise injection, where a proportion of the low-level movement embeddings of the test sets were interpolated with random values sampled from a uniform distribution; (2) within-participant drop-out, where a contiguous segment of each participant's was deleted in the test datasets, simulating shorter recordings while preserving temporal coherence; (3) training set reduction, where we progressively decreased the number of unique participants used to train the model; and (4) cluster reduction, where we gradually reduced the number of recurring patterns used to construct the movement feature matrix $X^{N \times C}$ (Supplemental Figure S21).

Corruption levels were increased in increments from 0% to 100%. At each corruption level, we evaluated model performance using the correlation coefficient between predicted and ground-truth scores, separately for cursor-based interface data, touch-based interface data, and touch-based drawing data.

7.3.13 Deception

To test whether human-computer interactions can identify inconsistent or false self-reports, we quantified how reliably mismatches between verbal reports and behavioural data could be detected as a function of the magnitude of distortion applied to otherwise valid mental-health profiles (Supplemental Figure S22). P_i and T_i denote participant i's MAILA-predicted and true mental-health profiles (z-scored). For each distortion level σ (in SD units), we created distorted profiles by adding independent Gaussian noise to each dimension,

$$T_i^{\text{fake}} = T_i + \varepsilon_i, \qquad \varepsilon_i \sim \mathcal{N}(0, \sigma^2),$$

and clipped each dimension to the empirical range $[z_{\min,d}, z_{\max,d}]$ observed in T. For each σ and repetition, we computed mismatch scores as the negative Euclidean distance between predictions and profiles,

$$s_i = -\|P_i - T_i\|_2, \qquad s_i^{\text{fake}} = -\|P_i - T_i^{\text{fake}}\|_2,$$

and used these to compute the AUC for discriminating true from distorted profiles. We repeated this procedure 1,000 times per distortion level and report the mean AUC and 95% confidence intervals across repetitions as a function of σ.

7.3.14 Identification analyses

To test whether human-computer interactions carry personally identifiable information, we trained a SVC to predict the identity of 4000 participants based on their movement feature matrix $X_1^{N \times C}$ from the baseline cursor-tracking dataset. Movement features at follow-up, $X_2^{N \times C}$, were derived using K-means clustering defined exclusively on segment embeddings from X_1. This fixed clustering ensured that no information from the follow-up dataset influenced feature construction. To assess statistical significance, we retrained the SVC on randomly permuted training labels over 10^6 iterations and compared the empirical results to the resulting null distribution.

To assess whether cursor movements contain sufficient information to track the continuity of identity across time, we trained a second SVC to distinguish whether two feature vectors X_1 and X_2 belonged to the same or to different individuals. For each participant in the follow-up dataset, we paired their movement features with those from the same individual in the training set (positive pairs), as well as with features from randomly selected individuals (negative pairs). Each pair was represented by the concatenated movement features from the two sessions. The classifier was trained using 5-fold stratified cross-validation and evaluated based on its ability to discriminate between positive and negative pairs. Statistical significance was assessed using a permutation test with 10^6 iterations.

We used logistic regression to examine whether classifier performance was influenced by the time elapsed between recordings or by the precision of the mental health predictions at follow-up,

7.4 Summary Statistics and Inference
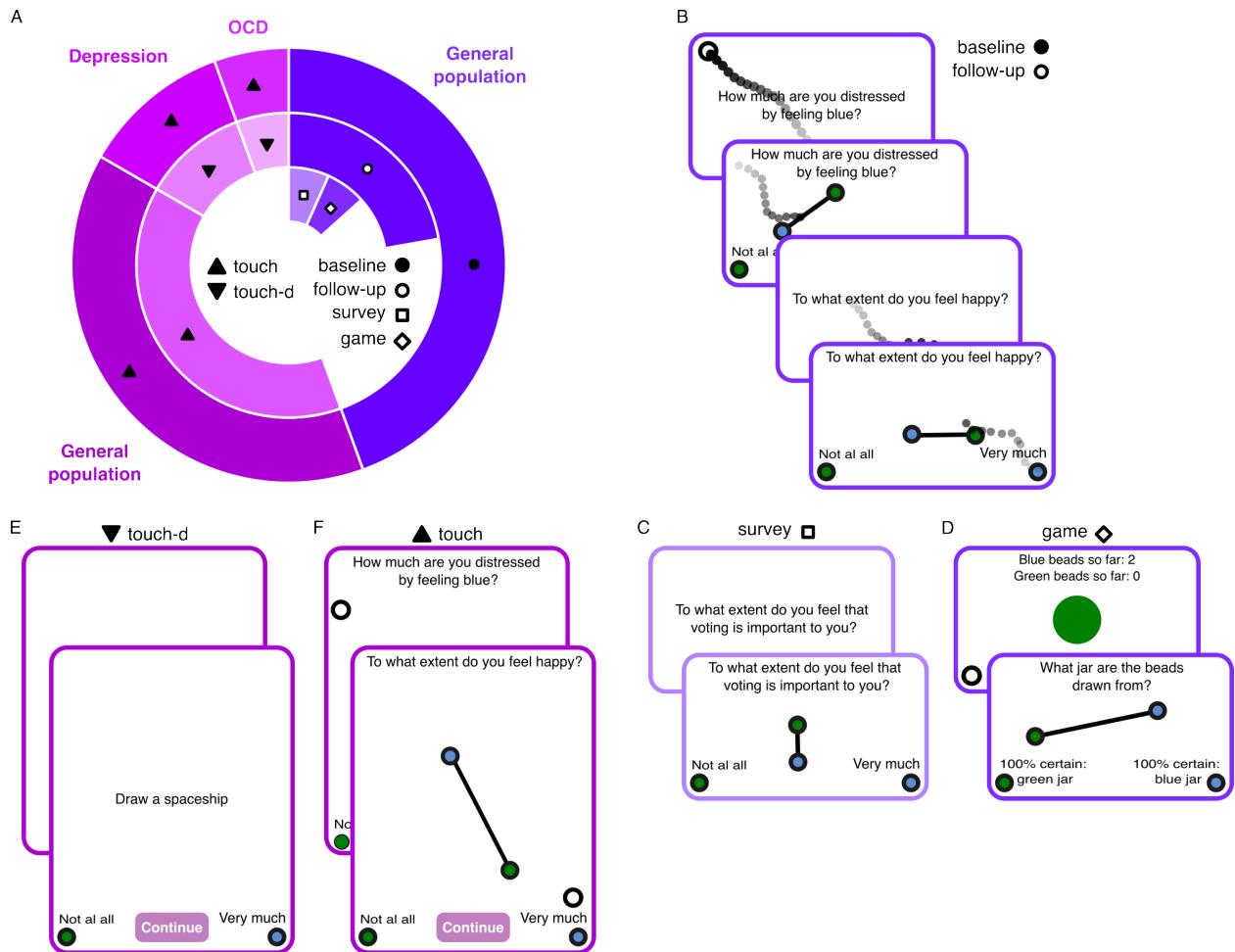
7.4.1 Support vector regression

To assess statistical significance, we compared observed model performance to null distributions obtained from 10^6 iterations with randomly shuffled target values. Permutation-based p-values quantify the proportion of permuted scores that were equal to or more extreme than the empirical metric. Unless otherwise indicated, we used t- and F-test statistics for group-level inferences. Linear mixed-effects models (LMEs) were applied in analyses where repeated measurements or hierarchical data structures required explicit modeling of dependency.

8 Acknowledgements

9 Supplementary Information

9.1 Supplemental Figure S1

Supplemental Figure S1. The MAILA dataset.

A. Dataset structure. We evaluated MAILA across structured and open-ended digital behaviour, repeated assessments, and participants with and without a self-reported mental-health diagnosis. Cursor movements were recorded from 4,000 general-population participants who completed a structured questionnaire interface designed to mimic everyday computer use ("baseline," purple section of the outer ring). Of these, 2,000 completed a follow-up session ("follow-up," purple section of the middle ring). Within this follow-up cohort, 600 also completed a non-mental-health survey ("survey") and 600 performed an interactive decision-making game ("game," inner-ring subsections). Separately, touchscreen activity was recorded from 5,000 participants who completed a creative drawing task ("touch-d") and a mobile version of the questionnaire interface ("touch," pink sections of the outer and middle rings). The touchscreen cohort comprised 3,500 general-population participants, 1,000 individuals who self-identified as having a diagnosis of depression, and 500 who

reported living with obsessive-compulsive disorder (OCD, pink subsection of the outer and middle rings).

B. Mental-health questionnaire. Participants reported on their current mental health using a randomized-response interface that dissociated cursor trajectories from the semantic content of their answers. Each trial began with a question screen; participants advanced by clicking a circle that appeared in one of the four screen corners at random. On the subsequent response screen, the same item reappeared and participants indicated their answer by clicking a randomly positioned and randomly oriented response line. Cursor trajectories (shown as grayscale traces with increasing opacity over time) were logged continuously but never displayed to participants.
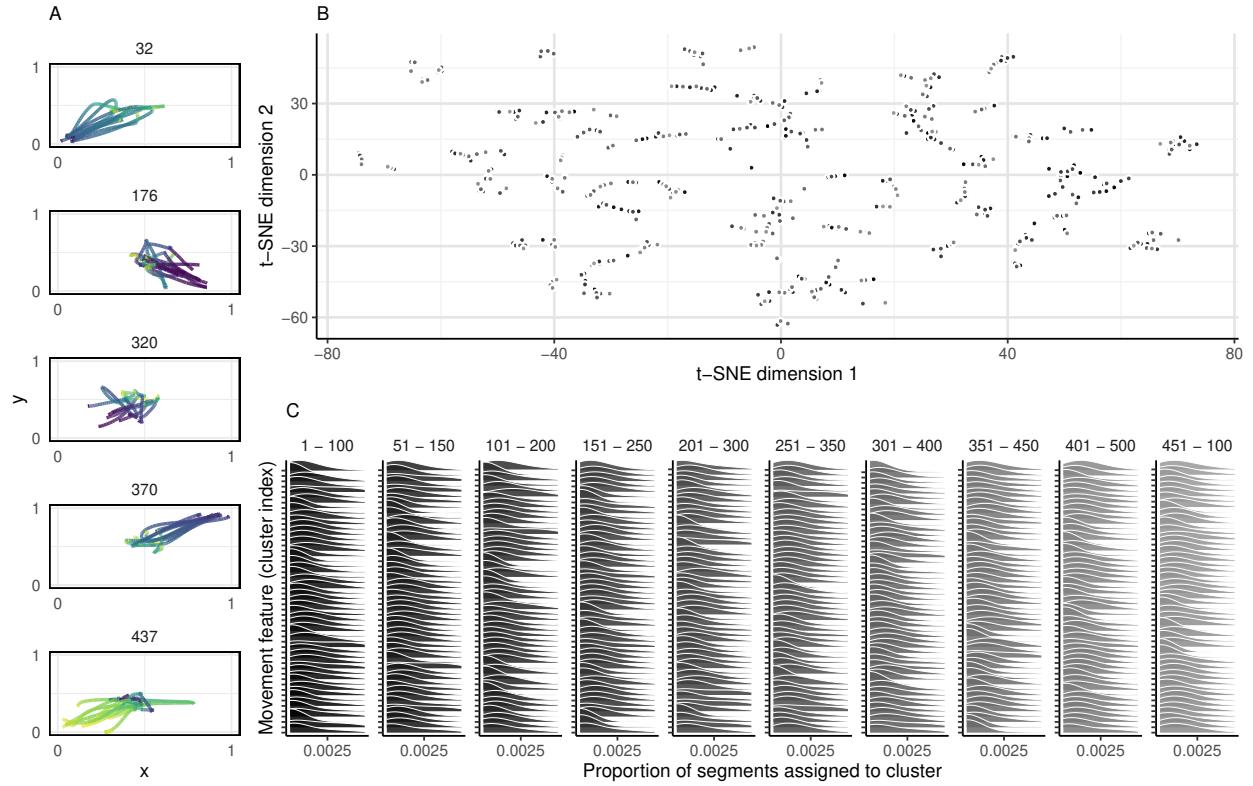
C. Mental-health questionnaire. Participants answered general survey questions unrelated to mental health using the same interface and randomized-response mapping as in **B**, isolating the effect of semantic content while holding the motor context constant.

D. Gamified decision-making task (beads task). Participants answered general survey questions unrelated to mental health using the same interface and randomized-response mapping as in **B**, isolating the effect of semantic content while holding the motor context constant.

E. Touchscreen drawing. Participants produced prompted, freehand drawings on their touchscreen device. Each prompt disappeared at first touch, and participants advanced by pressing a "Continue" button at the bottom center of the screen.

F. Touchscreen interface. After the drawing task, participants completed a touchscreen version of the randomized-response interface from **B**, adapted for vertical screens. Instead of clicking, participants dragged a response dot, initially placed in one of the four corners at random, onto the randomly positioned response line.
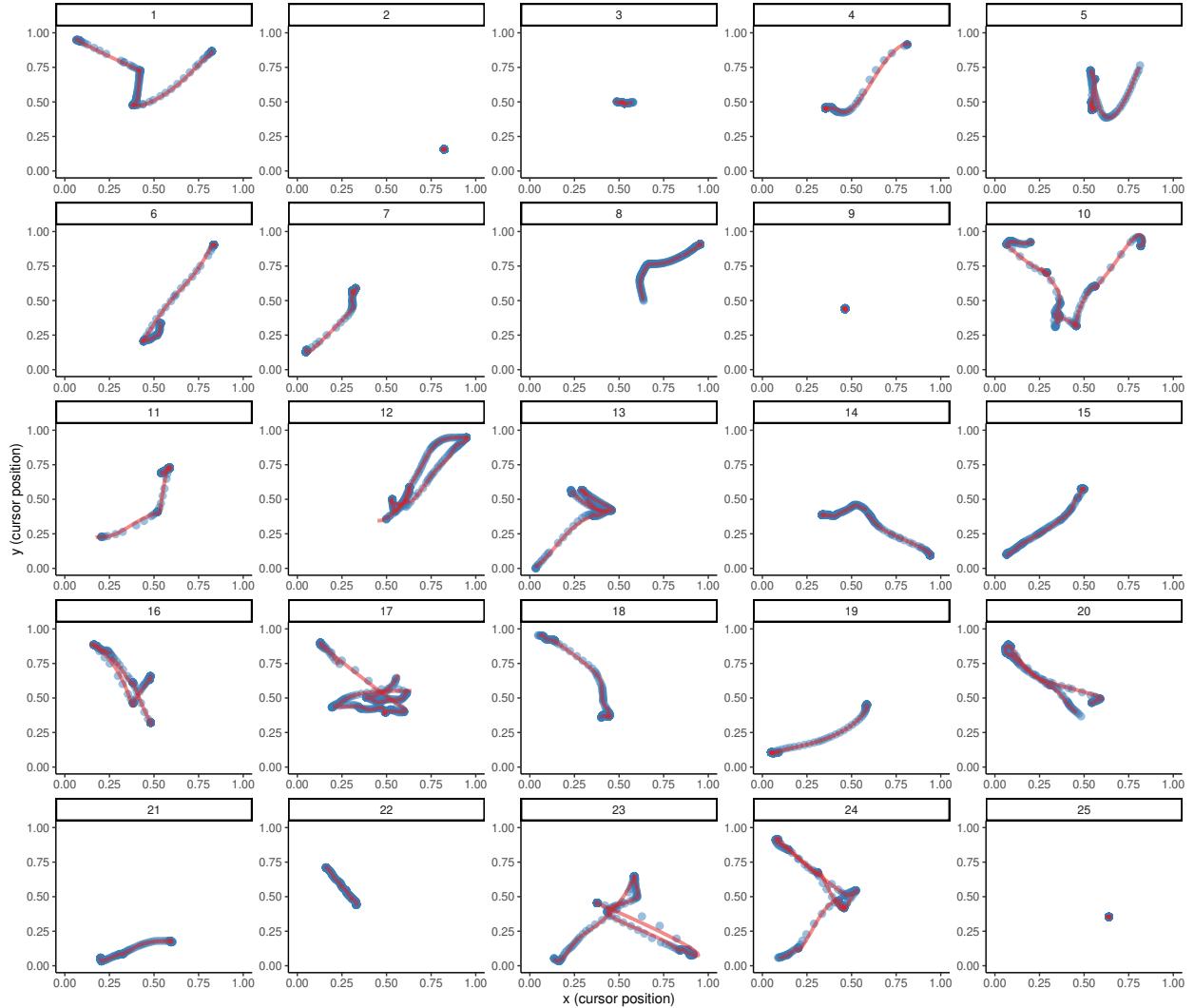
9.2 Supplemental Figure S2

Supplemental Figure S2. The space of human-computer interaction.

A. Clustered cursor movements. MAILA transform segments of cursor and touchscreen movement into low-dimensional embeddings. By clustering the embeddings across participants, MAILA discovers recurring patterns of human-computer interaction at the group-level. Here, we show five exemplary clusters derived from cursor movement (time progresses from darker to lighter colors; see Supplemental Figure S3 for examples from all 500 cursor clusters). While qualitatively similar patterns emerge for touchscreen data (not shown here), the specific clusters differ depending on the behavioral context of the interaction.

B. Structure of cursor movement features. Each dot represents a cursor movement cluster, positioned in t-SNE space based on its similarity to other clusters.
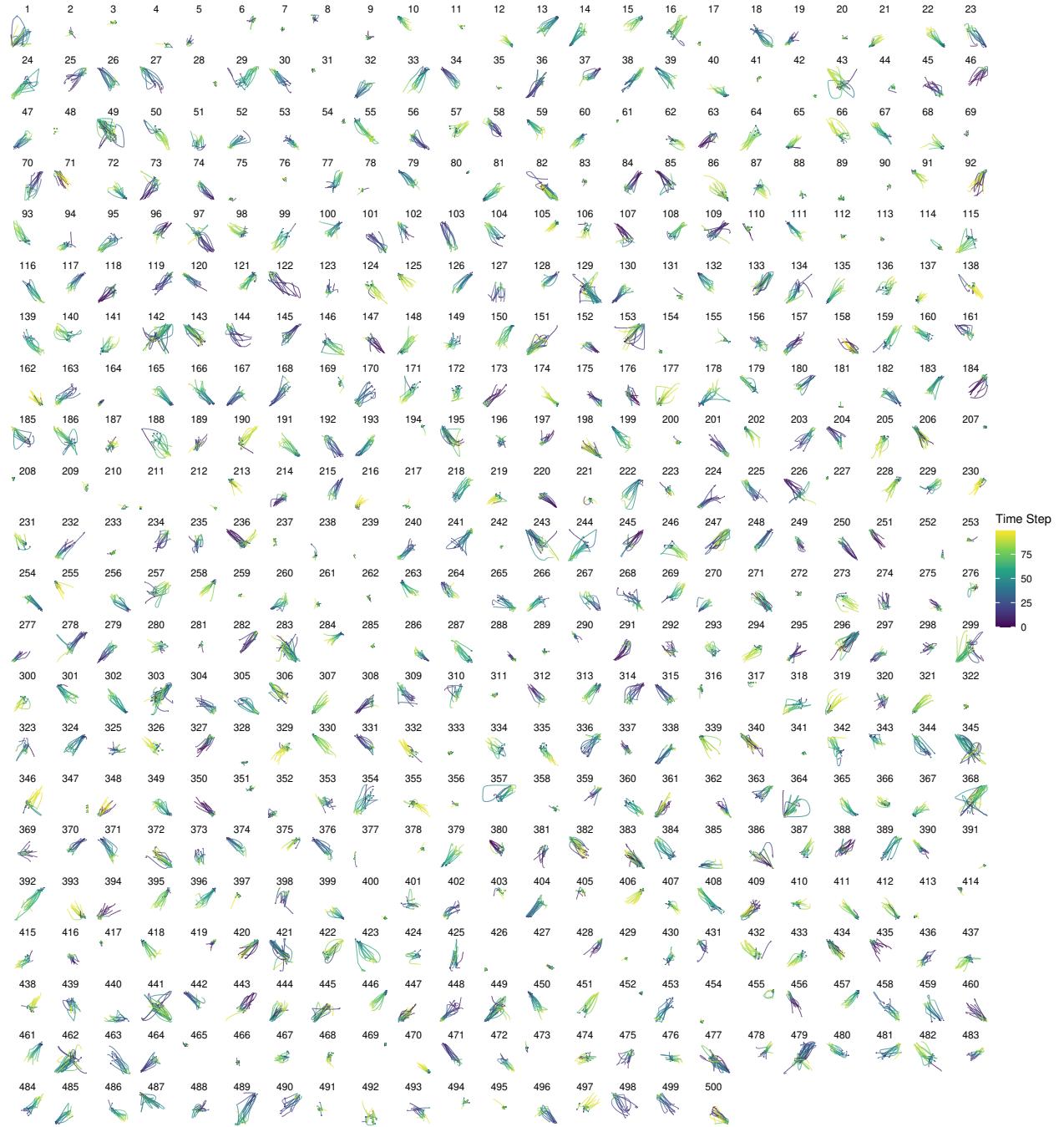
C. The cursor movement feature matrix. MAILA computes the per-participant (N) fraction of segments assigned to C = 500 clusters, resulting in a $X^{N \times C}$ movement feature matrix. Each row encodes a participant's location in a space of cursor movement patterns, derived from raw trajectories that are segmented, autoencoded, and assigned to discrete clusters defined at the group-level. Plots show the distribution of features across participants for the 500 cursor movement clusters. The shape of the clusters distributions are qualitatively similar for touchscreen interactions (not shown here).

41

9.3 Supplemental Figure S3

Supplemental Figure S3. Autoencoded cursor movements. Each subplot represents one of 25 example sequences of cursor movements from our experiment, with original cursor positions shown in blue and reconstructed trajectories in red. MAILA's LSTM autoencoder was trained on human-computer interaction from a public dataset of naturalistic computer use[41], frozen, and applied to the MAILA dataset, where it achieved a average reconstruction loss of 7.66×10^{-5} (relative to the participant's screen resolution). This confirms that MAILA captured and reconstructed human-computer interaction with high precision.
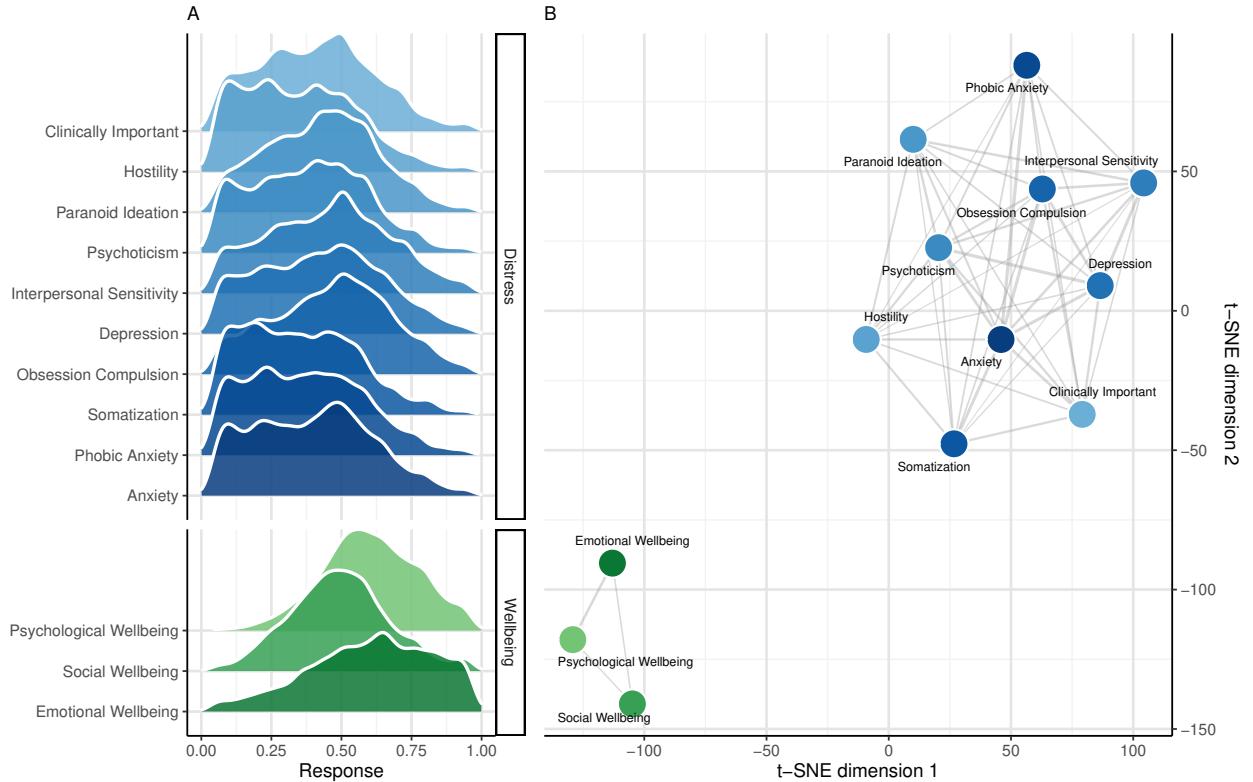
9.4 Supplemental Figure S4

Supplemental Figure S4. Clusters of cursor movement. Each subplot represents 10 example trajectories from one of the $C = 500$ cursor movement clusters. Lighter colors indicate later time steps within each sequence. Each cluster represents one distinct cursor movement motif observed in our experiment. For each of the N participants, we computed the fraction of embeddings assigned to each cluster C. This results in a participant-by-cluster $X^{N \times C}$ movement feature matrix. The

clusters are assigned automatically and without any hypotheses about what movement features are meaningful for the downstream task of predicting mental states from human-computer interaction. Different movement clusters emerge when MAILA is calibrated to structured cursor movement (shown here), structured touchscreen activity (not shown here), or free-form touchscreen activity (not shown here).
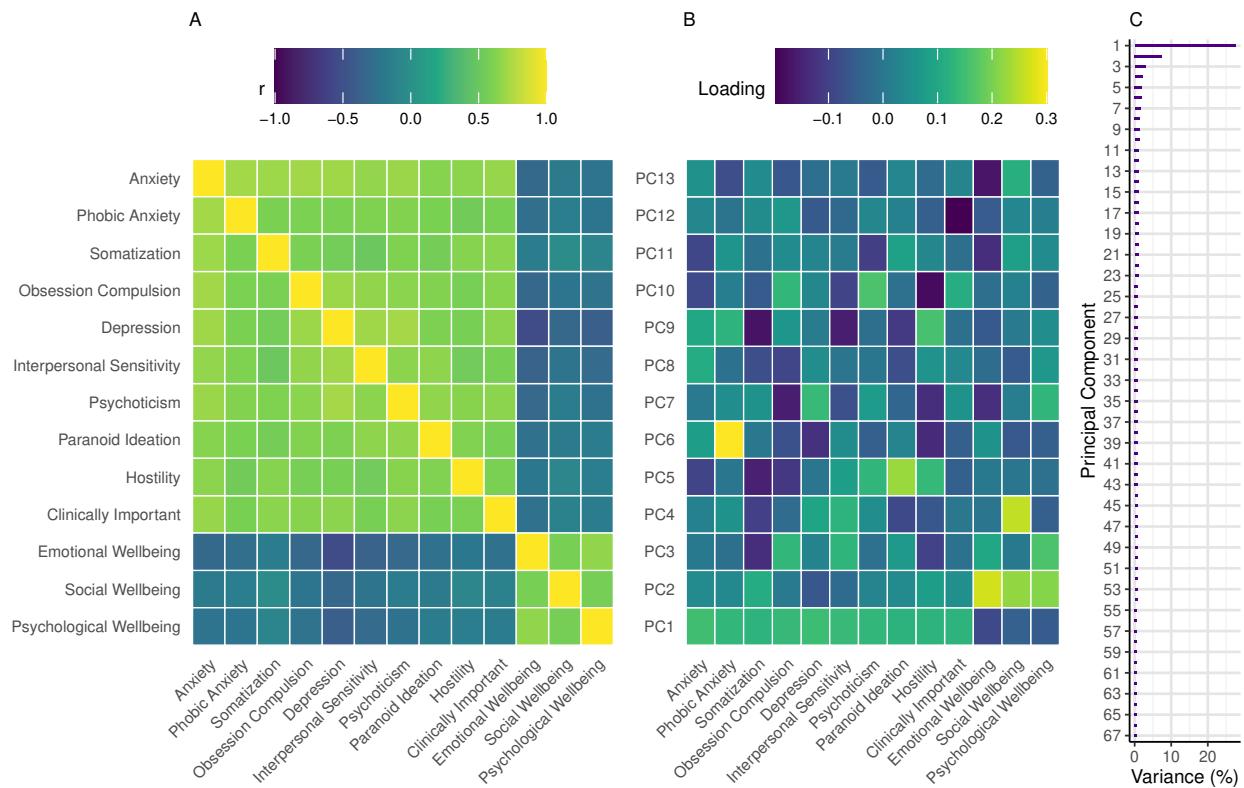
9.5 Supplemental Figure S5

Supplemental Figure S5. The space of mental health.

A. The mental health matrix. The mental health matrix $Y^{N \times Q}$ comprises self-reports for 67 questionnaire items, each belonging to an overarching dimension of distress and wellbeing. Distress distributions are shown in blue, wellbeing distributions in green, pooled across all participants from the general population in the MAILA dataset.

B. Structure and correlation of self-reported mental health. Each point represents a mental health dimension, positioned in t-SNE space based on its similarity to other dimensions. Line thickness corresponds to the strength of positive correlations (negative correlations not shown).
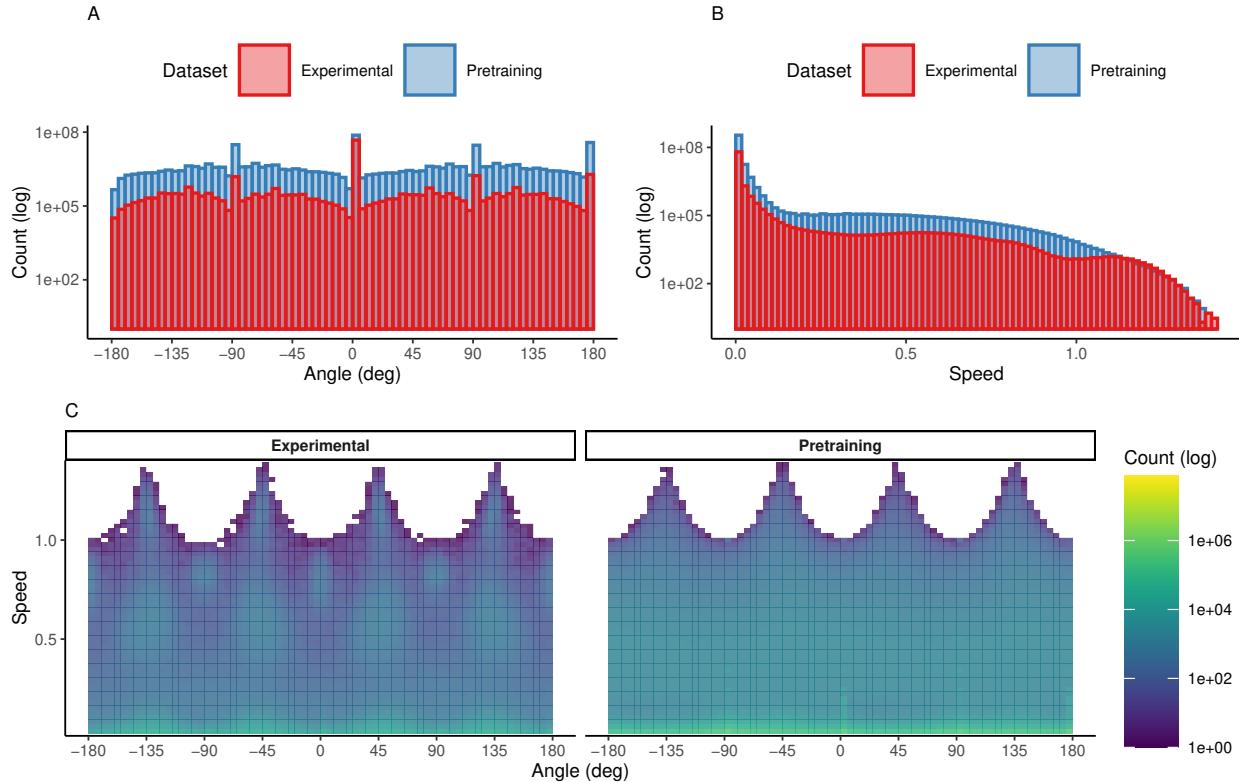
Supplemental Figure S6. Correlations and latent structure of self-reported mental health.

A. Correlation matrix. Correlations between self-reports in the distress and wellbeing domain, pooled across all participants from the general population in the MAILA dataset. Colors indicate the correlation strength and direction. Responses were negatively correlated between the domains of distress and wellbeing (R = -0.25 ± 0.02) and positively correlated between the dimensions of each domain (e.g., anxiety to depression, or emotional to psychological wellbeing). Average correlations reached R = 0.66 ± 0.02 between distress dimensions and R = 0.73 ± 0.09 within wellbeing dimensions.

B. PCA loadings. Loading of each mental health dimension onto the principal components (PCs) that captured 60% of the variance in mental health (across participants). Colors indicate the strength and direction of the loading on the respective PC. For example, a positive loading for depression on PC1 means that, when a participant experiences increasing depressive symptoms, their score on PC1 will increase.

C. Variance explained. The proportion of mental health variance explained by each principal component. Bars indicate the variance explained per component. Together, the first 3 components accounted for 37.91% of the variance.
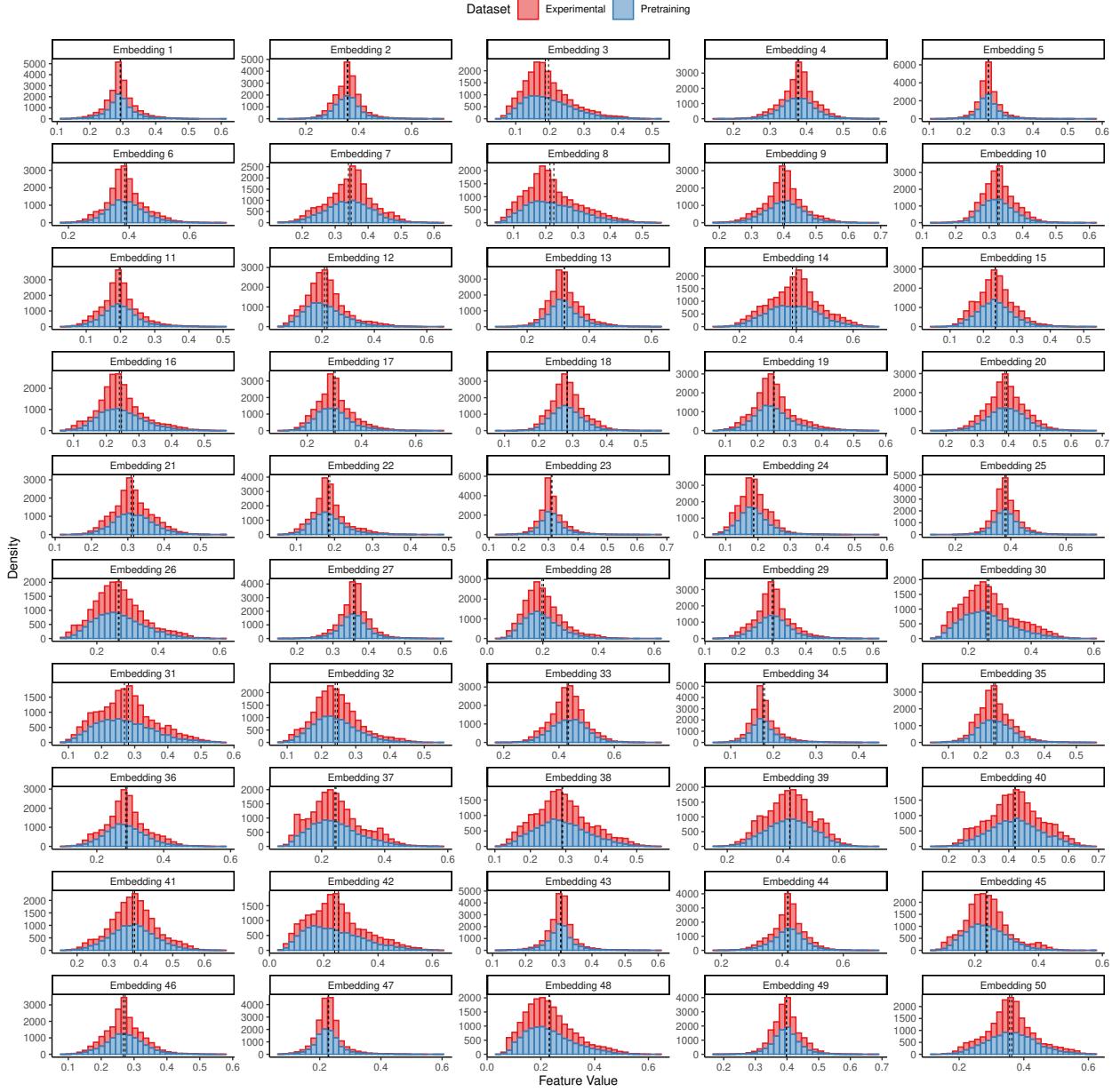
9.7 Supplemental Figure S7

Supplemental Figure S7. Distribution of cursor movement angles and speeds in the MAILA dataset and everyday cursor movements.

A. Angles. Histograms show the distribution of cursor movement directions (in degrees from -180° to 180°). The MAILA dataset (red) is compared to everyday cursor movements[41] (blue). The overlapping distributions indicate that MAILA captures the natural range of movement directions typically observed during everyday computer use.

B. Speeds. Histograms show the distribution of cursor speed (log-scaled y-axis). The MAILA dataset (red) and everyday cursor movements (blue) exhibit highly similar profiles, suggesting comparable dynamics of cursor motion across experimental and naturalistic settings.

C. Joint distribution of angle and speed. Heatmaps show the logarithmic density of cursor movements as a function of direction and speed for both datasets. Color intensity reflects movement frequency (log-scaled). The similarity in structure across datasets indicates that MAILA's response interface reproduces core features of natural cursor trajectories.
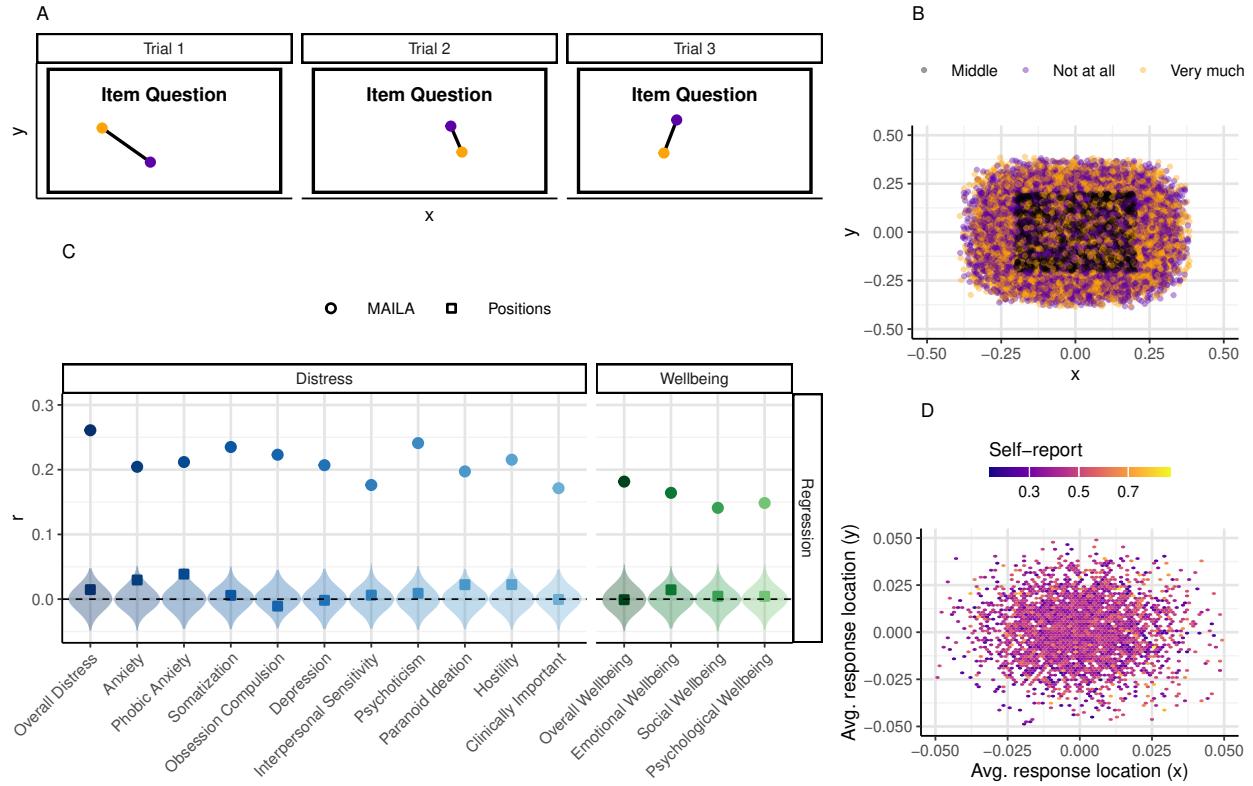
9.8 Supplemental Figure S8

Supplemental Figure S8. Feature space similarity between the MAILA dataset and everyday cursor movements. We compared LSTM embeddings from the MAILA dataset (experimentally induced cursor movements, red) to those from a public dataset of everyday computer use[41] (blue). Across all features, the distributions showed substantial overlap. On average, MAILA embeddings differed by only $0.94 \pm 0.67\%$ of the respective feature range, and $99.97 \pm 0.05\%$ of MAILA embeddings fell within the bounds of the pretraining distribution. Variance was slightly lower in the MAILA dataset compared to the naturalistic dataset ($\Delta_{var} = -2.21 \times 10^{-4} \pm 4.92 \times 10^{-4}$).

Together, these results suggest that, despite our dataset being experimental, it remained broadly representative of everyday computer use.

9.9 Supplemental Figure S9

Supplemental Figure S8. Questionnaire paradigm.

A. Task interface and randomized response mapping. Example response screens from the web-based questionnaire paradigm. Each panel shows one trial in which the response line appears at a random location and orientation. The line is flanked by two color-coded anchors: "Not at all" (illustrated here in purple) and "Very much" (illustrated here in orange). The item prompt (e.g., "How much are you distressed by feeling blue?") appears at the top of the screen. The spatial position, orientation, and length of the response line were independently randomized on every trial and for every participant, ensuring that motor behavior could not trivially encode the intended response. Note: In the actual experiment, the anchors were shown in green ("Not at all") and blue ("Very much").
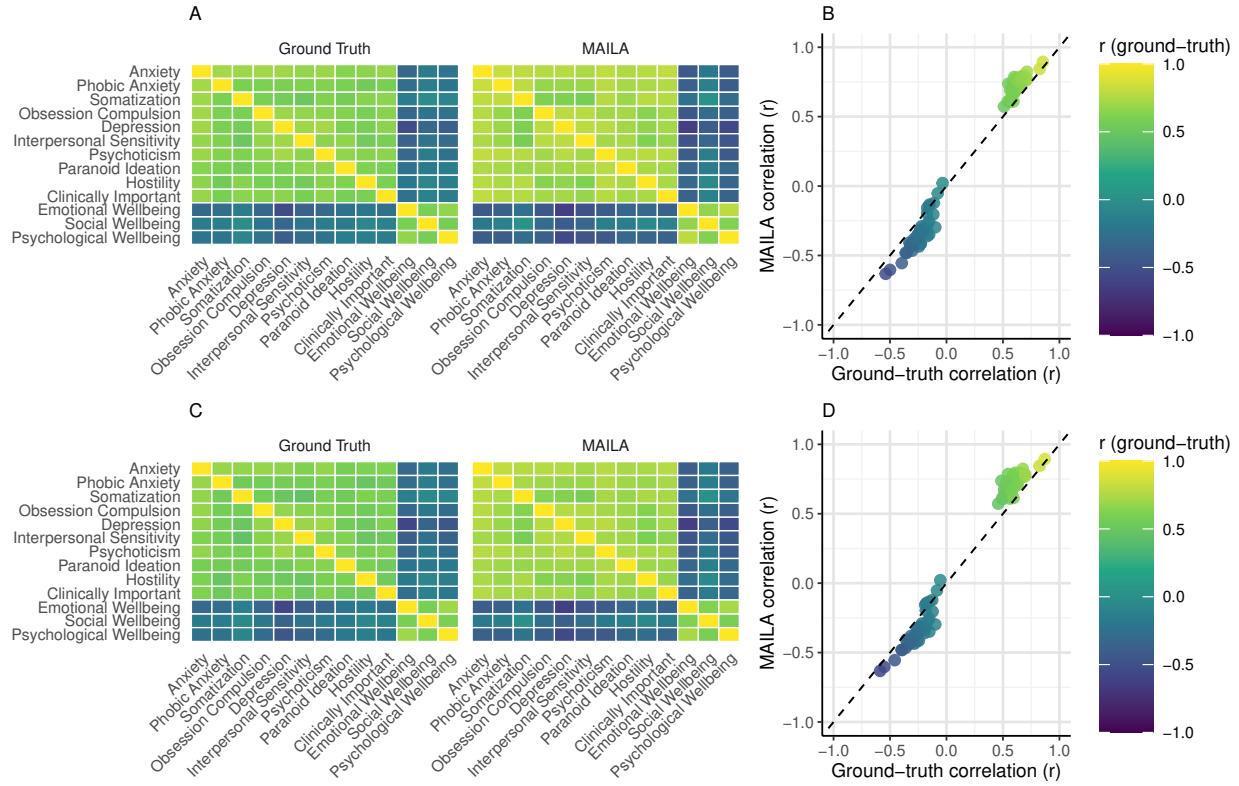
B. Spatial distribution of response endpoints. Screen coordinates of response-line midpoints and endpoints across 10,000 simulated trials. Endpoints labeled "Not at all" (purple) and "Very much" (orange) are symmetrically arranged around randomized center positions; midpoints (never displayed) are shown in black. This randomized spatial encoding prevents raw pointer coordinates from carrying systematic information about the meaning of participants' responses.

C. Regression analysis. To further confirm that screen positions did not permit trivial decoding of mental health, even when considering human-computer interactions recorded during survey com-

pletion, we trained support vector regression models to predict self-reported mental health from x and y screen coordinates. Their cross-validated performance did not exceed permuted baselines and remained well below MAILA's movement-based features (R = $0.01 \pm 7.31 \times 10^{-3}$; round versus square markers). These controls complement analyses where we applied frozen MAILA models to non-mental-health settings (non-psychological survey and gamified decision-making experiment) and on free-form digital activity without any link to self-reports (Figure 2-3), and demonstrate successful decoding of mental health.

D. Self-reports versus screen positions. The plot shows average x and y response cursor positions per participant, colored by average of the associated self-reports. The uniform color distribution indicates that eccentricity was not correlated with the self-reports (R = -1.46×10^{-3}, p = 0.93). Please note that MAILA received the entirety of the cursor or touch trajectory as it's input, without any labeling of the screen position of the response, or at what point in the recording a specific mental health item was presented (random order of intermixed distress and wellbeing items).

9.10 Supplemental Figure S10

Supplemental Figure S10. Overlapping correlation structure between MAILA and the ground truth.

A. MAILA recovers the correlation structure of ground-truth mental health. Heatmaps show pairwise correlations among mental-health dimensions in the ground truth (left) and in MAILA's predictions (right). Although MAILA was trained with separate support-vector regressions for each dimension, its predictions closely reproduced the correlation structure of the true self-reports ($R = 0.97$, $p = 1.23 \times 10^{-64}$). This indicates that human-computer interactions encode shared latent dimensions of mental health.
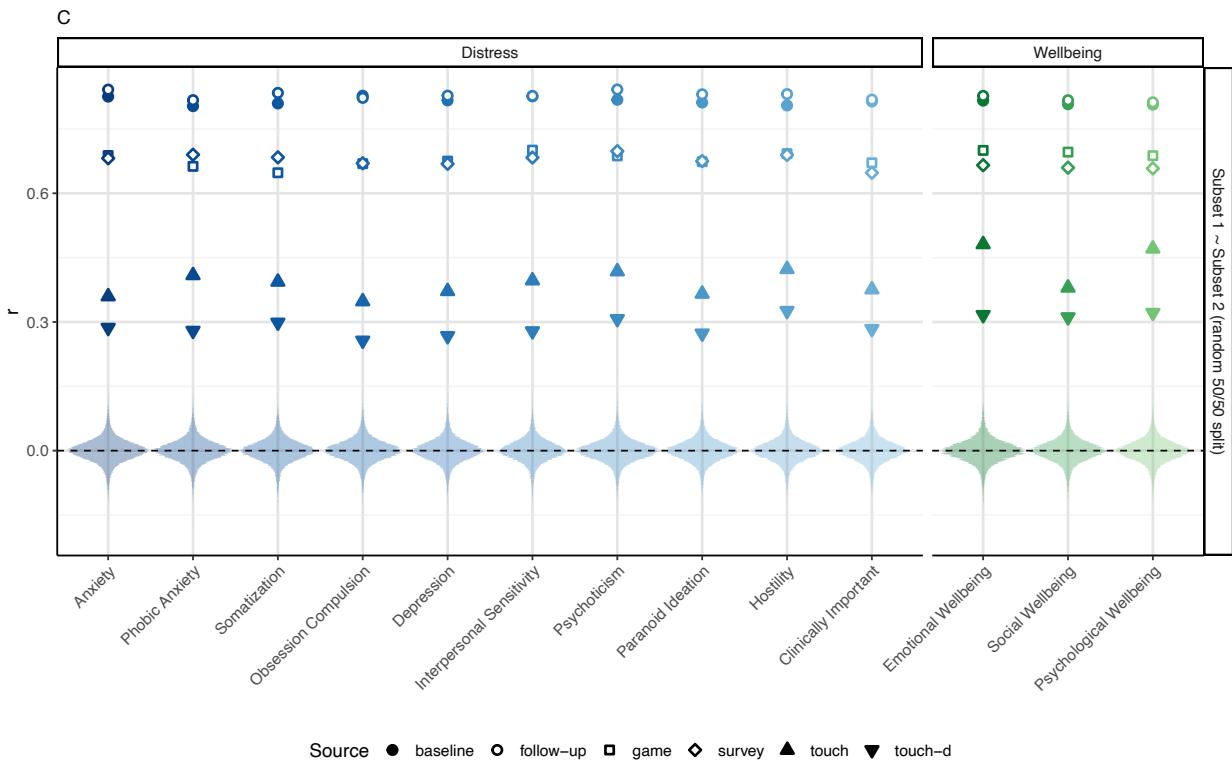
B. Agreement between ground-truth and MAILA correlations. Scatter plot comparing the pairwise correlation coefficients between mental-health dimensions derived from ground-truth data (x-axis) and MAILA's predictions (y-axis). Each point represents one unique pair of dimensions (e.g., anxiety ~ depression), colored by the corresponding ground-truth correlation strength. The diagonal marks perfect agreement. Points for negative ground-truth correlations lie mostly below the diagonal and positive ones mostly above, indicating that MAILA tends to overestimate the magnitude of inter-dimensional correlations overall (paired t-test on |r|: $p = 1.58 \times 10^{-35}$).

C. MAILA reproduces the correlation structure of changes in mental health. Heatmaps show pairwise correlations among changes in mental-health dimensions (follow-up relative to base-

line) for the ground truth (left, $y_{followup} - y_{baseline}$) and MAILA predictions (right, $\hat{y}_{followup} - \hat{y}_{baseline}$). MAILA's estimates of within-person change captured the inter-dimensional dependency structure of true longitudinal changes (R = 0.97, p = 2.51×10^{-68}), suggesting that shared latent trajectories of mental health are encoded in human-computer interactions.
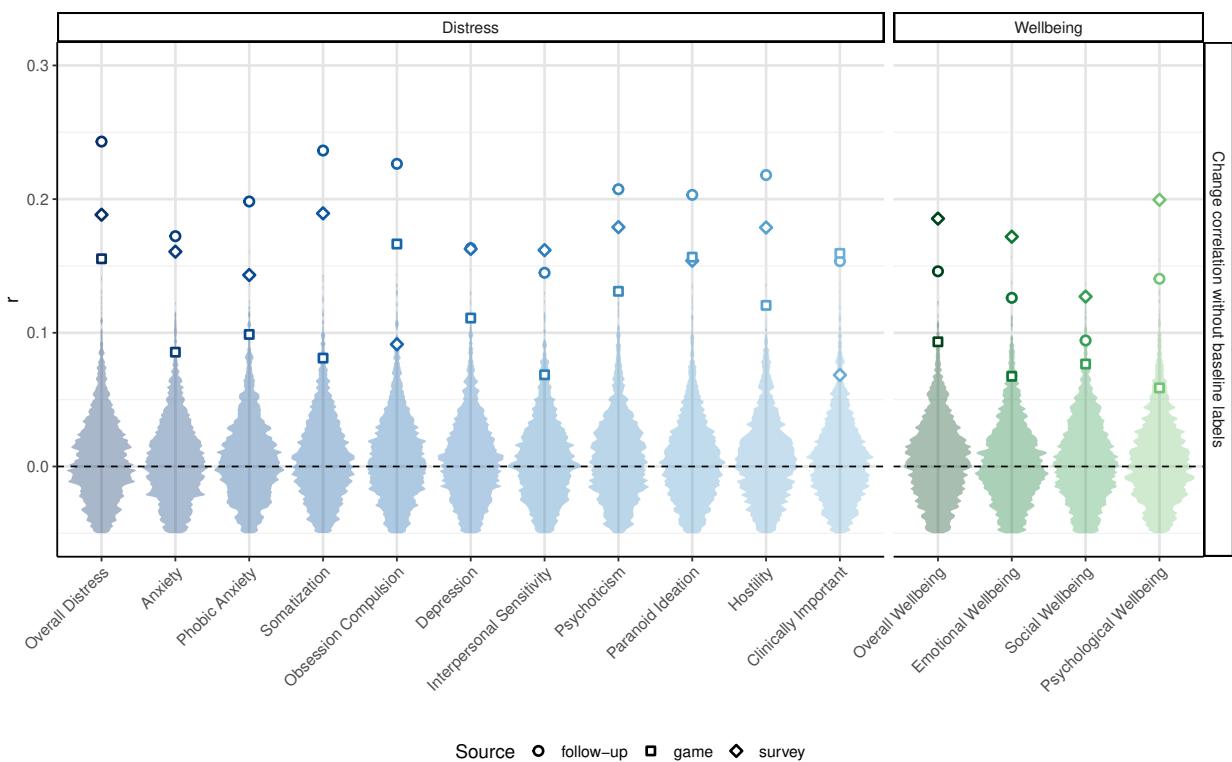
D. Agreement between ground-truth and MAILA correlations for changes in mental health. Scatter plot comparing the pairwise correlation coefficients between changes in mental-health dimensions computed from the ground truth (x-axis) and from MAILA's predictions (y-axis). Each point represents one pair of dimensions, colored by the ground-truth correlation strength. The diagonal marks perfect agreement. Negative ground-truth correlations tend to lie below and positive ones above the diagonal, again indicating that MAILA slightly overestimates inter-dimensional dependencies in changes (paired t-test on |r|: p = 3.32×10^{-35}).

9.11 Supplemental Figure S11
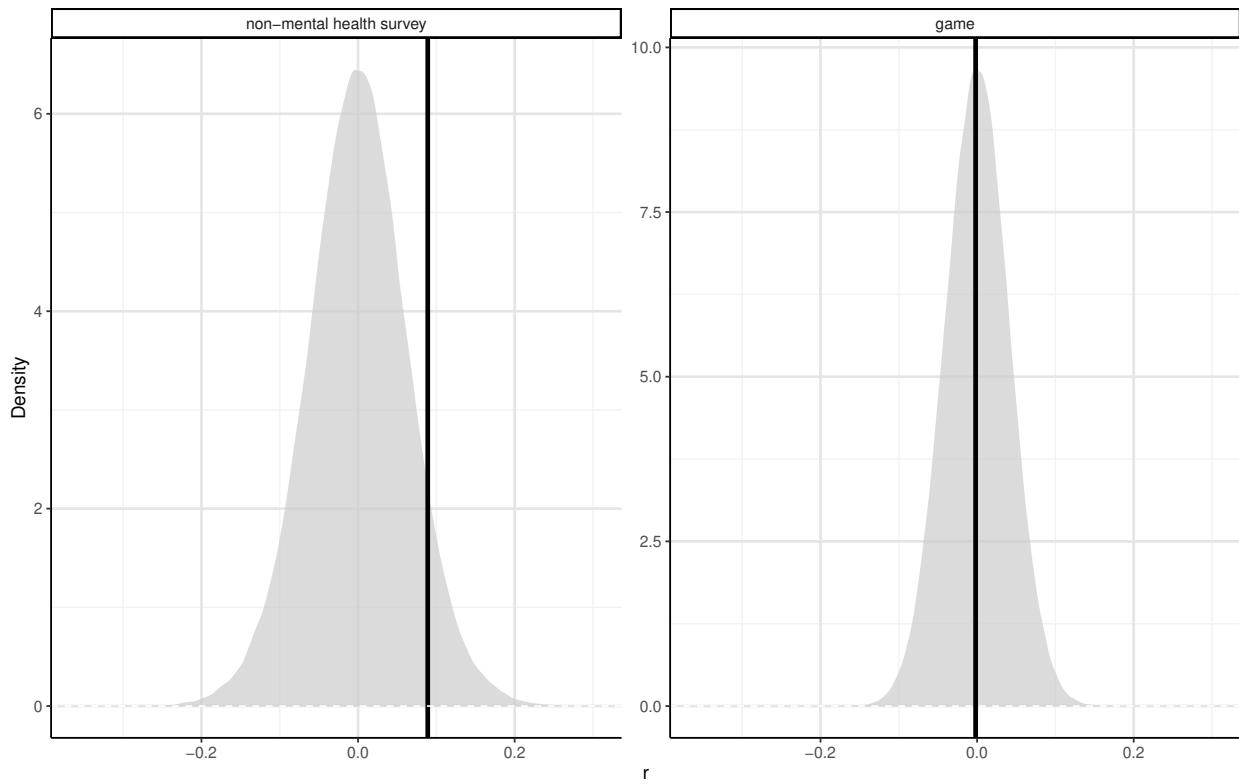
Supplemental Figure S11. Split-half reliability of MAILA across datasets and dimensions. To assess the internal reliability of MAILA, we divided each participant's cursor or touchscreen trajectories into randomized 50/50 subsets and trained support vector regression models on one half to predict self-reported mental health in the other. We repeated this procedure in the reverse direction, yielding two independent prediction vectors per participant. Violin plots depict permutation-based null distributions obtained by shuffling one split. Filled markers denote correlation coefficients from unseen participants in 5-fold cross-validation (baseline, touch, and touch-d); unfilled markers denote correlation coefficients when frozen MAILA models were applied to independent generalization datasets (follow-up, survey, and game). MAILA's predictions were highly consistent across randomized halves (R = 0.61 ± 0.05, across all dimensions and datasets), demonstrating a level of reliability that exceeded most behavioral and neuroimaging markers of mental health (Figure 3).

9.12 Supplemental Figure S12

Supplemental Figure S12. Direction-of-change prediction of mental health without baseline labels. Correlations between predicted and true changes within participants were higher than correlation between MAILA and the ground truth when only one time-point was considered (Figure 2-3). In this control analysis, predicted changes were defined as the difference between (i) MAILA's output at follow-up using models trained at baseline, and (ii) MAILA's output for held-out participants from models trained and tested at baseline (5-fold cross-validation). Violin plots depict permuted null distributions; hollow markers show observed correlations for when considering the follow-up (circles), survey (triangles), and game (squares) dataset. Predictive performance remained robust when only model-derived baseline estimates for held-out participants were used ($R = 0.15 \pm 0.01$, $p = 4.69 \times 10^{-24}$). These results confirm that digital behavior alone can track changes in mental health, while predictive accuracy is further enhanced in the clinically realistic setting where baseline symptom information is available (Figure 3).
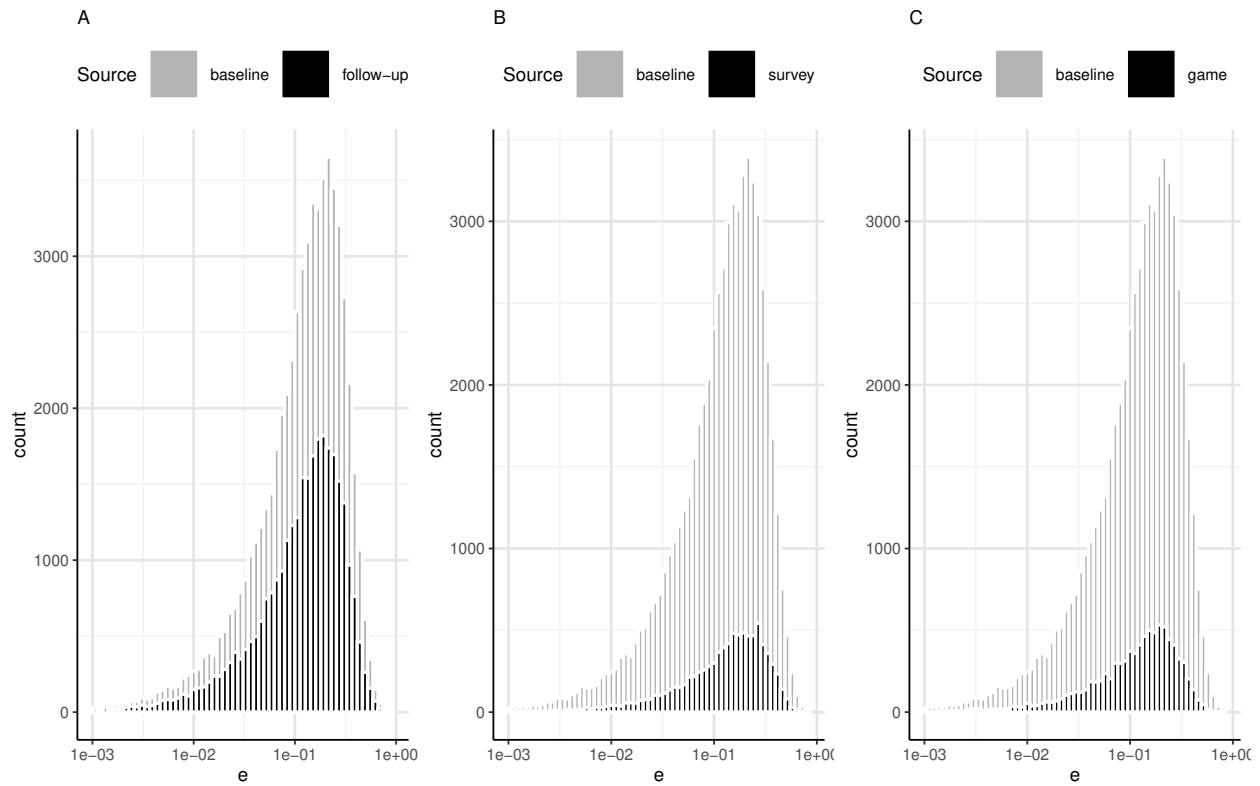
9.13 Supplemental Figure S13

Supplemental Figure S13. Predicting mental-health self-reports from responses in the non-mental heatlh survey and gameplay. We tested whether individual non-mental-health items from the non-mental-health survey or the game contained any above-chance information about the participants' mental-health self-reports. For each dataset, we trained linear models that predicted each of the 67 mental-health items from a single non-mental-health item using 5-fold cross-validation, and quantified prediction accuracy using the Spearman correlation between predicted and observed responses. The grey density curves show the permutation null distribution of cross-validated correlations. Solid vertical lines indicate the empirical mean cross-validated correlation across all predictor-target pairs (survey: $R = 0.09$, $p = 0.08$; game: -1.88×10^{-3}, $p = 0.52$). In both tasks, the empirical means fall within the permutation distributions, indicating that responses to non-mental-health items do not provide above-chance information about the participants' mental-health self-reports.

In addition to the randomized response mapping, the weak or absent association between non-mental-health items and mental-health items, together with the finding that human–computer interactions did not predict responses to the non-mental-health items themselves ($R = 0.01 \pm 0.03$, $p = 0.28$) or gameplay behavior ($R = 0.02 \pm 0.02$, $p = 0.09$; Supplemental Table S2), demonstrate that MAILA's predictions in the generalization experiments rely on context-invariant movement patterns rather than any trivial association with the non-mental-health content of the tasks.

9.14 Supplemental Figure S14
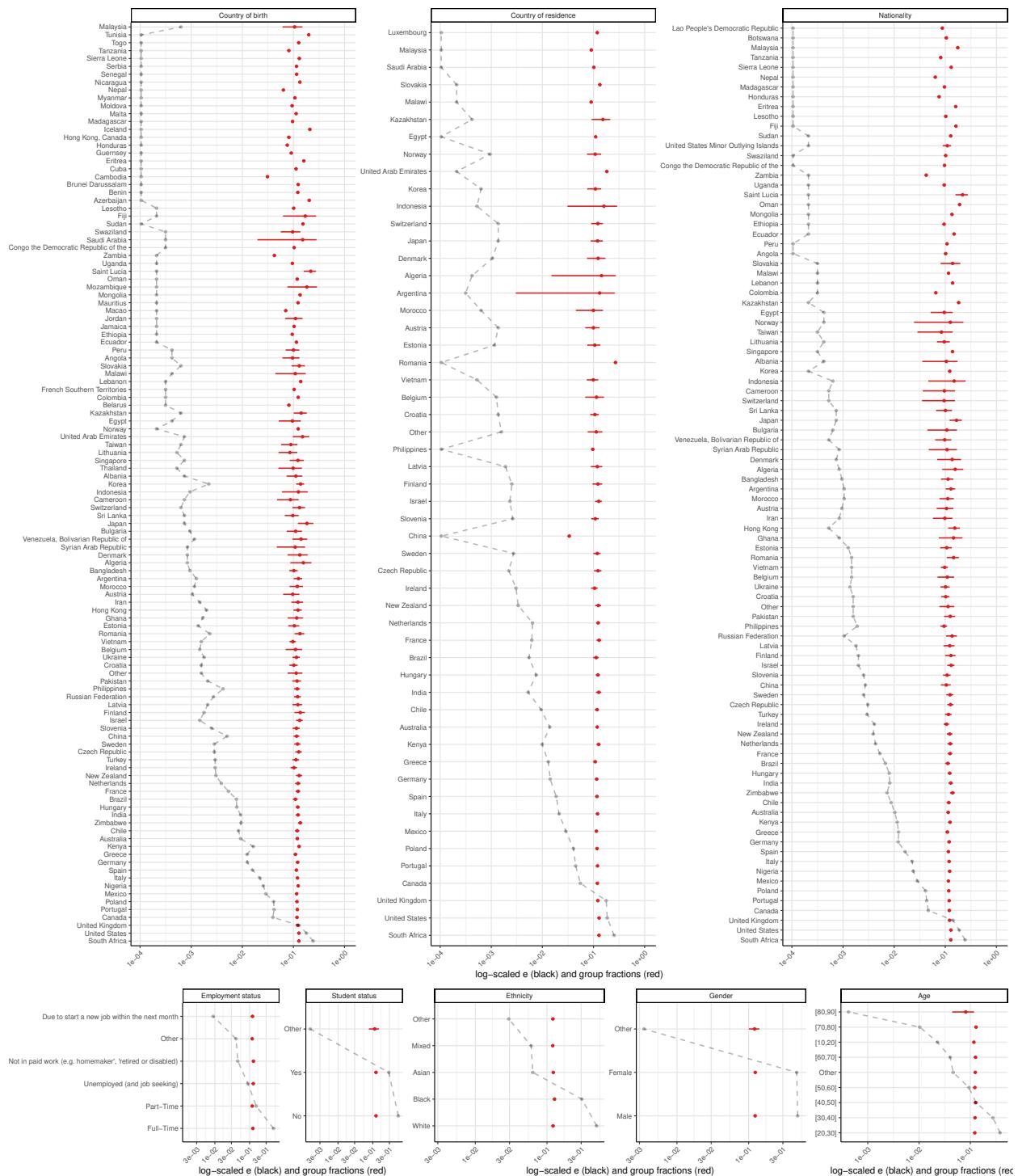
Supplemental Figure S14. Cursor-based mental health predictions generalize across contexts. Distributions of normalized mean root squared errors (e) are shown on a logarithmic scale for the baseline (grey) and three generalization datasets (black). Models trained on baseline cursor-movement data (N = 4000) were applied without retraining to follow-up sessions (**A**, subset of N = 2000), independent online surveys (**B**, subset of N = 600 within the follow-up dataset), and an interactive game (**C**, independent subset of N = 600 within the follow-up dataset). Compared to baseline cross-validation, prediction errors increased by $3.66 \pm 1.61\%$ when mental health was inferred from cursor movements during survey completion ($p = 1.69 \times 10^{-4}$), and decreased by $0.43 \pm 3.25\%$ for predictions based on gameplay ($p = 0.69$). The overlapping error distributions indicate that cursor-based predictions of mental health generalize robustly across time, task, and behavioral context.

9.15 Supplemental Figure S15

Supplemental Figure S15. Example drawings. Free-form touchscreen drawings from five randomly selected participants, with prompts displayed to the left. See Supplemental Table S3 for a list of prompts.
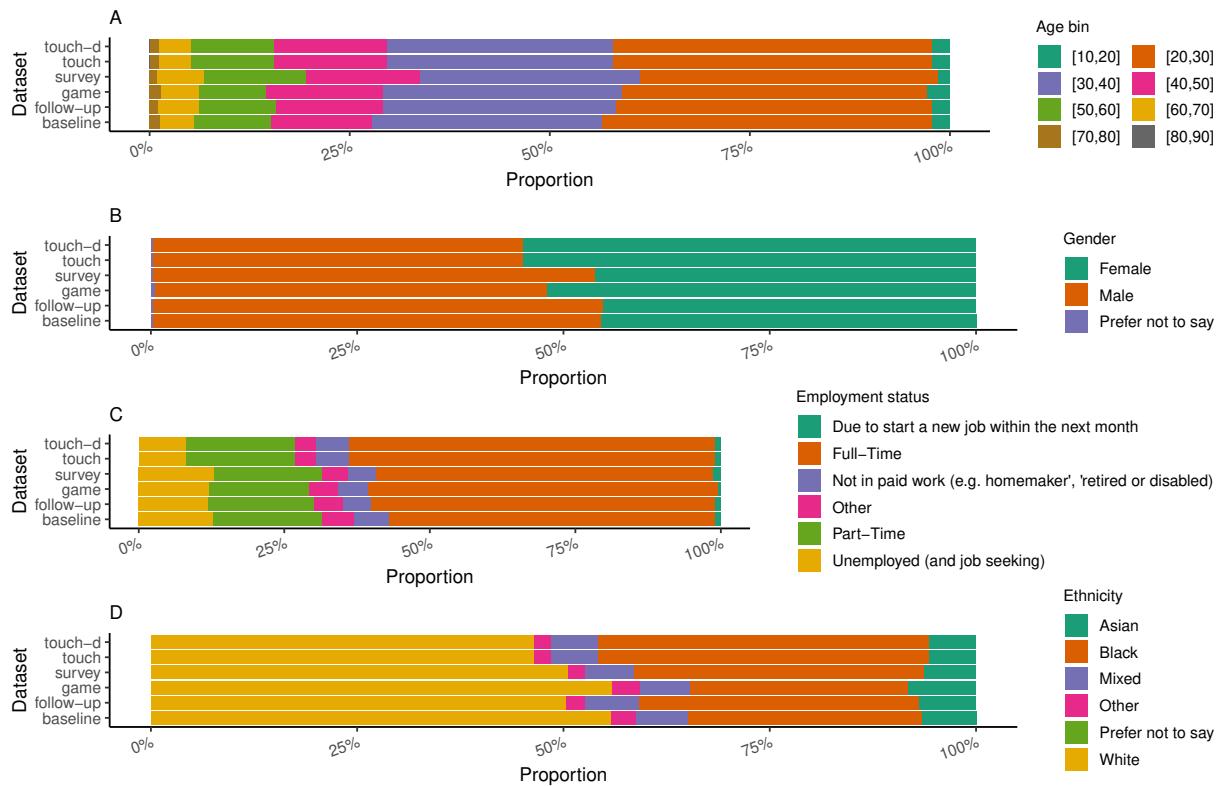
9.16 Supplemental Figure S16

Supplemental Figure S16. Algorithmic bias. MAILA's prediction errors pooled over the first three principle components of mental health (log-scaled normalized root mean squared error, e),
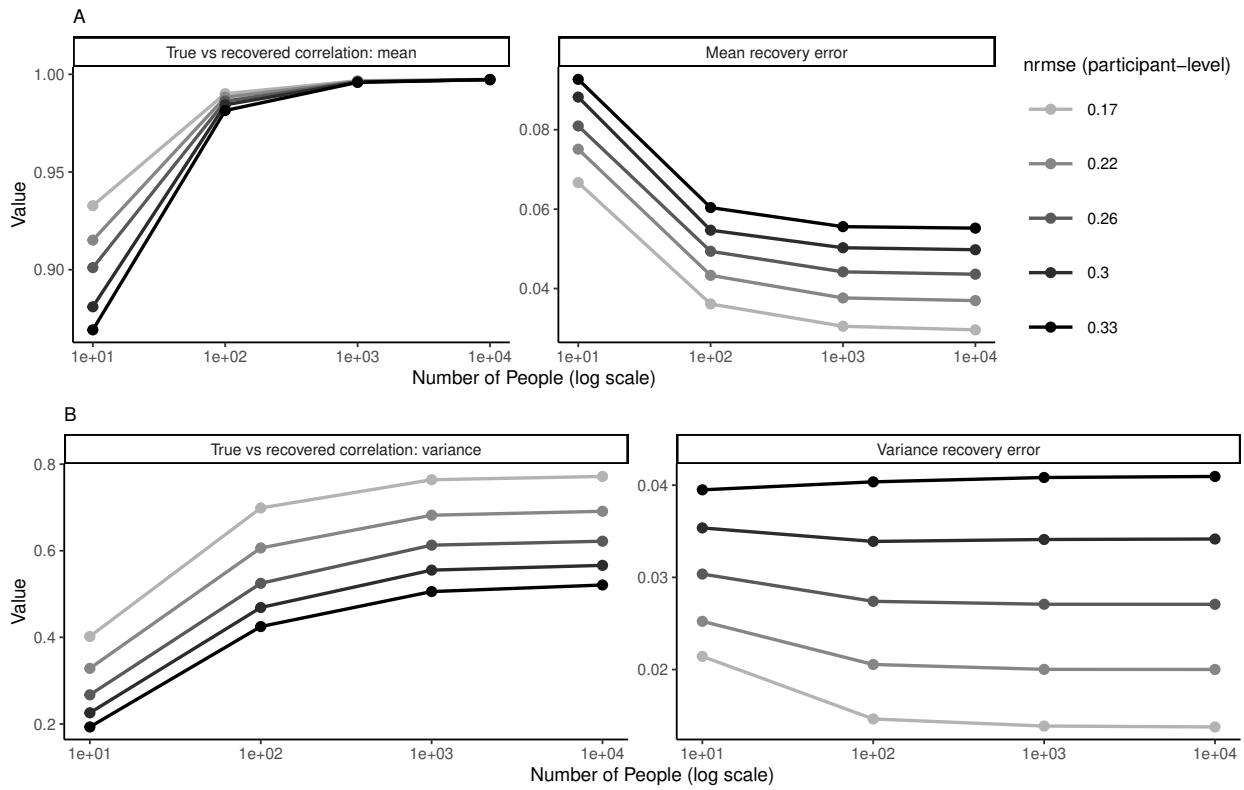
shown as mean $\pm$ 95% confidence intervals across participants. Errors are shown in red, and the log-scaled fraction of individuals within each demographic category is overlayed in grey. To assess the influence of each demographic factor, we fitted linear mixed-effects models to the errors, with fixed effects corresponding to the categorical levels of the respective factor and a random intercept to capture individual-level differences in predictive performance. We evaluated the significance of each demographic factor using type III analysis of variance (ANOVA) on the fixed effects. There was no significant effect of gender (F = 0.63, p = 0.67), ethnicity (F = 0.32, p = 0.92), country of birth (F = 1.1, p = 0.23), country of residence (F = 1.04, p = 0.4), nationality (F = 1.06, p = 0.35), student status (F = 0.91, p = 0.4), or age (F = 1.66, p = 0.11). MAILA's prediction errors varied significantly with employment status (F = 3.71, p = 1.1×10^{-3}), and there was a borderline significant effect of language (F = 1.34, p = 0.05).

9.17 Supplemental Figure S17

Supplemental Figure S17. Age, gender, employment, and ethnicity composition between MAILA's datasets. Stacked bar plots show the proportional distribution of participants across (**A**) age bins, (**B**) gender, (**C**) employment status, and ethnicity (**D**), separately for MAILA's dataset.

9.18 Supplemental Figure S18
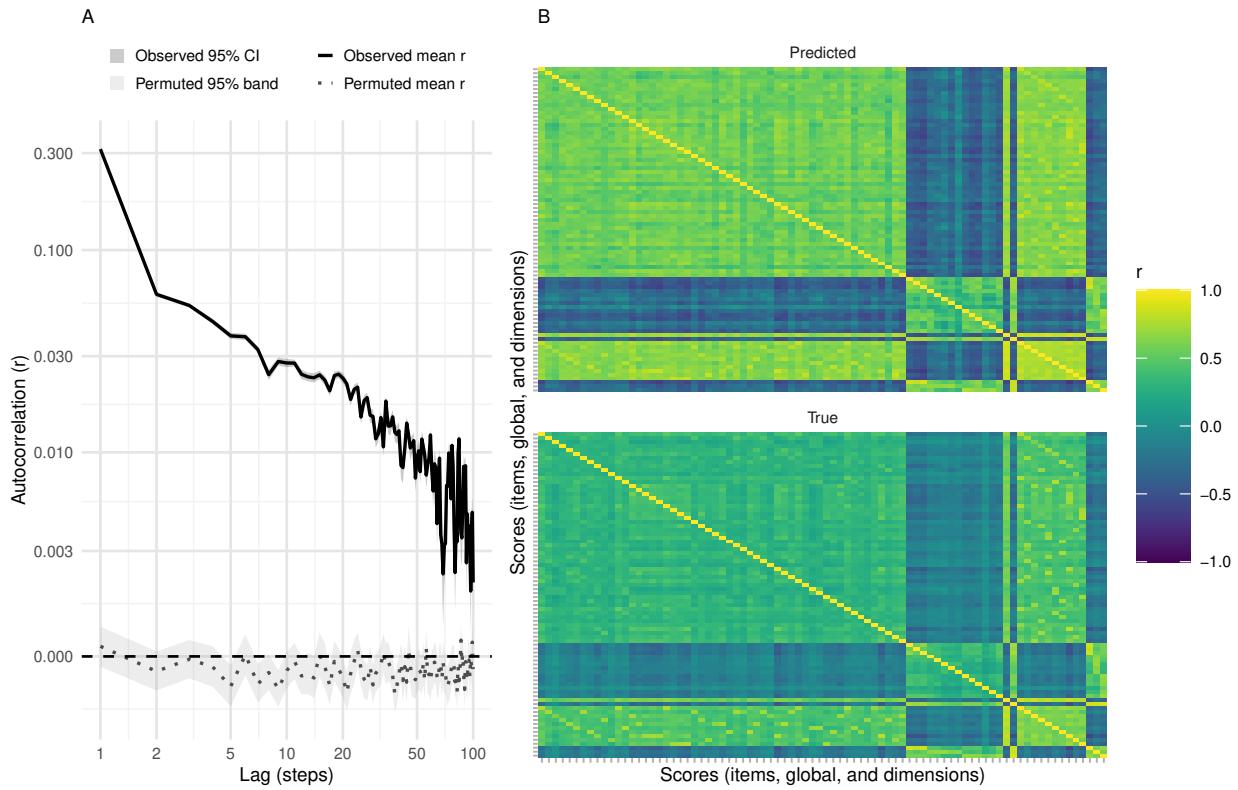
Supplemental Figure S18. Simulated recovery of population-level mental health. To assess whether human-computer interaction encode information about group-level mental health, we simulated populations of group size N, each defined by a specific mean and variance of a ground truth mental health feature. We then simulated MAILA's predictions, with noise levels defined by normalized mean squared errors (e) ranging from 17 to 35%. The resulting mental health predictions were clipped to the unit interval to ensure they remained within the bounds of mental health scores. We then recovered the population means (**A**) and variances (**B**) from the noisy participant-level predictions and compared them to the ground truth of the simulated populations. The law of large numbers predicts that accuracy improves as a function of population size and prediction error.

A. Recovery of the group-level mean. The left panel shows the correlation between the true and recovered population means. The right panel presents the corresponding absolute recovery error. The x-axis represents population size on a logarithmic scale, illustrating how larger sample sizes improve group-level accuracy. Shades of grey represent different error levels, which were informed by the range of prediction errors observed for items, dimensions, and global scores of distress and wellbeing in the MAILA dataset.

B. Recovery of the group-level variance. The left panel shows the correlation between the true and recovered population variances. The right panel presents the corresponding absolute error when recovering the variance.

9.19 Supplemental Figure S19
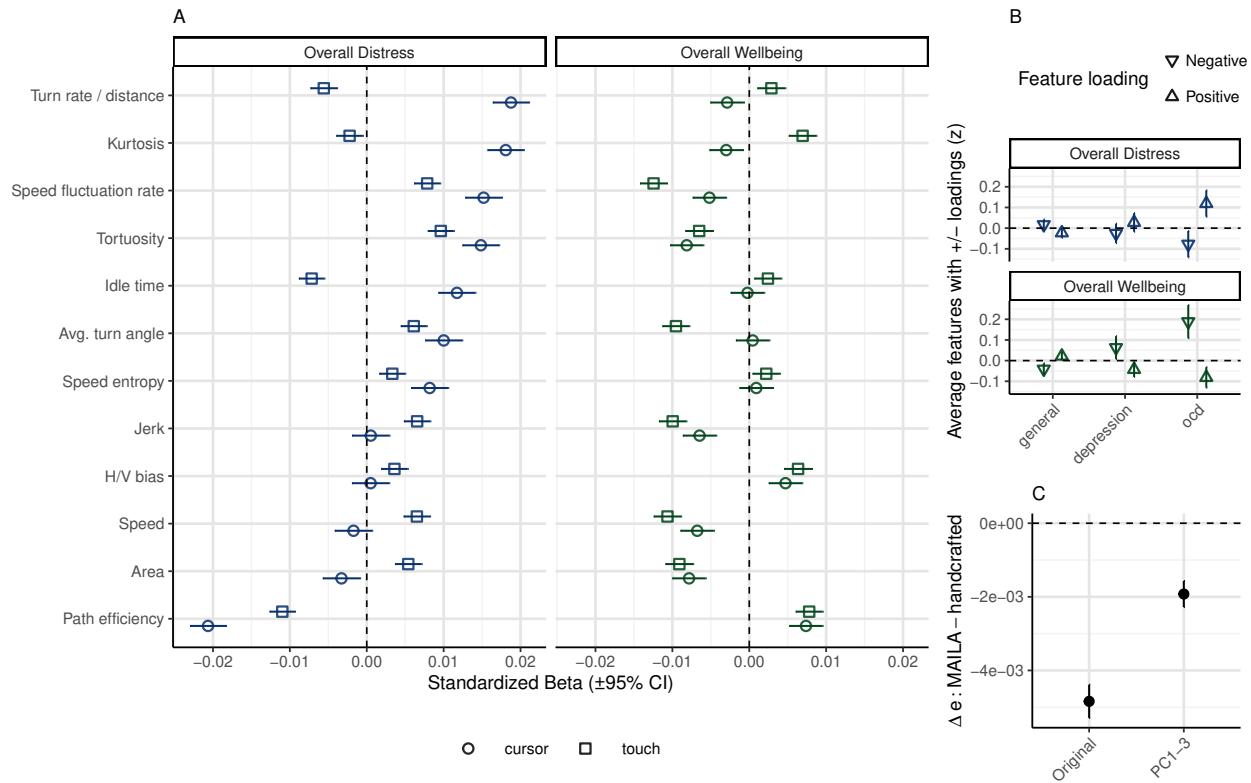
Supplemental Figure S19. Validating MILA on naturalistic cursor movement. MAILA was trained on cursor movements from the baseline and follow-up datasets and applied, without retraining, to naturalistic cursor activity from 19 individuals, each contributing muliple sessions recorded across an extended period of time and at multiple times of the day[41]. While these analyses rely on unlabeled data, the temporal continuity (**A**) and structural consistency (**B**) of MAILA's predictions provide an indirect validation for the embedding of meaningful, generalizable dimensions of mental states in everyday human-computer interaction.

A. Autocorrelation of predicted mental health. Predicted mental-health scores (pooled across participants and items) exhibited a significant positive autocorrelation that decayed monotonically with increasing lag on a log-scaled x-axis. The observed mean (solid line) remained above the participant-wise time-shuffled null (dashed line), with non-overlapping 95% confidence intervals at short lags and convergence toward zero at longer lags. This pattern supports the interpretation that naturalistic cursor movements reflect temporally coherent, slowly evolving latent mental states. The autocorrelation of MAILA's predictions extracted from independent naturalistic cursor movements closely mirrored that of self-reported scores in the MAILA dataset, where test-retest correlations declined from R = 0.88 for distress and R = 0.84 for wellbeing after one week to R = 0.69 after eight weeks.

B. Correlation structure of true and predicted mental health. To compare the internal structure of mental health across datasets, we z-scored each item separately for true and predicted scores and computed the pairwise correlations between items. The resulting correlation matrices were highly similar (R = 0.95), indicating that predictions derived from naturalistic cursor movements preserved the inter-item structure of mental health observed in the MAILA dataset.

Supplemental Figure S20. Interpreting MAILA.
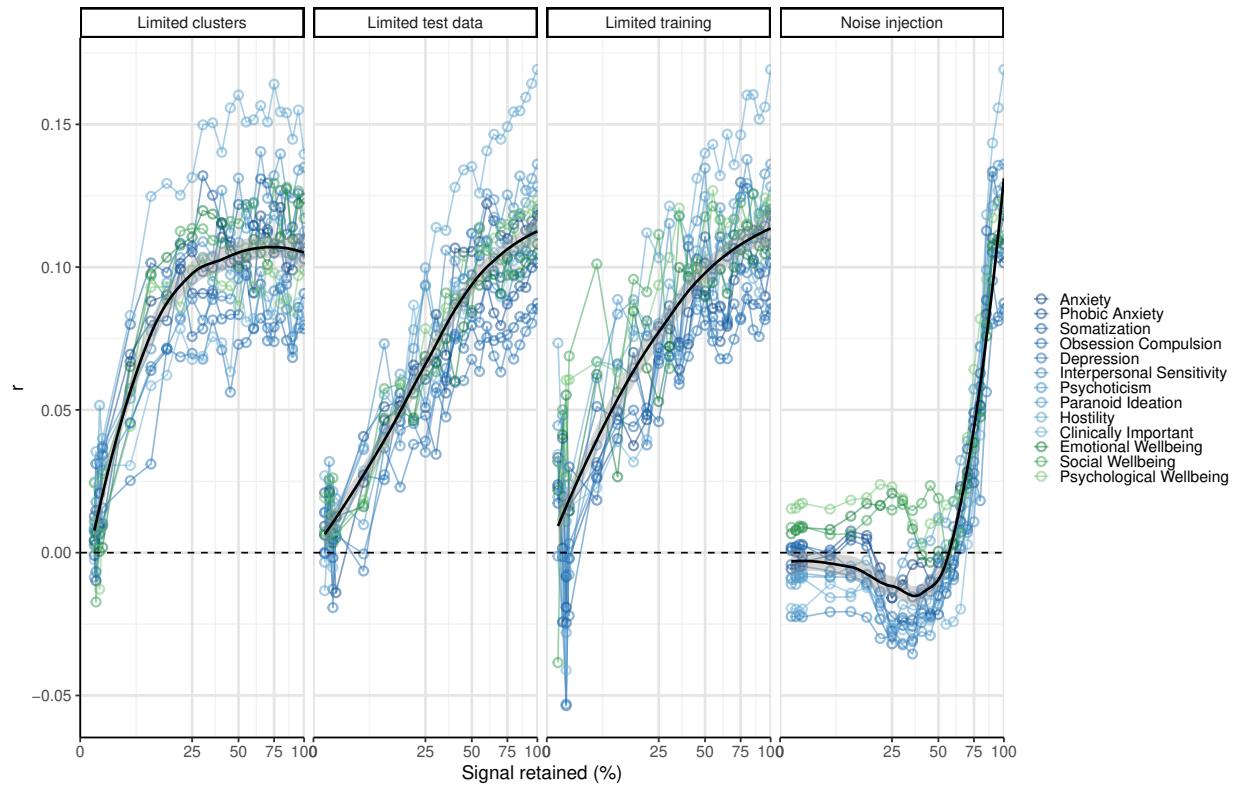
A. Associations between handcrafted movement features and MAILA's predictions in the general population. We correlated participant-level handcrafted movement features with MAILA's predictions, shown here for overall distress in blue and overall wellbeing in green. Markers show standardized regression coefficients estimated separately for cursor- and touch-based datasets (circles vs. squares), with horizontal bars indicating 95% confidence intervals across datasets. Across modalities, higher distress and lower wellbeing were associated with more tortuous trajectories and greater variability in speed, whereas higher path efficiency predicted greater wellbeing and lower distress. Despite these broad consistencies, several handcrafted metrics showed substantial cross-modal heterogeneity: only 62.5% of features loaded onto predicted mental health in the same direction across cursor and touchscreen data.

B. Expression of feature groups in clinical versus general populations. For each population (general, depression, OCD), handcrafted features were grouped according to whether they loaded positively or negatively on predicted wellbeing or distress. Mean z-scored feature values (±95% CI) are plotted for positively loading (upward arrow) and negatively loading (downward arrow) feature groups. In the general population, features associated with lower distress and higher

wellbeing were more strongly expressed. In participants who self-identified with depression or OCD, this pattern reversed for both distress ($p = 1.31 \times 10^{-6}$) and wellbeing ($p = 4.92 \times 10^{-15}$), indicating that interpretable aspects of human-computer interaction systematically tracked higher distress and lower wellbeing in clinical groups.
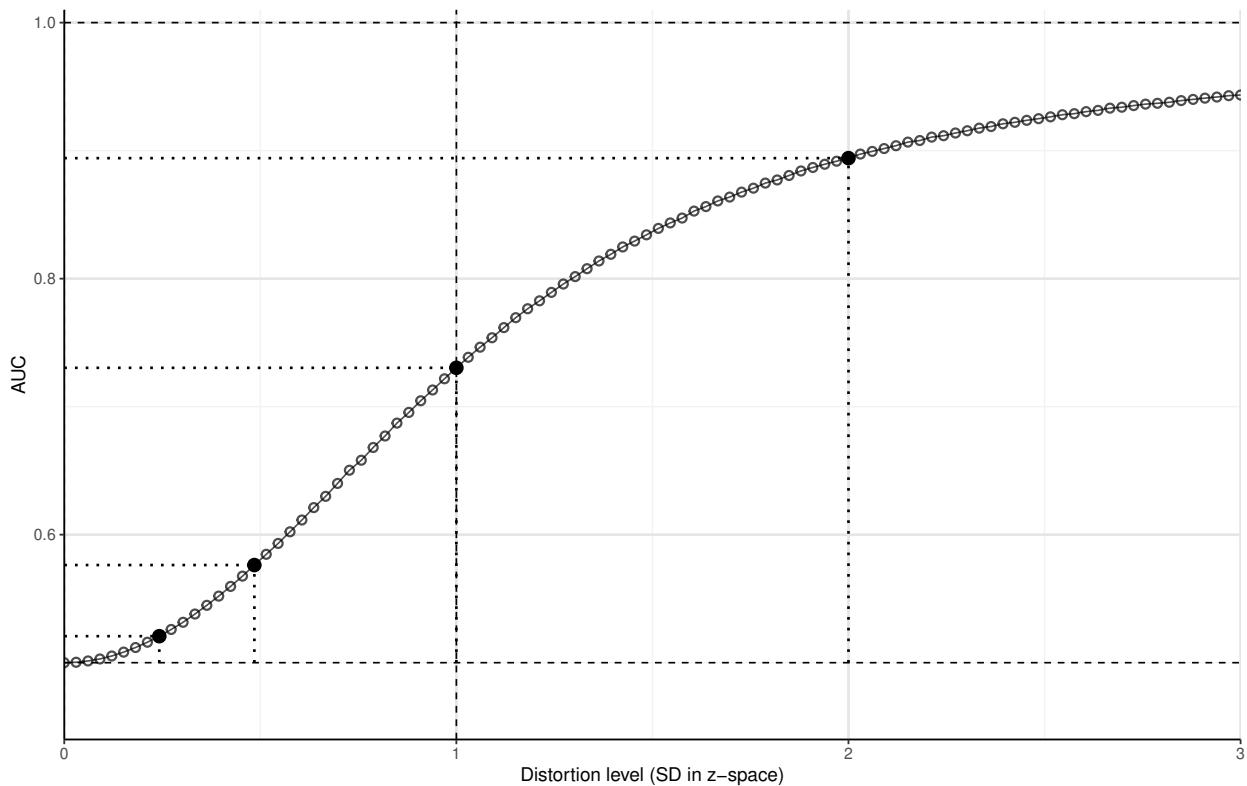
C. Predictive advantage of MAILA over handcrafted feature models. MAILA outperformed models built from handcrafted features across all benchmarks. In the original symptom space, MAILA achieved lower prediction errors for inter-individual differences in mental health in the general population ($p = 1.29 \times 10^{-97}$). Along PC1-3, which capture the level and specific causes of distress and wellbeing (Figure 4), MAILA also outperformed handcrafted models ($p = 2.67 \times 10^{-26}$). Together, these results demonstrate that MAILA provides more accurate and specific predictions of mental health than models based solely on handcrafted metrics.

9.21 Supplemental Figure S21

Supplemental Figure S21. Robustness of MAILA to information loss. We systematically degraded MAILA in four ways (from left to right panel): (i) we limited the number of K-means clusters used to construct the movement feature matrix $X^{N \times C}$, simulating reduced behavioral diversity; (ii) we reduced the amount of human-computer interaction available per participant in the test folds by removing contiguous segments from each trajectory, simulating inferences from shorter cursor or touch recordings; (iii) we subsampled the number of participants in the training folds, simulating the effect of smaller calibration datasets; (iv) we corrupted cursor/touch trajectories by linearly mixing true samples with random values drawn from a uniform distribution. In all cases, correlations declined smoothly with increasing degradation, indicating predictable performance loss under impoverished behavior, limited test data, limited training data, or injected noise.

9.22 Supplemental Figure S22

Supplemental Figure S22. Detectability of distorted self-reports from human-computer interaction. We simulated increasing levels of distortion in participants' true mental-health profiles by adding Gaussian noise in z-space and clipping values to the empirical range. Detection accuracy was quantified as the AUC of the negative Euclidean distance between predicted and distorted profiles. AUC increased monotonically with distortion magnitude, indicating that progressively inconsistent or fabricated self-reports become easier to detect from cursor and touchscreen behavior alone.

9.23 Supplemental Table S1

Question	Mean ± 95% CI (IQR)	MAILA's correlation to ground truth (r)					
		baseline	follow-up	survey	game	touch-q	touch-d
Distress - Anxiety							
How much are you distressed by nervousness or shakiness inside?	0.41 ± 0.02 (0.52)	0.16	0.11	0.13	-0.01	0.10	0.04
How much are you distressed by suddenly being scared for no reason?	0.36 ± 0.02 (0.48)	0.12	0.15	0.12	0.06	0.14	0.04
How much are you distressed by feeling fearful?	0.41 ± 0.02 (0.49)	0.13	0.11	0.07	0.07	0.11	0.04
How much are you distressed by feeling tense or keyed up?	0.45 ± 0.02 (0.49)	0.13	0.10	0.07	0.08	0.06	0.03
How much are you distressed by spells of terror or panic?	0.35 ± 0.02 (0.47)	0.13	0.15	0.13	0.10	0.09	0.02
How much are you distressed by feeling so restless you could not sit still?	0.36 ± 0.02 (0.48)	0.14	0.14	0.11	0.06	0.09	0.04
Distress - Clinically Important							
How much are you distressed by poor appetite?	0.32 ± 0.02 (0.45)	0.10	0.14	0.10	0.07	0.16	0.07
How much are you distressed by trouble falling asleep?	0.45 ± 0.02 (0.59)	0.07	0.07	0.04	0.08	0.03	0.01
How much are you distressed by thoughts of death or dying?	0.42 ± 0.02 (0.56)	0.06	0.11	0.01	0.02	0.10	0.03
How much are you distressed by feeling of guilt?	0.41 ± 0.02 (0.53)	0.13	0.12	0.06	0.11	0.08	0.03
Distress - Depression							
How much are you distressed by thoughts of ending your life?	0.27 ± 0.02 (0.39)	0.13	0.15	0.10	0.05	0.13	0.02
How much are you distressed by feeling lonely?	0.44 ± 0.02 (0.56)	0.12	0.11	0.05	0.04	0.07	0.00
How much are you distressed by feeling blue?	0.45 ± 0.02 (0.55)	0.12	0.11	0.14	0.04	0.11	0.01
How much are you distressed by feeling no interest in things?	0.43 ± 0.02 (0.54)	0.13	0.13	0.02	0.08	0.05	0.01
How much are you distressed by feeling hopeless about the future?	0.49 ± 0.02 (0.57)	0.14	0.10	0.04	0.20	0.07	-0.03
How much are you distressed by feelings of worthlessness?	0.42 ± 0.02 (0.58)	0.12	0.14	0.04	0.12	0.12	0.04
Distress - Hostility							
How much are you distressed by feeling easily annoyed or irritated?	0.47 ± 0.02 (0.52)	0.13	0.13	0.02	0.03	0.08	0.01
How much are you distressed by temper outbursts that you could not control?	0.35 ± 0.02 (0.48)	0.13	0.18	0.12	0.03	0.09	0.07
How much are you distressed by having urges to beat, injure, or harm someone?	0.25 ± 0.01 (0.31)	0.13	0.16	0.14	0.07	0.17	0.12
How much are you distressed by having urges to break or smash things?	0.27 ± 0.01 (0.36)	0.14	0.22	0.15	0.03	0.14	0.06
How much are you distressed by getting into frequent arguments?	0.38 ± 0.02 (0.51)	0.14	0.09	0.12	-0.03	0.11	0.08
Distress - Interpersonal Sensitivity							
How much are you distressed by your feelings being easily hurt?	0.48 ± 0.02 (0.55)	0.09	0.14	0.11	0.03	0.11	0.08
How much are you distressed by feeling that people are unfriendly or dislike you?	0.39 ± 0.02 (0.49)	0.12	0.12	0.05	0.09	0.13	0.00
How much are you distressed by feeling inferior to others?	0.41 ± 0.02 (0.53)	0.11	0.14	0.06	0.02	0.11	0.05
How much are you distressed by feeling very self-conscious with others?	0.50 ± 0.02 (0.49)	0.11	0.09	0.04	0.04	-0.01	-0.01
Distress - Obsession-Compulsion							
How much are you distressed by trouble remembering things?	0.45 ± 0.02 (0.56)	0.12	0.16	0.10	0.05	0.10	-0.02

Question	Mean ± 95% CI (IQR)	baseline	follow-up	survey	game	touch-q	touch-d
How much are you distressed by feeling blocked in getting things done?	0.51 ± 0.02 (0.53)	0.13	0.13	0.13	0.03	0.10	0.05
How much are you distressed by having to check and double check what you do?	0.49 ± 0.02 (0.52)	0.12	0.11	0.11	0.01	0.07	0.04
How much are you distressed by difficulty making decisions?	0.47 ± 0.02 (0.52)	0.16	0.15	0.01	0.04	0.10	0.07
How much are you distressed by your mind going blank?	0.40 ± 0.02 (0.51)	0.13	0.12	0.03	-0.04	0.07	0.04
How much are you distressed by trouble concentrating?	0.47 ± 0.02 (0.54)	0.16	0.21	0.05	0.10	0.09	0.04
Distress - Paranoid Ideation							
How much are you distressed by feeling others are to blame for most of your troubles?	0.33 ± 0.01 (0.40)	0.12	0.17	0.11	0.09	0.13	0.04
How much are you distressed by feeling that most people cannot be trusted?	0.50 ± 0.02 (0.48)	0.09	0.12	0.08	0.08	0.09	0.05
How much are you distressed by feeling that you are watched or talked about by others?	0.38 ± 0.02 (0.51)	0.12	0.10	0.15	0.02	0.12	0.06
How much are you distressed by others not giving you proper credit for your achievements?	0.43 ± 0.02 (0.49)	0.14	0.15	0.09	0.02	0.07	0.03
How much are you distressed by feeling that people will take advantage of you if you let them?	0.52 ± 0.02 (0.51)	0.08	0.11	0.06	0.02	0.06	0.05
Distress - Phobic Anxiety							
How much are you distressed by feeling afraid in open spaces?	0.30 ± 0.02 (0.40)	0.14	0.17	0.12	0.09	0.09	0.07
How much are you distressed by feeling afraid to travel on buses, subways, or trains?	0.31 ± 0.02 (0.43)	0.14	0.12	0.11	0.06	0.11	0.03
How much are you distressed by having to avoid certain things, places, or activities because they frighten you?	0.42 ± 0.02 (0.53)	0.10	0.15	0.14	0.06	0.12	0.01
How much are you distressed by feeling uneasy in crowds?	0.45 ± 0.02 (0.55)	0.08	0.08	0.10	-0.03	0.06	0.03
How much are you distressed by feeling nervous when you are left alone?	0.32 ± 0.02 (0.44)	0.13	0.18	0.14	0.02	0.12	0.07
Distress - Psychoticism							
How much are you distressed by the idea that someone else can control your thoughts?	0.31 ± 0.02 (0.46)	0.16	0.20	0.11	0.08	0.17	0.06
How much are you distressed by feeling lonely even when you are with people?	0.43 ± 0.02 (0.53)	0.12	0.14	0.10	0.04	0.10	0.04
How much are you distressed by the idea that you should be punished for your sins?	0.33 ± 0.02 (0.45)	0.19	0.18	0.11	0.02	0.12	0.10
How much are you distressed by never feeling close to another person?	0.41 ± 0.02 (0.52)	0.08	0.09	0.08	0.07	0.08	0.04
How much are you distressed by the idea that something is wrong with your mind?	0.41 ± 0.02 (0.56)	0.19	0.17	0.07	0.13	0.10	0.02
Distress - Somatization							
How much are you distressed by faintness or dizziness?	0.34 ± 0.02 (0.45)	0.13	0.17	0.10	0.03	0.12	0.02
How much are you distressed by pains in the heart or chest?	0.34 ± 0.02 (0.50)	0.12	0.11	0.09	0.00	0.09	0.09
How much are you distressed by nausea or upset stomach?	0.37 ± 0.02 (0.50)	0.09	0.13	0.12	0.00	0.05	0.02
How much are you distressed by trouble getting your breath?	0.32 ± 0.02 (0.43)	0.12	0.17	0.11	0.05	0.09	0.06
How much are you distressed by hot or cold spells?	0.31 ± 0.01 (0.40)	0.17	0.17	0.15	0.10	0.12	0.02

Question	Mean ± 95% CI (IQR)	baseline	follow-up	survey	game	touch-q	touch-d
How much are you distressed by numbness or tingling in parts of your body?	0.33 ± 0.02 (0.45)	0.14	0.15	0.12	0.02	0.09	0.06
How much are you distressed by feeling weak in parts of your body?	0.41 ± 0.02 (0.53)	0.12	0.12	0.03	-0.01	0.07	0.03
Wellbeing - Emotional Wellbeing							
To what extent do you feel happy?	0.60 ± 0.01 (0.39)	0.15	0.12	0.15	0.13	0.16	0.05
To what extent do you feel interested in life?	0.66 ± 0.01 (0.40)	0.09	0.14	0.10	0.08	0.15	0.03
To what extent do you feel satisfied with life?	0.55 ± 0.02 (0.46)	0.12	0.09	0.15	0.14	0.17	0.03
Wellbeing - Psychological Wellbeing							
To what extent do you feel that you like most parts of your personality?	0.62 ± 0.01 (0.38)	0.05	0.07	0.09	0.05	0.19	0.04
To what extent do you feel good at managing the responsibilities of your daily life?	0.61 ± 0.01 (0.41)	0.13	0.13	0.17	0.06	0.15	0.06
To what extent do you feel that you have warm and trusting relationships with others?	0.60 ± 0.01 (0.41)	0.06	0.09	0.13	0.08	0.10	0.02
To what extent do you feel that you have experiences that challenge you to grow and become a better person?	0.62 ± 0.01 (0.35)	0.06	0.04	0.17	0.04	0.10	0.02
To what extent do you feel confident to think or express your own ideas and opinions?	0.64 ± 0.01 (0.38)	0.08	0.12	0.12	0.04	0.15	0.01
To what extent do you feel that your life has a sense of direction or meaning to it?	0.56 ± 0.02 (0.51)	0.08	0.12	0.09	0.03	0.14	0.02
Wellbeing - Social Wellbeing							
To what extent do you feel that you have something important to contribute to society?	0.59 ± 0.02 (0.47)	0.11	0.13	0.06	0.09	0.15	0.06
To what extent do you feel that you belong to a community (like a social group, or your neighborhood)?	0.51 ± 0.02 (0.52)	0.09	0.09	0.01	0.10	0.06	0.06
To what extent do you feel that our society is a good place, or is becoming a better place, for all people?	0.41 ± 0.02 (0.41)	0.15	0.06	0.08	0.10	0.10	0.08
To what extent do you feel that people are basically good?	0.52 ± 0.01 (0.34)	0.01	0.03	0.04	-0.02	0.09	0.00
To what extent do you feel that the way our society works makes sense to you?	0.47 ± 0.01 (0.43)	0.06	0.05	0.07	0.07	0.02	0.08

Supplemental Table S1. Predicting mental health from human-computer interactions. For each questionnaire item, the average score is reported as mean ± 95% confidence interval (inter-quartile range). To the right, Spearman correlations (r) indicate the correspondence between predicted and true scores in the calibration cursor dataset (baseline, 5-fold cross-validation), follow-up data, an independent non-mental-health survey, and a gamified decision-making task. All generalization models were trained on the baseline dataset and applied without retraining to the respective target data. The final two columns show correlations from two touch-based tasks (interface interaction and free-form drawing), each evaluated using 5-fold cross-validation.

9.24 Supplemental Table S2

Question	Groun truth correlation (r)
Body Awareness	
To what extent do you feel that strong lights or sounds affect your ability to focus?	-0.01
To what extent do you feel that you can detect changes in your vision or hearing in different environments?	0.05
To what extent do you feel that you can distinguish between different textures or temperatures by touch?	0.16
To what extent do you feel that you can sense your body's position in space during movement?	0.00
To what extent do you feel that you notice subtle bodily sensations (e.g., heartbeat, muscle tension)?	-0.02
Civic	
To what extent do you feel that voting is important to you?	-0.01
To what extent do you feel that your voice matters in society?	0.04
Cognition	
To what extent do you feel that you can detect subtle differences in colors?	0.16
To what extent do you feel that you can easily identify objects in cluttered scenes?	-0.09
To what extent do you feel that you can recall specific events from two days ago?	-0.04
To what extent do you feel that you easily recall names of people you meet?	0.05
To what extent do you feel that you remember people's faces after meeting them once?	-0.11
Decision Making	
To what extent do you feel that uncertainty affects your decision-making?	-0.05
To what extent do you feel that you can consider long-term outcomes when making choices?	0.05
To what extent do you feel that you enjoy solving complex logical problems?	0.10
To what extent do you feel that you prefer making decisions quickly rather than deliberating?	0.01
To what extent do you feel that you rely on intuition when making difficult decisions?	-0.03
Economy	
To what extent do you feel that groceries are more expensive than last year?	-0.13
To what extent do you feel that people work harder now than 10 years ago for the same housing?	-0.16
To what extent do you feel that the economy has improved in the past year?	0.04
To what extent do you feel that you are paid fairly for your work?	0.02
To what extent do you feel that your income keeps up with the cost of living?	0.03
Head Impact	
To what extent do you feel that you can recall episodes of losing consciousness during or after sports?	0.02
To what extent do you feel that you've experienced head impacts during physical activities?	-0.05
To what extent do you feel that you've noticed changes in your memory after repeated sports-related impacts?	0.01
To what extent do you feel that your past participation in contact sports has affected your physical coordination?	0.11
To what extent do you feel that your sports training emphasized head safety?	0.05
Motor Control	
To what extent do you feel that you can adjust your body movements in response to unexpected changes in your environment?	0.04
To what extent do you feel that you can coordinate both hands effectively for tasks like tying shoelaces or typing?	0.17
To what extent do you feel that you can keep your body still when needed (e.g., holding a posture or standing motionless)?	0.19
To what extent do you feel that you can maintain balance when walking on uneven surfaces?	0.16
To what extent do you feel that your movements are precise when doing tasks that require fine motor skills (e.g., writing, threading a needle)?	0.13
Politics	
To what extent do you feel that immigration strengthens the country?	-0.07
To what extent do you feel that political news influences your daily decisions?	-0.06
To what extent do you feel that public healthcare is important?	-0.01
To what extent do you feel that the government should solve more social problems?	-0.03
Society	
To what extent do you feel that climate change affects your everyday life?	0.01
To what extent do you feel that news media are trustworthy?	-0.09
To what extent do you feel that people are treated equally regardless of race?	-0.15
To what extent do you feel that public transport meets your daily needs?	0.00
To what extent do you feel that your cultural background shapes your identity?	0.05
To what extent do you feel that your education prepared you well for life?	0.10
Technology	

Question	Groun truth correlation (r)
To what extent do you feel that fake news is easy to recognize?	0.01
To what extent do you feel that technology improves your quality of life?	0.10
To what extent do you feel that your online activity is private and secure?	-0.11
Values	
To what extent do you feel that learning about other cultures enriches your perspective?	0.06
To what extent do you feel that religion plays a role in your life?	-0.05

Supplemental Table S2. Predicting responses to non-mental health items from human-computer interactions. For each question from the non-psychological survey and gamified task, the table reports the Spearman correlation coefficient (R) between predicted and true item scores obtained within each dataset using 5-fold cross-validation. Dimensions correspond to thematic categories of items. Each group header indicates the corresponding dimension, and individual rows list the specific items within that domain. MAILA failed to predict the responses to the non-mental health survey (R = 0.01 ± 0.03, p = 0.28), suggesting that cursor movements capture dynamic mental states associated with psychological distress and wellbeing, but not more stable self-assessments of abilities, attitudes, or beliefs, or response artifacts induced by our interface.

9.25 Supplemental Table S3

Prompt: Draw ...
Digits
the digits "8047"
the digits "9846"
the digits "1237"
the digits "5912"
the digits "0356"
Objects
a human face with glasses
a bow shooting an arrow
a spaceship
lightning coming out of a cloud
a key
a tent and a campfire
a traffic light
a fish in a fishbowl
a house with a chimney
a flower in a pot
a cat
a coffee mug
a mountain range with a sun
a hand with a wristwatch
a person riding a bike

Supplemental Table S3. Predicting mental health from free-form digital behavior. Participants were instructed to draw each prompt using a touchscreen interface. For readability, prompts are grouped by their underlying semantic category (e.g., objects, digits). Each prompt was shown once in random order across participants.

9.26 Supplemental Table S4

	Status	
Recommendation	Current efforts	Future priorities
Explainability		
Define the need and requirements for explainability with end users	Assessed mechanism of prediction, provided explanations of performance in terms of human-centered movement features	Develop interactive visualizations or summaries for non-experts
Evaluate explainability with end users (e.g., correctness, impact on users)	N/A	Conduct usability studies to assess how well explanations improve understanding
Fairness		
Collect information on individuals' and data attributes	Collected demographics, self-reported mental health data, and hardware at the participant level	Expand data collection to include additional background information, e.g. electronic health records, additional dimensions of mental health, biomarkers (genetics, wearables, imaging)
Define any potential sources of bias from an early stage	Evaluated performance across demographic features available for participants recruited via an online experimental platform	Conduct targeted bias analyses for underrepresented (including clinical) populations; validate MAILA outside of online cohorts
Evaluate potential biases and, when needed, bias correction measures	Evaluated model stability across demographic groups, context, time, and input modality	Implement algorithmic fairness measures (e.g., re-weighting techniques) to actively mitigate bias
General		
Define adequate evaluation plan (e.g., datasets, metrics, reference methods)	Defined evaluation protocol for cursor and touchscreen activity for regression and classification	Incorporate additional fairness, robustness, and real-world performance metrics
Engage interdisciplinary stakeholders throughout the AI lifecycle	N/A	Expand involvement to include ethicists, data privacy experts, and policymakers
Identify and comply with applicable AI regulatory requirements	N/A	Anticipate compliance plans aligned with AI standards such as GDPR, HIPAA, or ISO standards
Implement measures for data privacy and security	Emphasized anonymization, explored strategies for preventing unintended use (client-side scrambling)	Build a browser plugin for client-side scrambling
Implement measures to address identified AI risks	Discussed risk mitigation	Develop targeted strategies for mitigating potential misuse of human-computer interactions, starting with scrambling tools
Investigate and address application specific ethical issues	Acknowledged ethical concerns such as consent and transparency	Develop detailed guidelines for ethical data use and informed consent practices
Investigate and address social and societal issues	Acknowledged ethical risks and societal implications	Conduct focus groups or interviews with key social groups to anticipate unintended consequences
Robustness		
Define sources of data variation from an early stage	Conducted stress testing for noise, incomplete data, reduced training set size, and impoverished movement clusters	Validate in cohorts with known movement variation (e.g., movement disorders)Assess atypical movement patterns in people with movement disorders
Evaluate and optimize robustness against real world variations	N/A	Expand data collection fully unconstrained computer use annotated with mental health labels
Train with representative real world data	Collected data various modalities intended to simulate everyday computer use, indirect validation on unlabeled naturalistic computer use	Expand data collection fully unconstrained computer use annotated with mental health labels
Traceability		
Define mechanisms for quality control of the AI inputs and outputs	Evaluated model performance using multiple metrics and targets (regression on inter-individual differences and classification of groups)	Implement ongoing quality control processes during deployment
Establish mechanisms for AI governance	N/A	Establish an advisory board to oversee ethical concerns and data management

Recommendation	Current efforts	Future priorities
Implement a logging system for usage recording	N/A	Develop secure logging protocols to track system performance and failures
Implement a risk management process throughout the AI lifecycle	Addressed ethical considerations regarding privacy and security, outlined scrambling as a way to mitigate unwanted digital profiling	Formalize a risk management framework, identifying potential failure points, build scrambler browser plugin & safety hardware
Implement a system for periodic auditing and updating	N/A	Develop procedures for continuous model updates based on evolving data
Provide documentation (e.g., technical, clinical)	Developed detailed methodology documentation for feature extraction, data analysis, and model development	Develop user-facing documentation for non-technical stakeholder, publish code & data on GitHub at the time of publication
Universality		
Define intended clinical settings and cross setting variations	Tested generalization from models trained on the general population to populations with self-identified diagnoses (depression & OCD)	Define specific contexts for deployment (e.g., telehealth, digital wellbeing platforms)
Evaluate and demonstrate local clinical validity	N/A	Conduct clinical trials in real-life healthcare settings
Evaluate using external datasets and/or multiple sites	Evaluated performance in several generalization datasets, applied trained models to external datasets	Evaluate model performance across multiple sites and diverse real-world conditions, e.g. gaming, naturalistic browsing, office work, coding, entertainment applications in large cohorts
Use community defined standards (e.g., clinical definitions, technical standards)	Used an novel questionnaire tool with favorable psychometric properties	Integrate structured interviews (e.g., SCID), expand to other self-report questionnaires, expand to predefined cohorts
Usability		
Define intended use and user requirements from an early stage	Defined human-computer interactions as a scalable signal for mental health prediction	Develop specific deployment strategies for use in clinical or public health contexts
Establish mechanisms for human-AI interactions and oversight	N/A	Design user feedback mechanisms to improve model trustworthiness
Evaluate clinical utility and safety (e.g., effectiveness, harm, cost-benefit)	N/A	Conduct clinical safety and efficacy evaluations before deployment in clinical settings
Evaluate user experience and acceptance with independent end users	N/A	Conduct studies evaluating usability, interpretability, and trust
Provide training materials and activities (e.g., tutorials, hands-on sessions)	N/A	Develop educational content for clinicians, researchers, and end users

Supplemental Table S4. Recommendations for responsible and transparent use of AI in mental health research (FAIR). Each row summarizes a key recommendation grouped by overarching category. The table outlines how the FAIR principles are currently addressed and highlights proposed next steps for advancing best practices.

References

1. GBD 2019 Mental Disorders Collaborators. Global, regional, and national burden of 12 mental disorders in 204 countries and territories, 1990-2019: A systematic analysis for the Global Burden of Disease Study 2019. *The Lancet. Psychiatry* **9**, 137–150 (2022).

2. WHO. Mental disorders Factsheet.

3. Ghio, L. *et al.* Duration of untreated illness and outcomes in unipolar depression: A systematic review and meta-analysis. *Journal of Affective Disorders* **152-154**, 45–51 (2014).

4. Pablo, G. S. de *et al.* What is the duration of untreated psychosis worldwide? – A meta-analysis of pooled mean and median time and regional trends and other correlates across 369 studies. *Psychological Medicine* **54**, 652–662 (2024).

5. Kraus, C. *et al.* Prognosis and improved outcomes in major depression: A review. *Translational Psychiatry* **9**, 127 (2019).

6. Preece, D. A. *et al.* Alexithymia profiles and depression, anxiety, and stress. *Journal of Affective Disorders* **357**, 116–125 (2024).

7. Clement, S. *et al.* What is the impact of mental health-related stigma on help-seeking? A systematic review of quantitative and qualitative studies. *Psychological Medicine* **45**, 11–27 (2015).

8. Miteva, D. *et al.* Impact of language proficiency on mental health service use, treatment and outcomes: "Lost in Translation". *Comprehensive Psychiatry* **114**, 152299 (2022).

9. Keynejad, R. C. *et al.* WHO Mental Health Gap Action Programme (mhGAP) Intervention Guide: A systematic review of evidence from low and middle-income countries. *Evidence Based Mental Health* **21**, (2018).

10. Binz, M. *et al.* A foundation model to predict and capture human cognition. *Nature* **644**, 1002–1009 (2025).

11. Dohnány, S. *et al.* Technological folie à deux: Feedback Loops Between AI Chatbots and Mental Illness. (2025) doi:10.48550/arXiv.2507.19218.

12. Lewis, C. M. *et al.* Polygenic risk scores: From research tools to clinical instruments. *Genome Medicine* **12**, 44 (2020).

13. Murray, G. K. *et al.* Could Polygenic Risk Scores Be Useful in Psychiatry?: A Review. *JAMA Psychiatry* **78**, 210–219 (2021).

14. Sanchez-Roige, S. *et al.* Emerging phenotyping strategies will advance our understanding of psychiatric genetics. *Nature neuroscience* **23**, 475–480 (2020).

15. Kambeitz, J. *et al.* Detecting Neuroimaging Biomarkers for Depression: A Meta-analysis of Multivariate Pattern Recognition Studies. *Biological Psychiatry* **82**, 330–338 (2017).

16. Marek, S. *et al.* Reproducible brain-wide association studies require thousands of individuals. *Nature 2022 603:7902* **603**, 654–660 (2022).

17. Liu, J. J. *et al.* Digital phenotyping from wearables using AI characterizes psychiatric disorders and identifies genetic associations. *Cell* **188**, 515–529.e15 (2025).

18. Abd-Alrazaq, A. *et al.* Systematic review and meta-analysis of performance of wearable artificial intelligence in detecting and predicting depression. *npj Digital Medicine* **6**, 84 (2023).

19. Open Science Collaboration. Estimating the reproducibility of psychological science. *Science* **349**, aac4716 (2015).

20. Schurr, R. *et al.* Dynamic computational phenotyping of human cognition. *Nature Human Behaviour* **8**, 917–931 (2024).

21. Gillan, C. M. *et al.* Smartphones and the Neuroscience of Mental Health. *Annual Review of Neuroscience* **44**, 129–151 (2021).

22. Mirea, D.-M. *et al.* Cognitive modeling of real-world behavior for understanding mental health. *Trends in Cognitive Sciences* (2025) doi:10.1016/j.tics.2025.07.009.

23. Freeman, J. B. Doing Psychological Science by Hand. *Current Directions in Psychological Science* **27**, 315–323 (2018).

24. Jain, S. H. *et al.* The digital phenotype. *Nature Biotechnology* **33**, 462–463 (2015).

25. Insel, T. R. Digital Phenotyping: Technology for a New Science of Behavior. *JAMA* **318**, 1215–1216 (2017).

26. Wainberg, M. L. *et al.* Challenges and Opportunities in Global Mental Health: A Research-to-Practice Perspective. *Current Psychiatry Reports* **19**, 28 (2017).

27. Barrett, P. M. *et al.* Digitising the mind. *The Lancet* **389**, 1877 (2017).

28. Topol, E. J. High-performance medicine: The convergence of human and artificial intelligence. *Nature Medicine* **25**, 44–56 (2019).

29. Onnela, J.-P. Opportunities and challenges in the collection and analysis of digital phenotyping data. *Neuropsychopharmacology* **46**, 45–54 (2021).

30. Hauser, T. U. *et al.* The promise of a model-based psychiatry: Building computational models of mental ill health. *The Lancet Digital Health* **4**, e816–e828 (2022).

31. Koutsouleris, N. *et al.* From promise to practice: Towards the realisation of AI-informed mental health care. *The Lancet Digital Health* **4**, e829–e840 (2022).

32. Darwin, C. *et al.* *The Expression of the Emotions in Man and Animals, Definitive Edition.* (Oxford University Press, 1998).

33. Ekman, P. Emotional and Conversational Nonverbal Signals. in *Language, Knowledge, and Representation* (eds. Larrazabal, J. M. et al.) 39–50 (Springer Netherlands, 2004).

34. Wolpert, D. M. *et al.* A unifying computational framework for motor control and social interaction. *Philosophical Transactions of the Royal Society B: Biological Sciences* **358**, 593–602 (2003).

35. Shadmehr, R. *et al.* Error correction, sensory prediction, and adaptation in motor control. *Annual Review of Neuroscience* **33**, 89–108 (2010).

36. Schoemann, M. *et al.* Using mouse cursor tracking to investigate online cognition: Preserving methodological ingenuity while moving toward reproducible science. *Psychonomic Bulletin & Review* **28**, 766–787 (2021).

37. Freihaut, P. *et al.* Tracking stress via the computer mouse? Promises and challenges of a potential behavioral stress marker. *Behavior Research Methods* **53**, 2281–2301 (2021).

38. De Angel, V. *et al.* Digital health tools for the passive monitoring of depression: A systematic review of methods. *npj Digital Medicine* **5**, 3 (2022).

39. Insel, T. *et al.* Research domain criteria (RDoC): Toward a new classification framework for research on mental disorders. *The American Journal of Psychiatry* **167**, 748–751 (2010).

40. Kotov, R. *et al.* A paradigm shift in psychiatric classification: The Hierarchical Taxonomy Of Psychopathology (HiTOP). *World Psychiatry* **17**, 24–25 (2018).

41. Kılıç, A. A. *et al.* Bogazici mouse dynamics dataset. *Data in Brief* **36**, 107094 (2021).

42. Westerhof, G. J. *et al.* Mental Illness and Mental Health: The Two Continua Model Across the Lifespan. *Journal of Adult Development* **17**, 110–119 (2010).

43. Dinga, R. *et al.* Predicting the naturalistic course of depression from a wide range of clinical, psychological, and biological data: A machine learning approach. *Translational Psychiatry* **8**, 241 (2018).

44. Karvelis, P. *et al.* Individual differences in computational psychiatry: A review of current challenges. *Neuroscience & Biobehavioral Reviews* **148**, 105137 (2023).

45. Obermeyer, Z. *et al.* Dissecting racial bias in an algorithm used to manage the health of populations. *Science* **366**, 447–453 (2019).

46. So, S. H. *et al.* Jumping to conclusions data-gathering bias in psychosis and other psychiatric disorders — Two meta-analyses of comparisons between patients and healthy individuals. *Clinical Psychology Review* **46**, 151–167 (2016).

47. DataReportal – Global Digital Insights. *DataReportal – Global Digital Insights.*

48. StatCounter. Desktop vs Mobile vs Tablet Market Share Worldwide. *Global Stats.*

49. Keyes, K. M. *et al.* UK Biobank, big data, and the consequences of non-representativeness. *Lancet (London, England)* **393**, 1297 (2019).

50. Caspi, A. *et al.* All for One and One for All: Mental Disorders in One Dimension. *American Journal of Psychiatry* **175**, 831–844 (2018).

51. Arena, A. F. *et al.* Mental health and unemployment: A systematic review and meta-analysis of interventions to improve depression and anxiety outcomes. *Journal of Affective Disorders* **335**, 450–472 (2023).

52. Charles, S. T. *et al.* Social and Emotional Aging. *Annual Review of Psychology* **61**, 383–409 (2010).

53. Kuehner, C. Why is depression more common among women than among men? *The Lancet Psychiatry* **4**, 146–158 (2017).

54. Golder, S. A. *et al.* Diurnal and Seasonal Mood Vary with Work, Sleep, and Daylength Across Diverse Cultures. *Science* **333**, 1878–1881 (2011).

55. Perris, F. *et al.* Duration of Untreated Illness in Patients with Obsessive-Compulsive Disorder and Its Impact on Long-Term Outcome: A Systematic Review. *Journal of Personalized Medicine* **13**, 1453 (2023).

56. Trepka, E. *et al.* Entropy-based metrics for predicting choice behavior based on local response to reward. *Nature Communications* **12**, 6567 (2021).

57. Bennett, D. *et al.* The Two Cultures of Computational Psychiatry. *JAMA Psychiatry* **76**, 563–564 (2019).

58. Torous, J. *et al.* The growing field of digital psychiatry: Current evidence and the future of apps, social media, chatbots, and virtual reality. *World psychiatry: official journal of the World Psychiatric Association (WPA)* **20**, 318–335 (2021).

59. LeCun, Y. *et al.* Deep learning. *Nature* **521**, 436–444 (2015).

60. Lebowitz, M. S. *et al.* Testing positive for a genetic predisposition to depression magnifies retrospective memory for depressive symptoms. *Journal of Consulting and Clinical Psychology* **85**, 1052–1063 (2017).

61. Lekadir, K. *et al.* FUTURE-AI: International consensus guideline for trustworthy and deployable artificial intelligence in healthcare. (2025) doi:10.1136/bmj-2024-081554.

62. Derogatis, L. R. *et al.* The Brief Symptom Inventory: An introductory report. *Psychological Medicine* **13**, 595–605 (1983).

63. Keyes, C. L. M. *et al.* Evaluation of the mental health continuum-short form (MHC-SF) in setswana-speaking South Africans. *Clinical Psychology & Psychotherapy* **15**, 181–192 (2008).